Supplementary Information for

Degradable semiconducting polymers without long-range order for on-demand degradation of transient electronics

Jerika A. Chiong,[1,2] Lukas Michalek,[2] Amnahir E. Peña-Alcántara,[3] Xiaozhou Ji,[2] Nathaniel J. Schuster,[2] and Zhenan Bao[1,2,*]

[1]Dept. of Chemistry, Stanford University, Stanford, CA 94305, USA

[2]Dept. of Chemical Engineering, Stanford University, Stanford, CA 94305, USA

[3]Dept. of Materials Science and Engineering, Stanford University, Stanford, CA 94305, USA

Materials and Methods

Monomer and Polymer Synthesis and Characterization:

All starting materials and reagents were purchased and used without further purification. 1D NMR spectra were recorded on a Bruker Neo spectrometer (500 MHz) at 298 K. The spectra were internally referenced to the residual solvent signal ($CDCl_3$: δ 7.26 for ^1H and δ 77.16 for ^{13}C; CD_2Cl_2: δ 5.32 for ^1H and δ 53.84 for ^{13}C; $C_2D_2Cl_4$: δ 6.0 for ^1H; toluene-d_8: δ 7.01 for ^1H; THF-d_8: δ 1.72 and δ 3.58 for ^1H). Mass spectrometry (MS) of small molecules was carried out using electrospray ionization on a Waters Acquity LC/MS with SQD Quadrupole MS and H-Class UPLC, and matrix-assisted laser desorption/ionization-time of flight (MALDI-TOF) analysis was performed using Bruker Microflex MALDI-TOF instrument in reflectron mode. Number average molecular weight (M_n), dispersity ($Đ$), and number average degree of polymerization (DP_n) were characterized by size exclusion chromatography (SEC) on the Tosoh High-temperature EcoSEC at 180 °C with 1,2,4-trichlorobenzene as the solvent. The system was equipped with a single TSK gel GPC column (GMH_{HR}-HT2; 300 mm×7.8 mm) and was calibrated against monodisperse polystyrene standards.

DFT and TD-DFT Calculations:

The DFT and TD-DFT calculations were executed by Jaguar, version 13.3, release 2022-4, Schrödinger, Inc.[1] on the Sherlock computing cluster at Stanford University. In the DFT models, IDT units were replaced with thiophene units to simplify the calculations. Additionally, in the TD-DFT models, the alkyl chains on the IDT units were truncated to methyl groups to expedite the calculations. We modeled thiophene units with its sulfur atom oriented toward the hydrogens on the benzo group of the BT unit based on reported understanding of stabilizing non-covalent interactions between the two units.[2,3] The geometries of our DFT models were optimized without symmetry restrictions in the gas phase using the B3LYP-D3 functional and 6-31G** basis set. For the modeled degradation products, the 20 lowest-energy singlet excited states were calculated in the gas phase using the CAM-B3LYP-D3 functional and 6-31G++** basis set. The corresponding UV-vis absorption spectra were generated at the purely electronic level without vibronic character.

Thin Film Preparation:

Octadecyltrimethoxysilane (OTS)-modified Si and SiO_2 wafers were prepared by first subjecting the wafers to O_2 plasma at 50 W for 10 min and 3 min, respectively. A solution of OTS in anhydrous trichloroethylene (18 μL OTS in 15 mL trichloroethylene) was syringe filtered, dropped

onto the wafers, and spincoated onto the wafers at 2000 rpm for 30 s after a 30 s wait. Wafers were left in a desiccator purged with NH_3 overnight, proceeded by sonication in toluene for 15 min. In all thin film preparation, IDT-based polymers were dissolved at a concentration of 10 mg/mL in anhydrous chlorobenzene by stirring overnight on a hotplate at 70 °C. The DPP-based polymer reference was dissolved at a concentration of 5 mg/mL using the same method. Solutions were then raised to 80 °C an hour before spincoating, and then spincoated at various rpm for 60 s to achieve comparable film thicknesses and optimal electronic performance (pIDT-BTiBT: 1000/500 rpm/accel, 150 °C anneal; pIDT-10BTiPh: 1200/1000 rpm/accel, 150 °C anneal; pIDT-BTiPh: 2500/1000 rpm/accel, 80 °C anneal; pIDT-BT: 1200/1000 rpm/accel, 150 °C anneal; pDPP(C4E)-TIT: 1000/1000 rpm/accel, 200 °C anneal). All IDT films were thermally annealed for 30 min and were allowed to cool slowly to 50 °C after the hotplate was turned off. All processes were conducted in a glovebox under nitrogen.

Thin Film Characterization:
UV-vis spectra were collected using an Agilent Cary 6000i spectrophotometer. PESA measurements were taken on a Riken AC-2 photoelectron spectrometer with a power setting of 5 nW and a power number of 0.5. Films were deposited on OTS-modified SiO_2 substrates.

GIXD of polymeric thin films were performed at beamline 11-3 in the Stanford Synchrotron Radiation Light Source (SSRL) with a beam energy of 12.7 keV. All the measurements were collected in a helium-purged environment with an X-ray incident angle of 0.12°. Diffraction images were recorded with an exposure time of 120 s. Samples were fabricated by spincoating on OTS-modified Si substrates (Si was used to avoid background scattering from SiO_2). Data was processed using Python code developed within the Bao group.

AFM images were taken in peak-force quantitative nanomechanical mapping (PF-QNM) mode on a Bruker Dimension Icon AFM. A NSC19 probe (from MikroMasch, Tallinn, Estonia with a nominal spring constant of 0.5 N/m, resonance frequency of 60 kHz, and a tip radius of 8 nm) was calibrated prior measurements on a hard sapphire sample resulting in a spring constant of 1.26 N/m. All nanomechanical images were recorded at a setpoint of ~700 pN with a Peak Force frequency of 2 kHz and amplitude of 150 nm. The scan resolution was set to 256x256 pixel with a scan-rate of 0.9 Hz. The data was evaluated and depicted with Gwyddion SPM software, which was also used to generate the histograms through a 1D statistical function to estimate the apparent DMT-modulus. Films were deposited on OTS-modified SiO_2 substrates.

Optical microscope images for mechanical testing were taken on a Leica Microsystems DM4000 M LED Microscope. Contact angle images were taken with a Prosilica GC camera and analyzed using a First Ten Angstroms (FTA32) goniometer. Polymer film thicknesses were measured using a Bruker Dektak XT-A profilometer.

Device Fabrication:
The edges of OTS-modified SiO_2 wafers were etched with O_2 plasma at 150 W for 20 s to remove OTS for spincoating. For bottom-gate top-contact (BGTC) devices, 40 nm Au source and drain contacts were thermally evaporated through a shadow mask (W = 1000 μm, L = 50 μm). For top-gate bottom-contact (TGBC) devices, 3/40 nm Cr/Au source and drain electrodes were thermally evaporated through a shadow mask (W= 2000 μm, L = 50 μm). Before spincoating of

semiconductors, OTS-SiO_2 substrates patterned with Au electrodes were soaked in isopropanol solution (20 mL) of pentafluorothiophenol (PFBT) (2.6 µL, 1:7700 v/v) for 10 min for electrode modification and then washed with isopropanol. Semiconductors were spincoated using the procedure detailed in thin film preparation. CYTOP dielectric (Asahi Glass, type CTL-809M) was prepared by mixing with CYTOP CT-SOLV180 (1:0.2 v/v CYTOP:CT-SOLV180) and spincoating to form ~700 nm dielectric layer and annealed at 80 °C for 1 h (pIDT-BTiPh) or 150 °C for 30 min (all other polymers). The 45 nm Au gate was also thermally evaporated using Kapton sheets as masks. All transistors were characterized using a Keithley 4200 semiconductor parameter analyzer in a glovebox under nitrogen atmosphere at room temperature. A gate-channel capacitance per unit area of 11.5 nF/cm^2 (for BGTC SiO_2 dielectric) or 2.6-2.9 nF/cm^2 (for TGBC CYTOP dielectric, calculated depending on CYTOP thickness) was used for determination of saturation mobilities. All transistor measurements were averaged from six total channels selected at random from two different substrates.

UV-vis, GPC, NMR, and QCM Degradation Studies:

For UV-vis solution studies, 150x molar excess of TFA and DI H_2O were added to polymer solution samples (~0.01 mg/mL). For chloroform solutions, chloroform stabilized with amylenes was used as the ethanol stabilizer reacted with TFA. Samples were left to degrade at room temperature. To quantify the degradation over time, absorbance (A) at λ_{max} was calculated after normalizing over the allowed degradation range, where $A_{\lambda max,final}$ was subtracted from $A_{\lambda max,initial.}$ The following equation $Normalized\ A_{\lambda max,\ i} = \frac{A_{\lambda max,\ i} - A_{\lambda max,\ f}}{A_{\lambda max,\ 0} - A_{\lambda max,\ f}}$ was used.

For UV-vis thin film studies, thin film samples were prepared by spincoating polymers onto OTS-SiO_2 substrates using the same processing conditions as detailed in thin film preparation. PDMS (Sylgard 184, 12:1 w/w base:crosslinker, 13 g total) was prepared by mixing for 3 min at 3000 rpm, pouring into a 150 mm x 15 mm petri dish, and curing overnight at 70 °C. PDMS stamps were used to peel off the polymer films and placed facing downwards into an acidic aqueous solution in water (3 mL) in a 20 mL scintillation vial with a Teflon cap. Vials were placed in a 70 °C oven to heat evenly.

GPC degradation studies were measured by size exclusion chromatography (SEC) at room temperature with HPLC THF as the solvent. The system was equipped with two PolyPore columns (Agilent) connected in series with a DAWN multiangle laser light scattering (MALLS) detector and an Optilab T-rEX differential refractometer (both from Wyatt Technology). 150x molar excess of TFA and DI H_2O were added to polymer solution samples (~0.01 mg/mL). At each timepoint, solutions were evaporated to dryness and dried under high vacuum overnight. ~1 mg/mL solutions in HPLC THF were used to run on GPC.

In situ NMR degradation experiments were conducted at a higher concentration of polymer solution in THF (~5 mg/mL) using a 150x molar excess of deuterated TFA and D_2O. NMR spectra were recorded on a Bruker Neo spectrometer (500 MHz) at 298 K.

QCM sensors were prepared by spincoating polymers onto QSense QSX 303 SiO2 sensors using the same processing conditions as detailed in thin film preparation. QCM measurements were

performed using a Biolin Scientific QSense Explorer and flow module with 40 µL volume above the sensor. For water swelling measurements, temperature was kept at 25 °C. For acid degradation experiments, temperature was kept at 65 °C. Each measurement was started by recording a stable baseline in air for > 30 min and subsequent flow of water or acid at a constant flow rate of 50 µL/min.

Synthesis of BT-derivative monomers

The synthetic schemes of the two degradable BT-derivative monomers *N*,1-bis(7-bromobenzo[*c*][1,2,5]thiadiazol-4-yl)methanimine (Br-BTiBT-Br) and 1-(7-bromobenzo[*c*][1,2,5]thiadiazol-4-yl)-*N*-(4-bromophenyl)methanimine (Br-BTiPh-Br) are shown below.

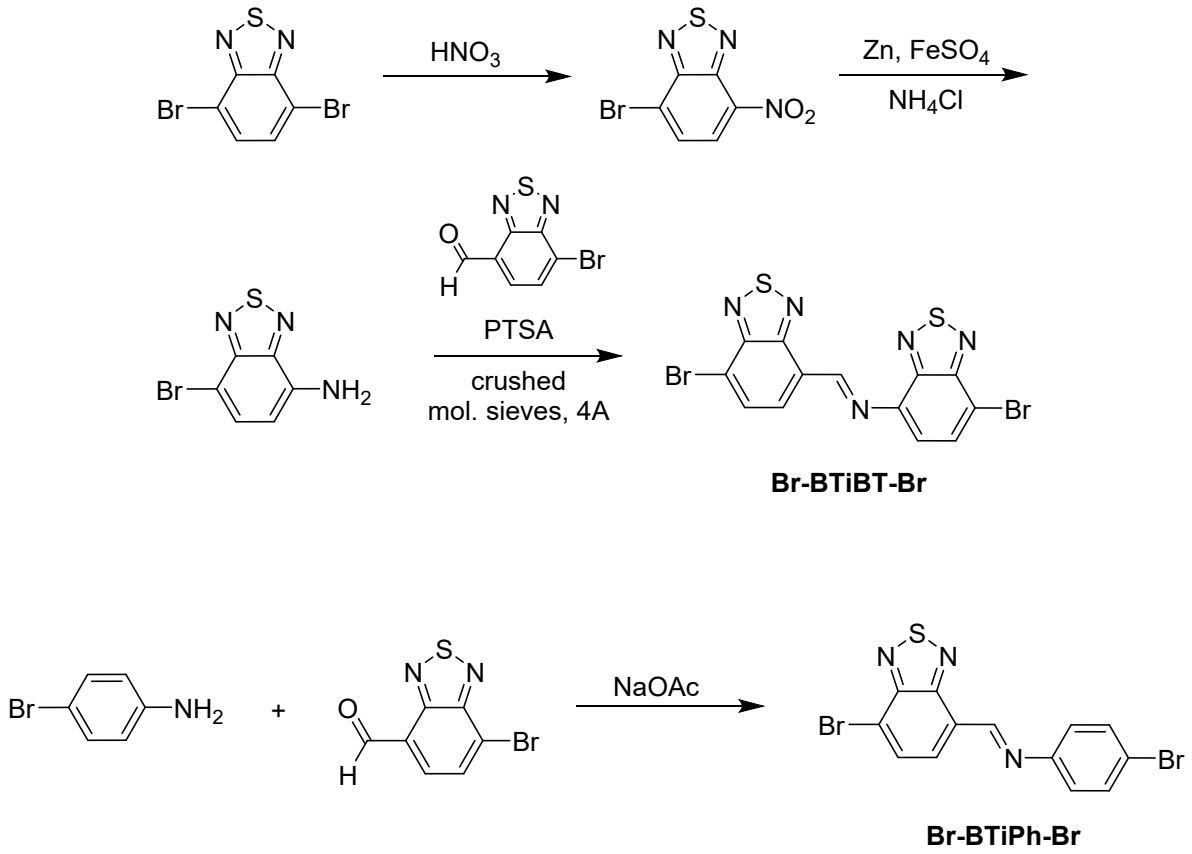

Figure S1. The preparation of Br-BTiBT-Br and Br-BTiPh-Br monomers.

Synthesis of 4-bromo-7-nitrobenzo[*c*][1,2,5]thiadiazole

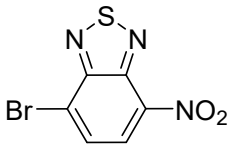

To a 250 mL round-bottom flask with stir bar, 4,7-dibromobenzo[*c*][1,2,5]thiadiazole (5.00 g, 17.0 mmol) and conc. nitric acid (80 mL) were added. The reaction was covered from light and refluxed for 5 h. The top joint of the condenser was connected by Teflon tubing to a flask containing 1 M NaOH for quenching of nitrogen oxide fumes. The reaction was cooled and then slowly poured into ice water (200 mL). The yellow precipitate that formed was filtered and washed well with H_2O. The crude precipitate was dissolved in DCM and washed with H_2O, sat. $NaHCO_3$, and brine. The organic layer was dried over Na_2SO_4 and dried *in vacuo*. The crude product was purified by silica column chromatography using 70% DCM in hexanes as the eluent. The final product was a pale-yellow solid. Yield: 2.20 g (50%).

^{1}H NMR: (500 MHz, $CDCl_3$) δ 8.47 (d, J = 8.1 Hz, 1H), 8.05 (d, J = 8.1 Hz, 1H).
^{13}C NMR: (126 MHz, $CDCl_3$) δ 154.79, 145.99, 139.14, 130.52, 127.85, 123.22.

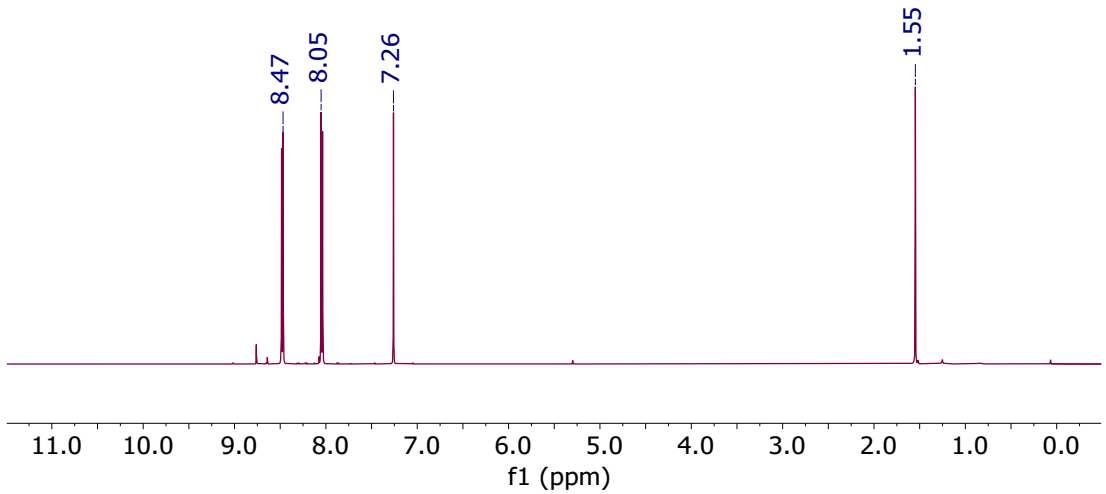

Figure S2. ^{1}H NMR spectra of 4-bromo-7-nitrobenzo[*c*][1,2,5]thiadiazole in $CDCl_3$.

Synthesis of 7-bromobenzo[*c*][1,2,5]thiadiazol-4-amine

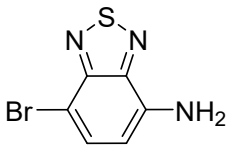

4-bromo-7-nitrobenzo[*c*][1,2,5]thiadiazole (1.90 g, 7.31 mmol, 1.0 equiv.) and EtOH (40 mL) were added to a 200 mL round-bottom flask with a stir bar. $FeSO_4 \cdot 7H_2O$ (6.09 g, 21.9 mmol, 3.0 equiv.), NH_4Cl (3.13 g, 58.4 mmol, 8.0 equiv.), and H_2O (7 mL) were added with efficient stirring. Then, Zn powder (1.43 g, 21.9 mmol, 3.0 equiv.) was added to the reaction mixture. The yellow suspension turned a brown-black color upon addition. The reaction mixture was heated at 55 °C for 3 h. After 3 h, the black mixture turned into an orange color. The reaction was cooled to room temperature and filtered over Celite. The precipitate on Celite was washed with EtOH (70 mL) and ethyl acetate (30 mL). The filtrate was concentrated *in vacuo* until a residue was formed. To the residue, ethyl acetate (80 mL) and 25% w/v NH_4Cl aqueous solution (20 mL) were added. The biphasic mixture was shaken and then washed with H_2O, sat. $NaHCO_3$, and brine. The organic layer was dried over Na_2SO_4 and dried *in vacuo*. The crude product was purified by silica column chromatography using 30% ethyl acetate in hexanes as the eluent. The final product was red-orange solid. Yield: 893 mg (53%)

^{1}H NMR: (500 MHz, $CDCl_3$) δ 7.57 (d, J = 7.7 Hz, 1H), 6.53 (d, J = 7.9 Hz, 1H), 4.71 (s, 2H).
^{13}C NMR: (126 MHz, $CDCl_3$) δ 153.67, 147.57, 138.68, 133.61, 107.43, 99.80.

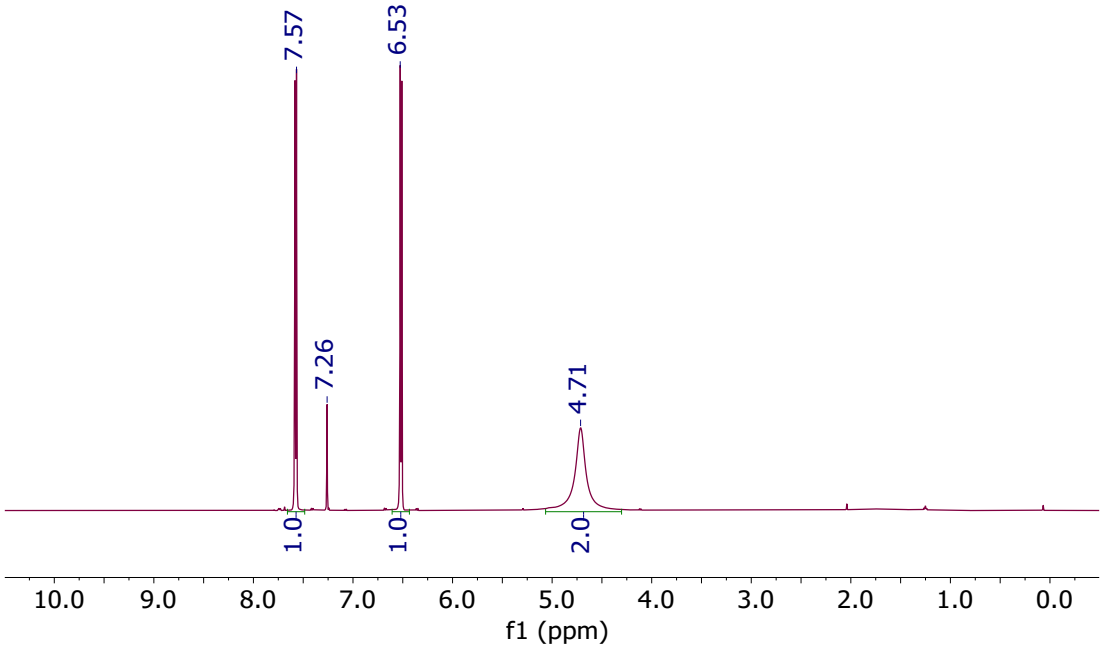

Figure S3. ^{1}H NMR spectra of 7-bromobenzo[*c*][1,2,5]thiadiazol-4-amine in $CDCl_3$.

Synthesis of *N*,1-bis(7-bromobenzo[*c*][1,2,5]thiadiazol-4-yl)methanimine (Br-BTiBT-Br)

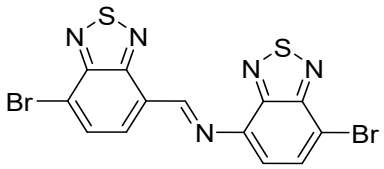

To an oven-dried 2-neck 50 mL round-bottom flask with a stir bar, 7-bromobenzo[*c*][1,2,5]thiadiazol-4-amine (400 mg, 1.74 mmol, 1.05 equiv.), 7-bromobenzo[*c*][1,2,5]thiadiazole-4-carbaldehyde (4.02 mg, 1.66 mmol, 1.0 equiv.), and PTSA monohydrate (15.7 mg, 82.8 µmol, 0.05 equiv.) were added. The flask was attached to a reflux condenser, and crushed molecular sieves were added. Anhydrous toluene (20 mL) was added, and the reaction was refluxed overnight (16 h). The reaction was cooled to room temperature, and the precipitate was filtered and washed with chloroform. To separate the product from the molecular sieves, the mixture was dissolved in hot chloroform and filtered through a frit. The filtrate was dried *in vacuo*, washed with minimal room temperature chloroform and filtered again. The precipitate was dried *in vacuo*. The final product was a yellow-orange solid. Yield: 392 mg (52%).

^{1}H NMR: (500 MHz, CD_2Cl_2) δ 9.97 (s, 1H), 8.46 (d, J = 7.7 Hz, 1H), 8.08 (d, J = 7.6 Hz, 1H), 7.93 (d, J = 7.7 Hz, 1H), 7.40 (d, J = 7.7 Hz, 1H).
^{13}C NMR: (126 MHz, CD_2Cl_2) δ 159.25, 154.18, 154.06, 150.23, 149.98, 142.97, 133.97, 133.02, 132.75, 132.30, 128.80, 122.00, 111.88.
Calculated ($M + H^+$): 455.83, measured (m/z): 455.85.

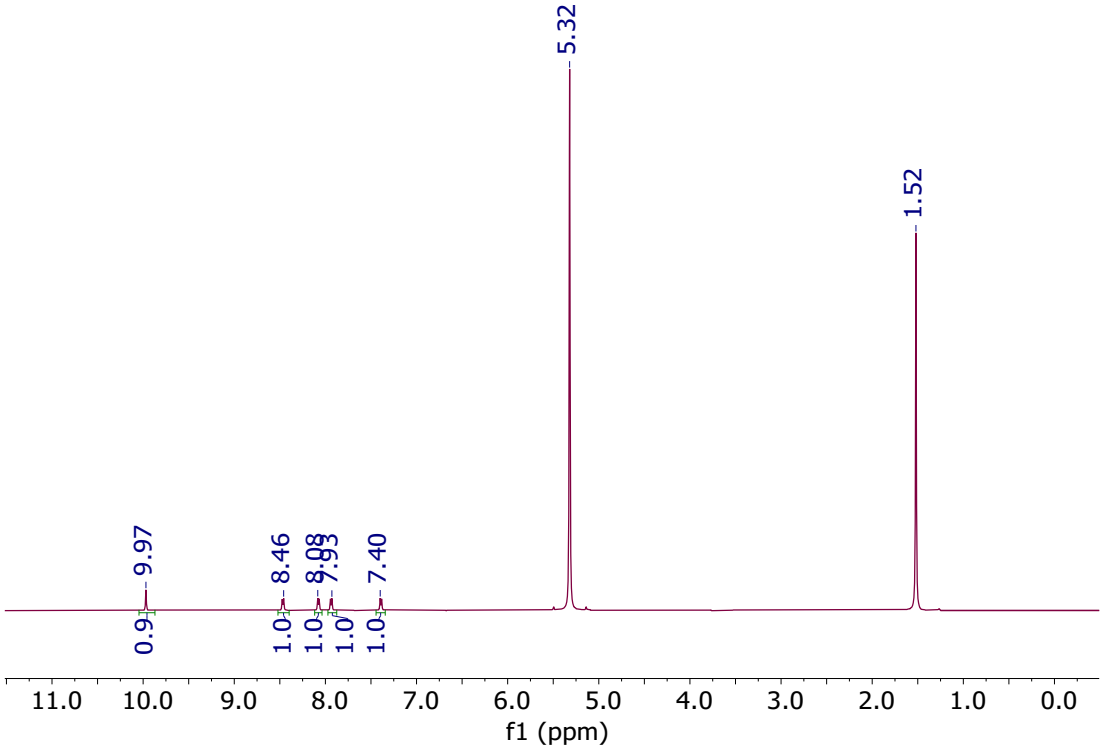

Figure S4. ^{1}H NMR spectra of Br-BTiBT-Br in CD_2Cl_2.

Synthesis of 1-(7-bromobenzo[*c*][1,2,5]thiadiazol-4-yl)-*N*-(4-bromophenyl)methanimine (Br-BTiPh-Br)

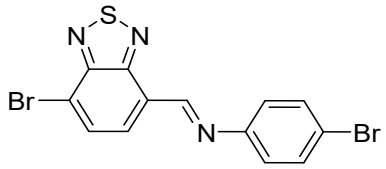

To a 50 mL round-bottom flask with stir bar, 7-bromobenzo[*c*][1,2,5]thiadiazole-4-carbaldehyde (300 mg, 1.23 mmol, 1.0 equiv.) and EtOH (200 proof, 15 mL) were added. Then, 4-bromoaniline (212 mg, 1.23 mmol, 1.0 equiv.) and sodium acetate (111 mg, 1.36 mmol, 1.1 equiv.) were added to the flask. The reaction was heated at 70 °C overnight (16 h). The reaction mixture was dried *in vacuo*. The crude product was extracted into chloroform, washed with H_2O, and dried over Na_2SO_4 and *in vacuo*. Then, the crude product was dissolved in minimal 1:1 chloroform:EtOH (200 proof) and heated until fully dissolved. The solution was left to cool to room temperature and slowly evaporate. After 3 h, precipitates of the starting material formed. The precipitate was filtered off, and the filtrate was dried *in vacuo*. The final product was yellow-orange solid. Yield: 400 mg (82%)

^{1}H NMR: (500 MHz, CD_2Cl_2) δ 9.29 (s, 1H), 8.31 (d, J = 7.6 Hz, 1H), 8.03 (d, J = 7.7 Hz, 1H), 7.56 (d, J = 8.4 Hz, 2H), 7.25 (d, J = 8.4 Hz, 2H).
^{13}C NMR: (126 MHz, CD_2Cl_2) δ 155.63, 154.09, 153.98, 150.96, 132.74, 132.68, 128.14, 123.31, 120.51, 117.87.
Calculated ($M + H^+$): 397.87, measured (m/z): 397.83.

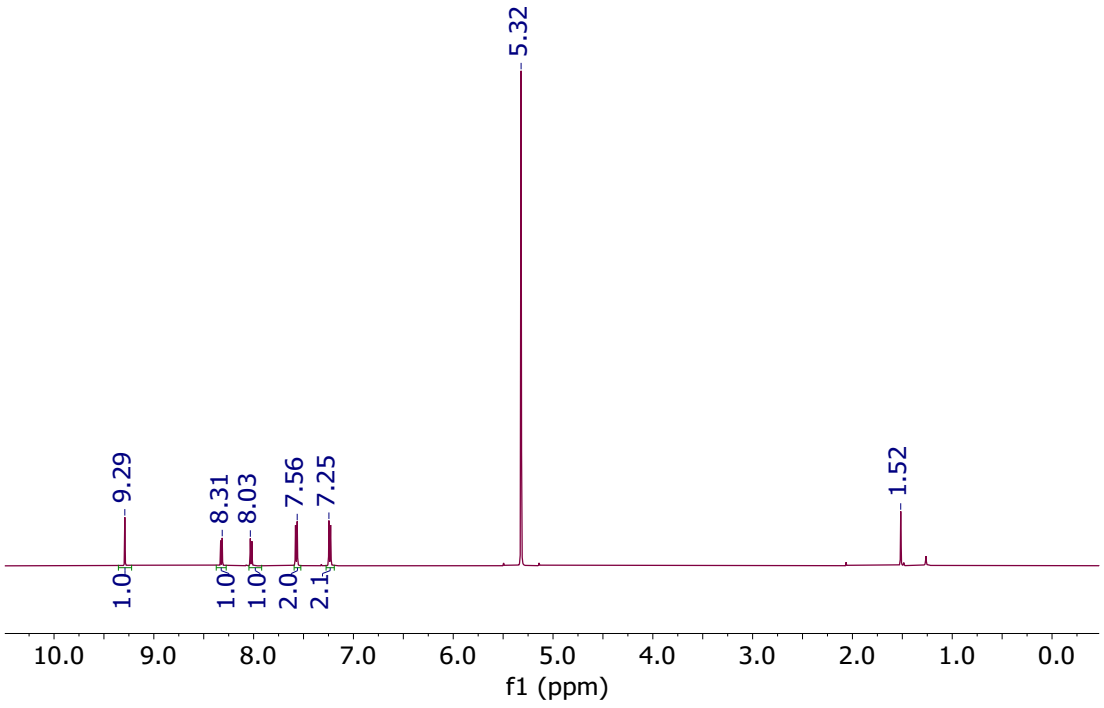

Figure S5. ^{1}H NMR spectra of Br-BTiPh-Br in CD_2Cl_2.

Synthesis of pIDT-BTiBT and pIDT-BTiPh semiconducting polymers

The IDT-based polymers were prepared using a similar procedure with XPhos Pd G3 as the catalyst.[4] Below, the preparations of pIDT-BTiBT and pIDT-BTiPh are detailed. pIDT-10BTiPh was prepared using the same procedure as for pIDT-BTiBT but with 0.91 equiv. of Br-BTiBT-Br and 0.1 equiv. of Br-BTiPh-Br.

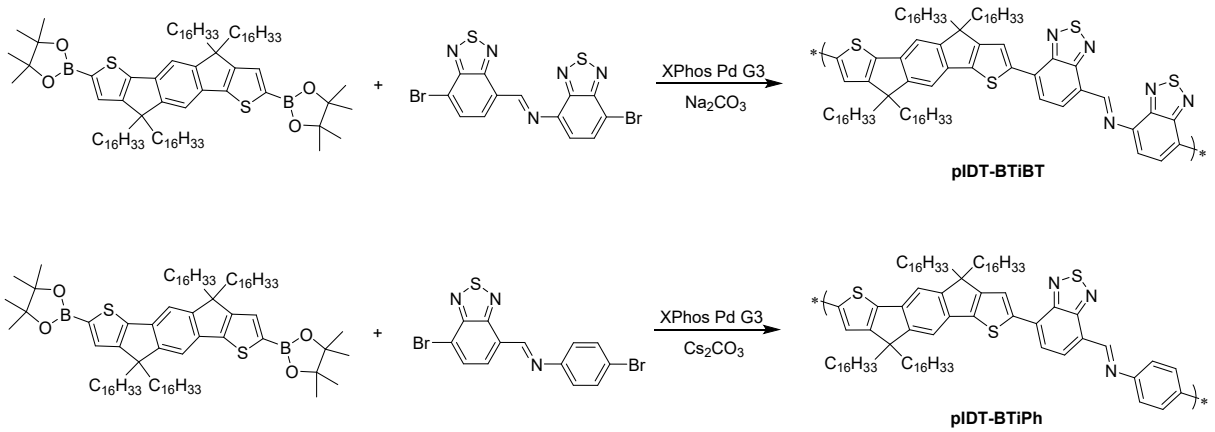

pIDT-BTiBT:

To a 10 mL round-bottom flask, anhydrous toluene (5 mL) and 1 drop of Aliquat 336 were added. To a 5 mL round-bottom flask, 2 M aqueous Na_2CO_3 solution (1 mL) was made. Both solutions were degassed for 1 h. To a microwave reaction vessel with stir bar, 2,2'-(4,4,9,9-tetrahexadecyl-4,9-dihydro-*s*-indaceno[1,2-*b*:5,6-*b*′]dithiophene-2,7-diyl)bis(4,4,5,5-tetramethyl-1,3,2-dioxaborolane) (75.0 mg, 53.0 µmol, 1.0 equiv.), Br-BTiBT-Br (25.3 mg, 55.6 µmol, 1.05 equiv.), and XPhos Pd G3 (0.897 mg, 1.06 µmol, 0.02 equiv.) were added. The vial was sealed with a cap with septum in a N_2-filled glovebox. Then, the toluene solution (0.55 mL) was added, and the reaction was stirred until all solids dissolved. 2 M Na_2CO_3 solution (0.11 mL) was added to make a 5:1 v/v toluene:H_2O ratio. The reaction was degassed for 10 min. Then, the reaction was heated at 50 °C for 4 d. The reaction mixture was precipitated in methanol. The dark blue solid was collected and purified via Soxhlet extraction in methanol and acetone. The polymer was collected with chloroform and precipitated in cold methanol to yield a dark blue solid. Yield: 60 mg (76%)

pIDT-BTiPh:

To a 10 mL round-bottom flask, anhydrous toluene (5 mL) and 1 drop of Aliquat 336 were added. To a 5 mL round-bottom flask, 2 M aqueous Cs_2CO_3 solution (1 mL) was made. Both solutions were degassed for 1 h. To a microwave reaction vessel with stir bar, 2,2'-(4,4,9,9-tetrahexadecyl-4,9-dihydro-*s*-indaceno[1,2-*b*:5,6-*b*′]dithiophene-2,7-diyl)bis(4,4,5,5-tetramethyl-1,3,2-dioxaborolane) (75.0 mg, 53.0 µmol, 1.0 equiv.), Br-BTiPh-Br (21.0 mg, 53.0 µmol, 1.0 equiv.), and XPhos Pd G3 (0.897 mg, 1.06 µmol, 0.02 equiv.) were added. The vial was sealed with a cap with septum in a N_2-filled glovebox. Then, the toluene solution (0.55 mL) was added, and the reaction was stirred until all solids dissolved. 2 M Cs_2CO_3 solution (0.11 mL) was added to make a 5:1 v/v toluene:H_2O ratio. The reaction was degassed for 10 min. Then, the reaction was heated at 80 °C for 3 d. The reaction mixture was precipitated in methanol. The dark blue solid was

collected and purified via Soxhlet extraction in methanol and acetone. The polymer was collected with chloroform and precipitated in cold methanol to yield a dark blue solid. Yield: 68 mg (90%)

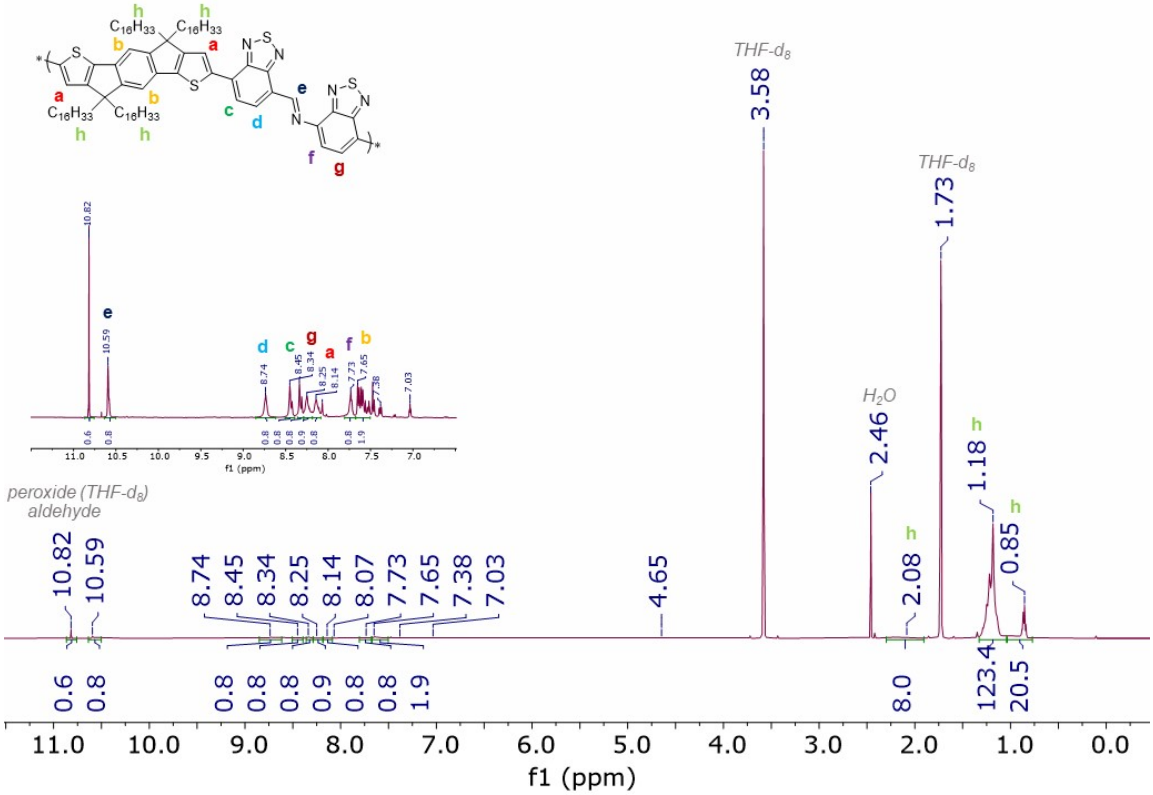

Figure S6. ^{1}H NMR spectra of pIDT-BTiBT in THF-d_8.

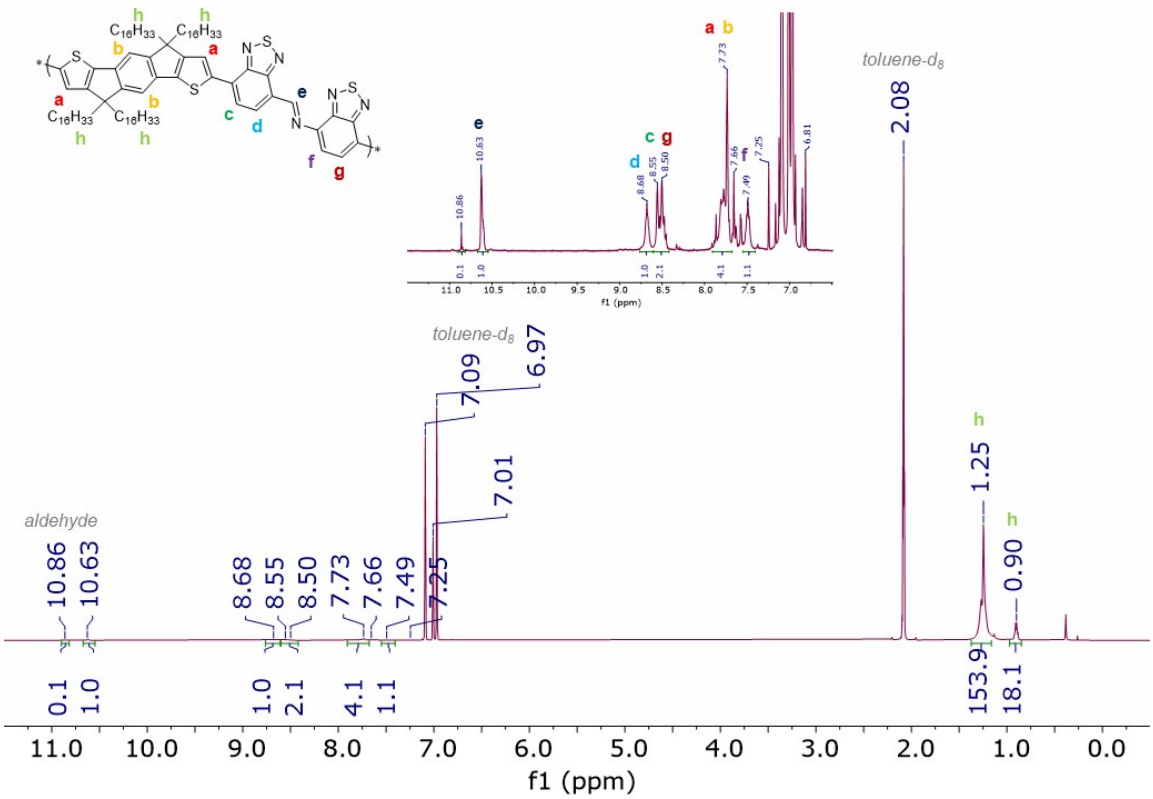

Figure S7. ^{1}H NMR spectra of pIDT-BTiBT in toluene-d_8.

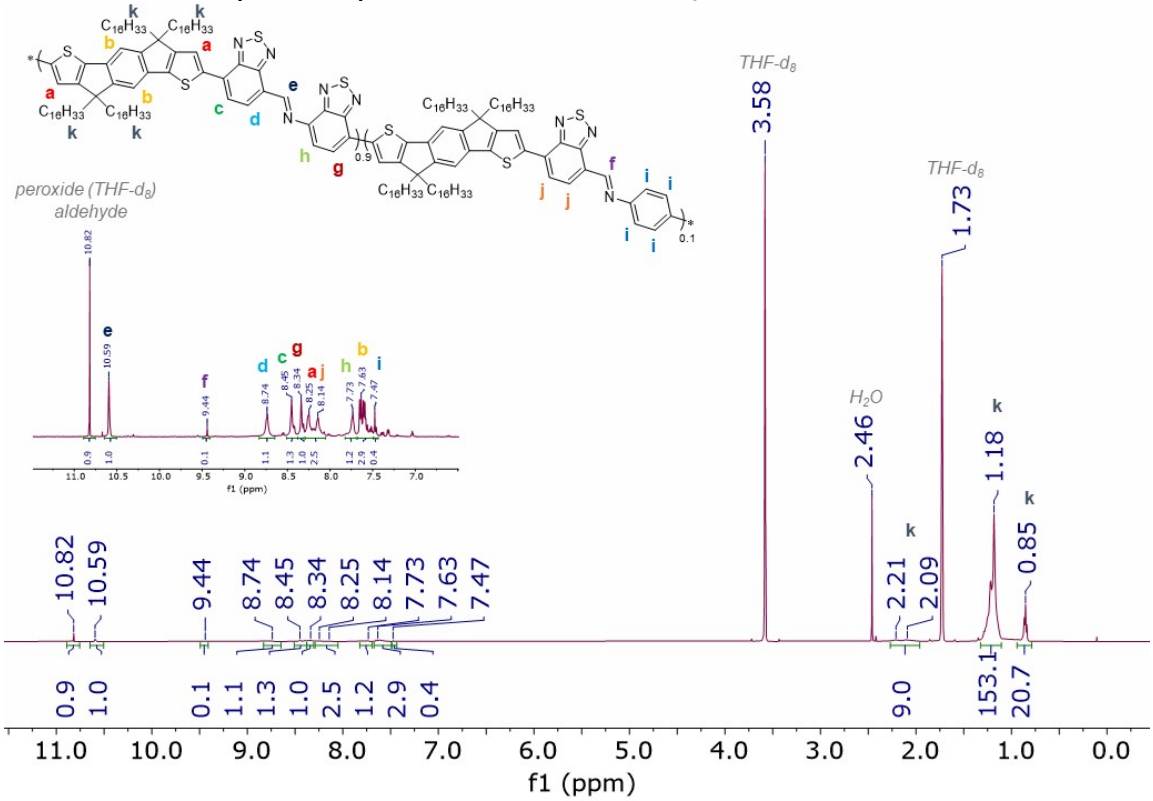

Figure S8. ^{1}H NMR spectra of pIDT-10BTiPh in THF-d_8.

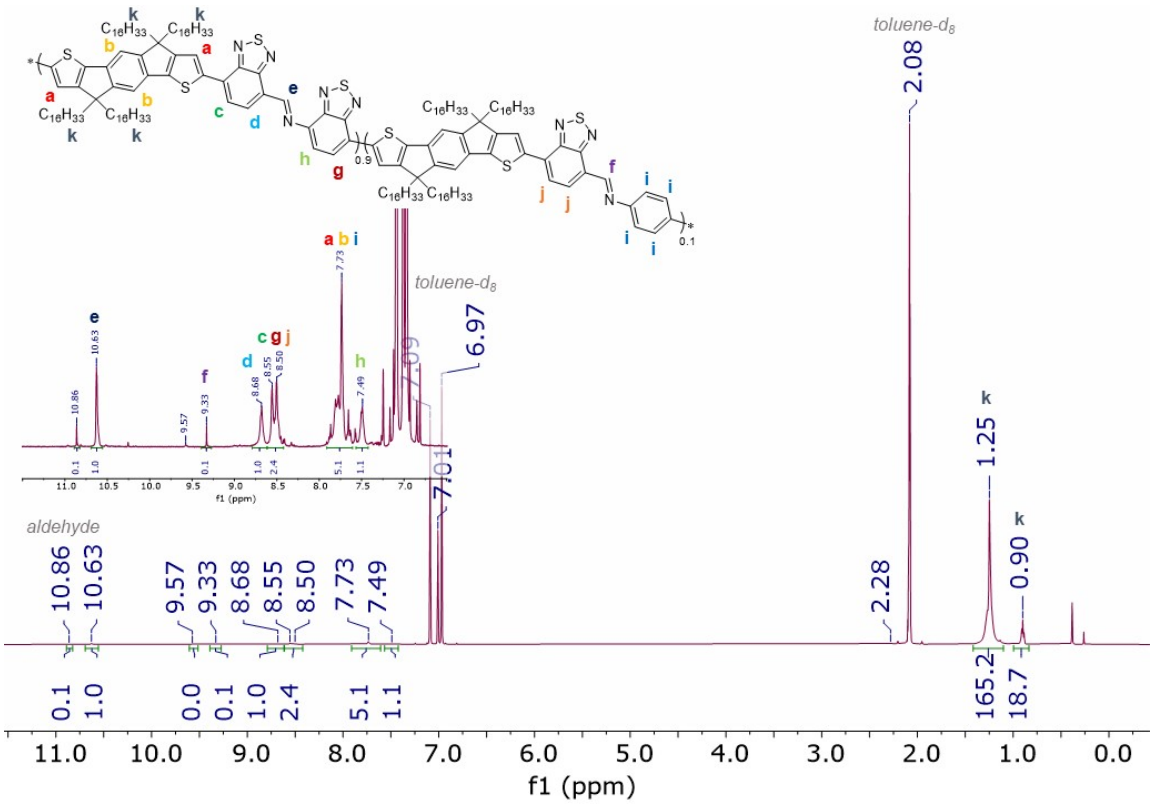

Figure S9. ^{1}H NMR spectra of pIDT-10BTiPh in toluene-d_8.

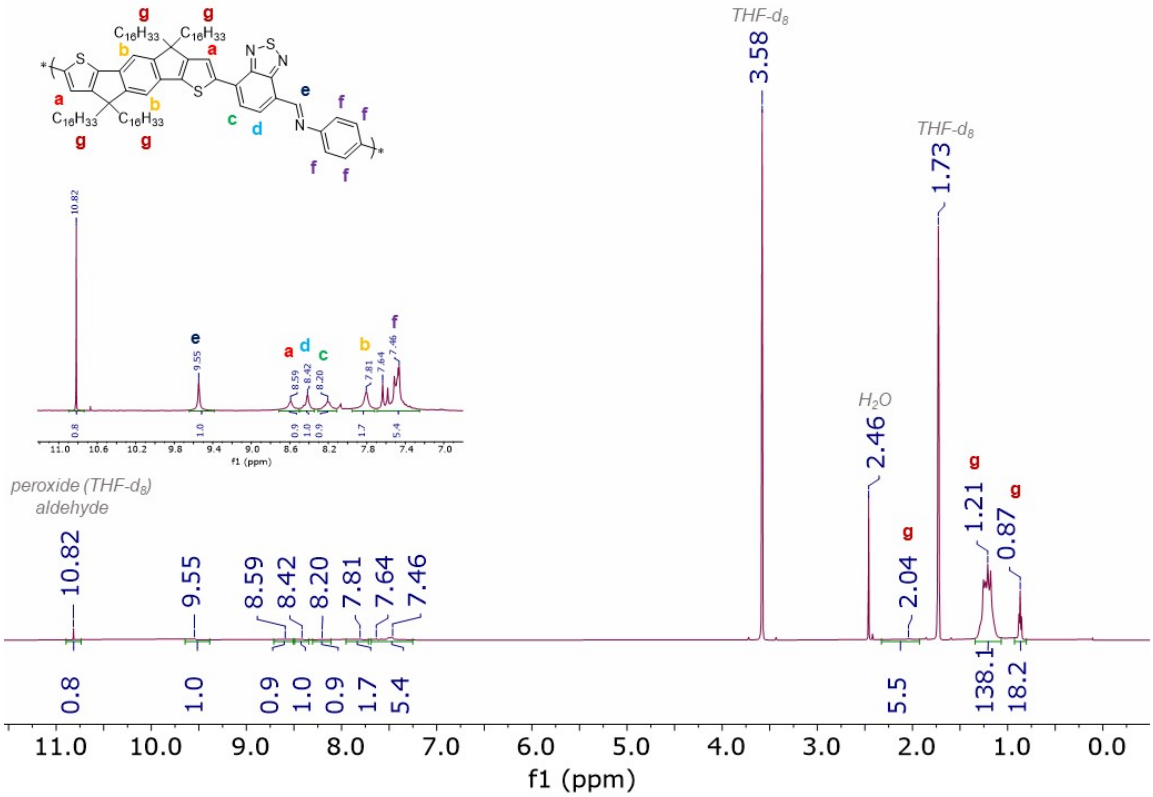

Figure S10. ^{1}H NMR spectra of pIDT-BTiPh in THF-d_8.

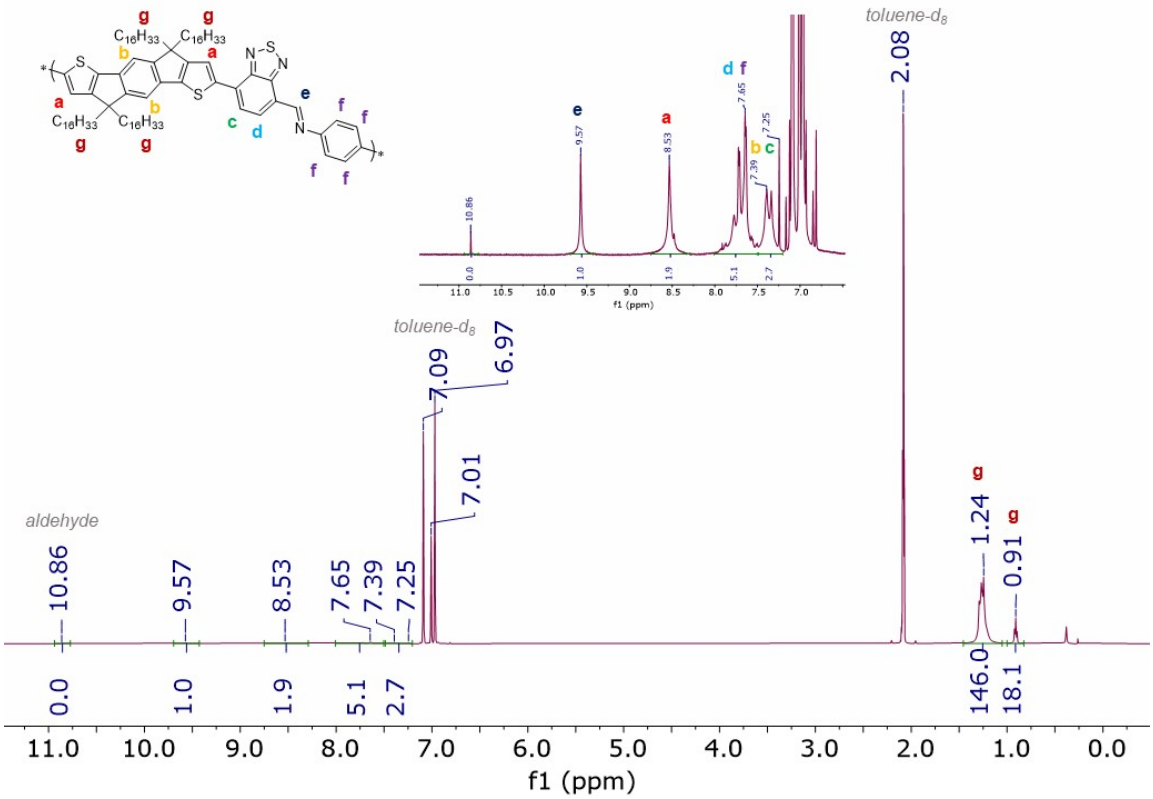

Figure S11. ^{1}H NMR spectra of pIDT-BTiPh in toluene-d_8.

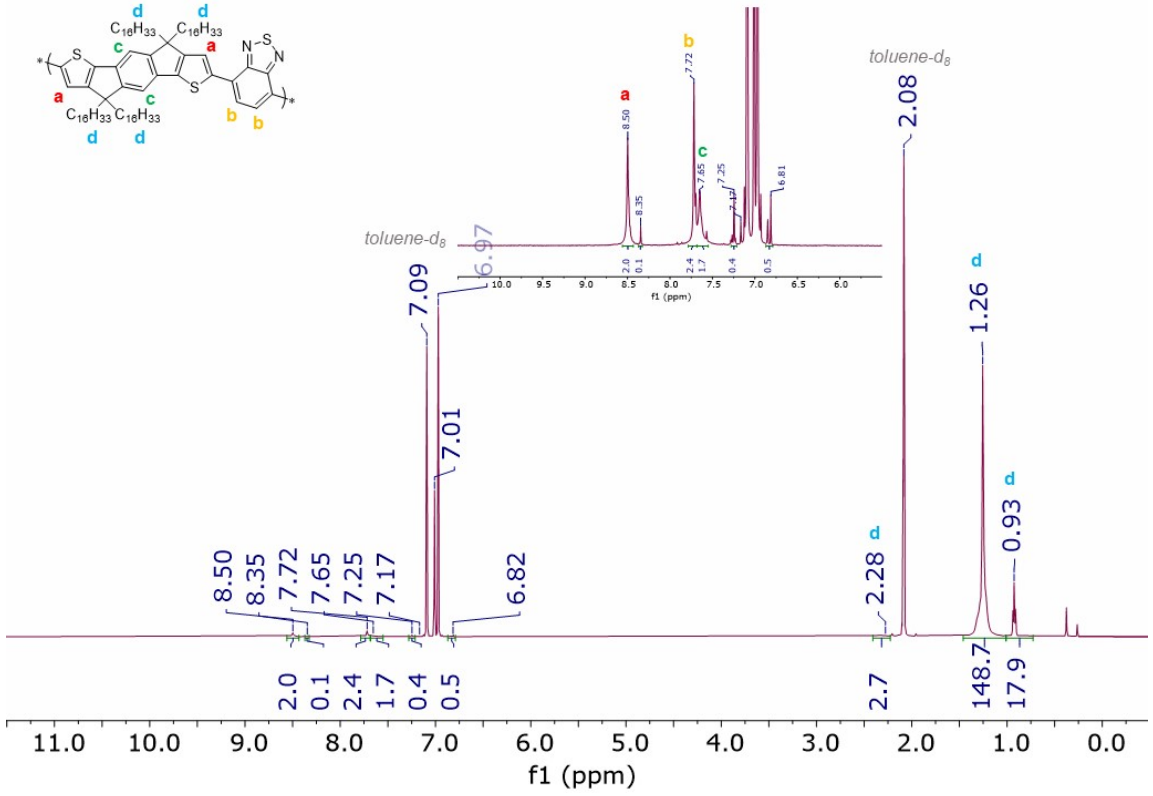

Figure S12. ^{1}H NMR spectra of pIDT-BT in toluene-d_8.

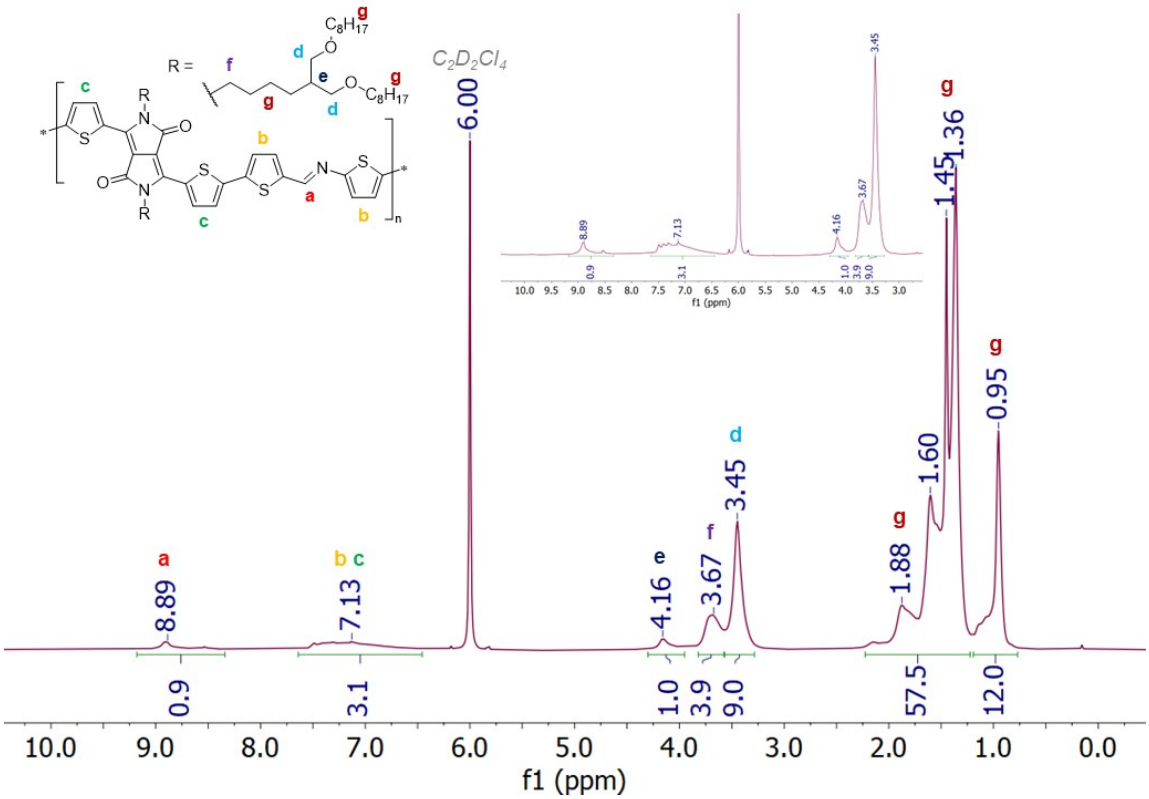

Figure S13. ^{1}H NMR spectra of pDPP(C4E)-TIT in $C_2D_2Cl_4$ at 393 K.

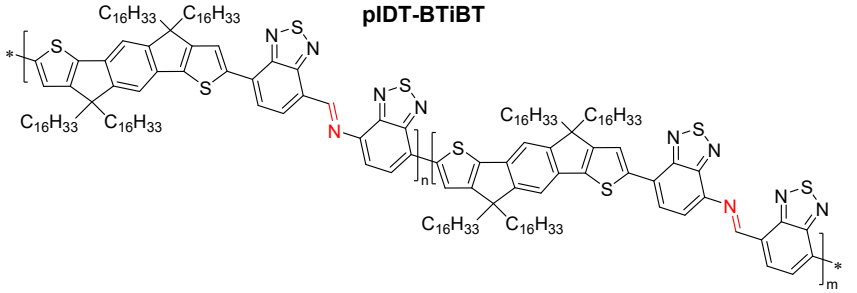

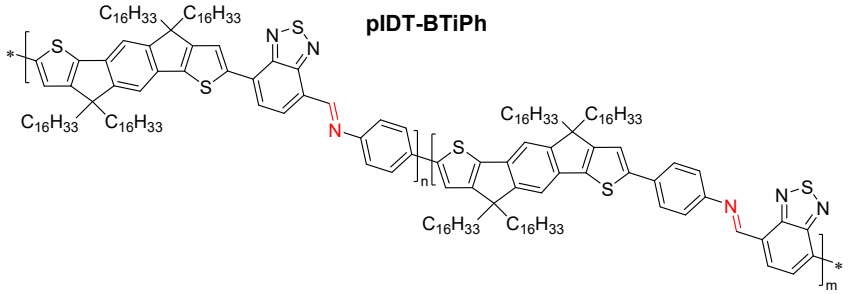

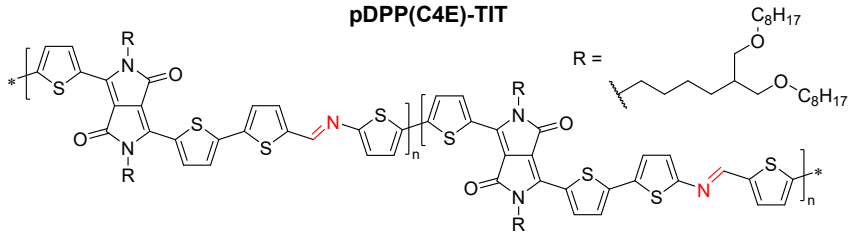

Figure S14. Chemical structures displaying regiorandom incorporation of imine co-monomers for all degradable, imine-based polymers.

Synthesis of 7,7'-(4,4,9,9-tetrahexadecyl-4,9-dihydro-*s*-indaceno[1,2-*b*:5,6-*b*′]dithiophene-2,7-diyl)bis(benzo[*c*][1,2,5]thiadiazole-4-carbaldehyde)

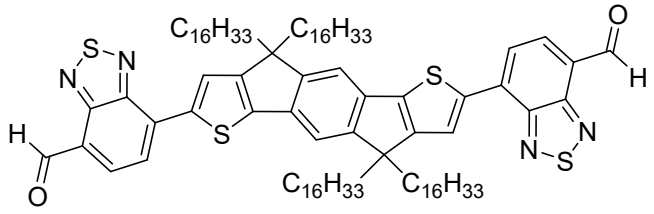

To a 10 mL round-bottom flask, anhydrous toluene (5 mL) and 1 drop of Aliquat 336 were added. To a 5 mL round-bottom flask, 2 M aqueous Na_2CO_3 solution (1 mL) was made. Both solutions were degassed for 1 h. To a microwave reaction vessel with stir bar, 2,2'-(4,4,9,9-tetrahexadecyl-4,9-dihydro-*s*-indaceno[1,2-*b*:5,6-*b*′]dithiophene-2,7-diyl)bis(4,4,5,5-tetramethyl-1,3,2-dioxaborolane) (75.0 mg, 53.0 μmol, 1.0 equiv.), 7-bromobenzo[*c*][1,2,5]thiadiazole-4-carbaldehyde (36.0 mg, 148 μmol, 2.8 equiv.), and XPhos Pd G3 (2.24 mg, 2.65 μmol, 0.05 equiv.) were added. The vial was sealed with a cap with septum in a N_2-filled glovebox. Then, the toluene solution (1.50 mL) was added, and the reaction was stirred until all solids dissolved. 2 M Na_2CO_3 solution (0.30 mL) was added to make a 5:1 v/v toluene:H_2O ratio. The reaction was degassed for 10 min. Then, the reaction was heated at 80 °C overnight (16 h). The reaction mixture was extracted into chloroform and washed with H_2O. The organic layer was dried over Na_2SO_4 and dried *in vacuo*. The crude product was purified by silica column chromatography using 70% DCM in hexanes as the eluent. The final product was a dark blue solid. Yield: 59 mg (75%).

^{1}H NMR: (500 MHz, CD_2Cl_2) δ 10.73 (s, 2H), 8.28 (s, 2H), 8.24 (d, J = 7.6 Hz, 2H), 8.06 (d, J = 7.6 Hz, 2H), 7.45 (s, 1H), 2.17 – 2.07 (m, 4H), 2.02 – 1.91 (m, 4H), 1.23 – 1.05 (m, 106H), 0.90 – 0.83 (m, 18H).
^{13}C NMR: (126 MHz, CD_2Cl_2) δ 188.55, 157.17, 154.44, 154.14, 152.39, 147.14, 140.81, 136.57, 134.26, 133.01, 125.01, 124.99, 122.90, 114.24, 77.36, 54.57, 39.25, 32.05, 30.08, 29.82, 29.78, 29.71, 29.48, 29.45, 24.38, 22.82, 14.25.
Calculated (M): 1488.00, measured (m/z, MALDI-TOF): 1488.23.

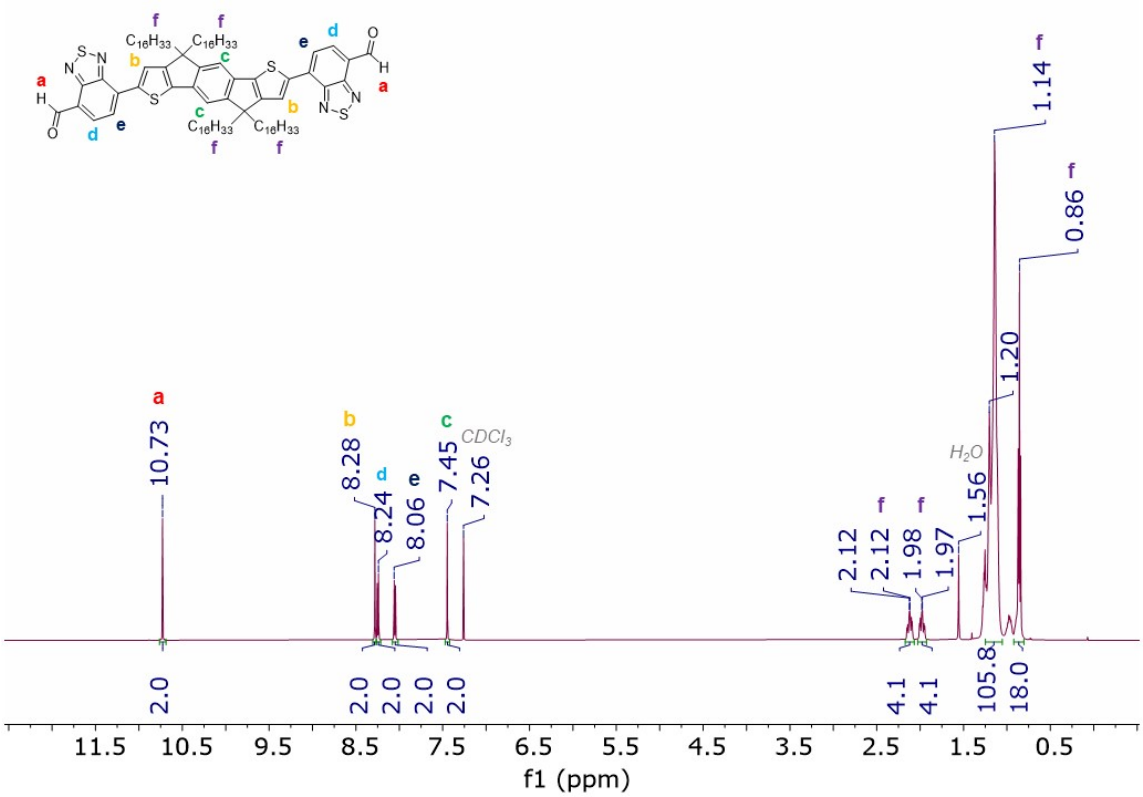

Figure S15. ^{1}H NMR spectra of 7,7'-(4,4,9,9-tetrahexadecyl-4,9-dihydro-*s*-indaceno[1,2-*b*:5,6-*b'*]dithiophene-2,7-diyl)bis(benzo[*c*][1,2,5]thiadiazole-4-carbaldehyde) in $CDCl_3$.

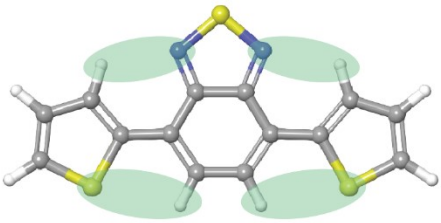

Figure S16. Preferred "cis" orientation of BT unit with thiophenes of IDT units due to stabilizing non-covalent interactions (green).[2]

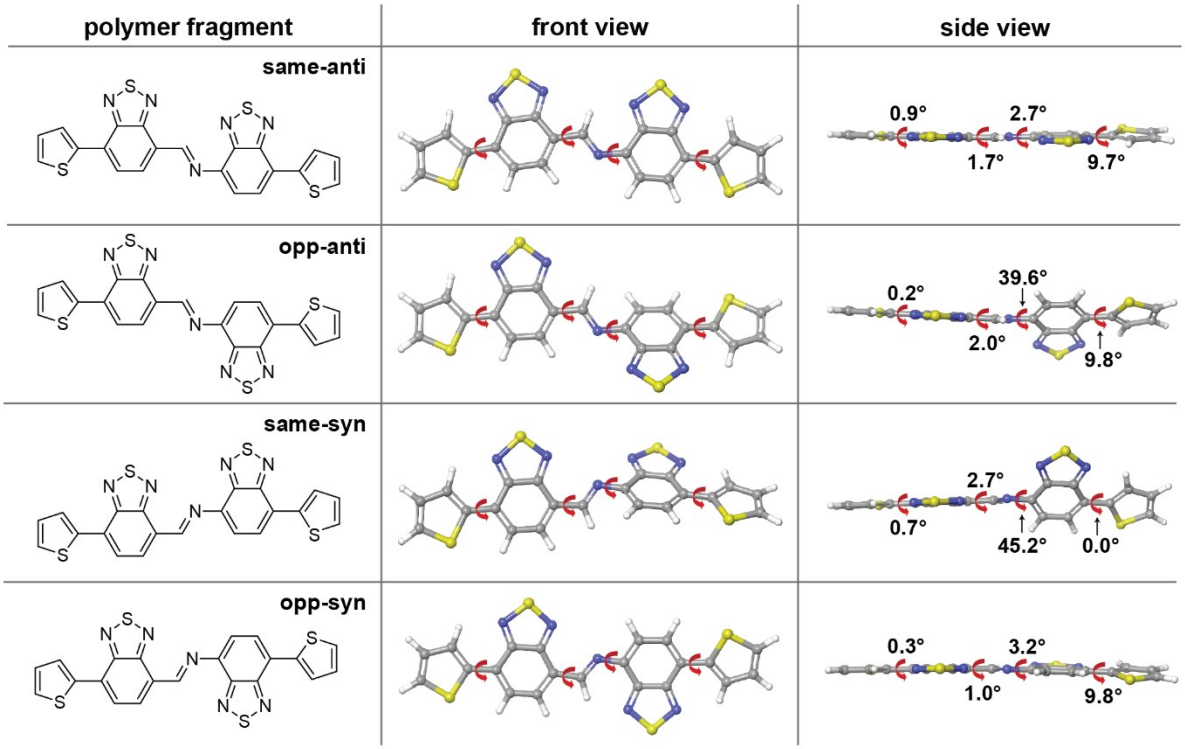

Figure S17. Chemical structures and corresponding DFT-optimized geometries for T-BTiBT-T polymer fragments. The conformers are labeled "same" for the BT units being on the same side and "opp" for being on opposite sides. They are also labeled "anti" for the imine nitrogen pointing away from the neighboring BT unit and "syn" for pointing toward the BT unit. Dihedral angles are marked by red arrows in both the front and side view. The unit preferred to be oriented with the imine hydrogen pointed toward the nitrogen on the neighboring BT unit likely due to potential hydrogen bonding interactions. Additionally, the BT units were energetically favored to be on the same side when in this configuration as there were less steric effects between the imine hydrogen and BT hydrogen, resulting in a more planar geometry for BTiBT.

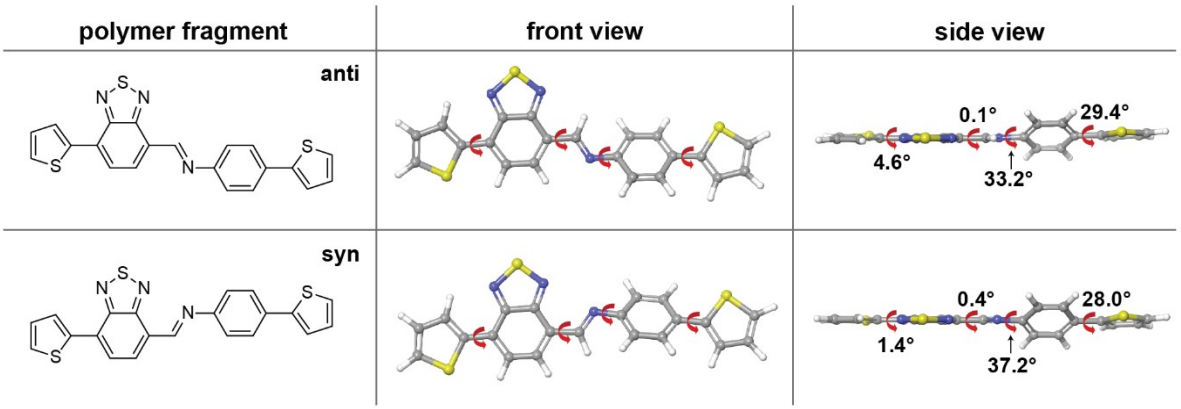

Figure S18. Chemical structures and corresponding DFT-optimized geometries for T-BTiPh-T polymer fragments. The conformers are labeled "anti" for the imine nitrogen pointing away from the neighboring BT unit and "syn" for pointing toward the BT unit. Dihedral angles are marked by red arrows in both the front and side view. BTiPh also preferred to be oriented with the imine hydrogen interacting with the BT nitrogen, agreeing with the results for BTiBT.

Table S1. Calculated Optimized Geometry Energies and Boltzmann Probabilities

polymer fragment	conformer	ΔG_{298K} (kcal/mol)	probability[a]
T-BTiBT	same-anti	0	94.47%
	opp-anti	1.75	4.96%
	same-syn	5.67	0.01%
	opp-syn	3.03	0.57%
T-BTiPh-T	anti	0	99.74%
	syn	3.53	0.26%

[a]Probabilities were calculated by the Boltzmann distribution equation $\frac{p_i}{p_{sum}} = \frac{e^{-\frac{\Delta G}{kT}}}{\Sigma e^{-\frac{\Delta G}{kT}}}$ where T = 298.15 K and k is the Boltzmann constant.

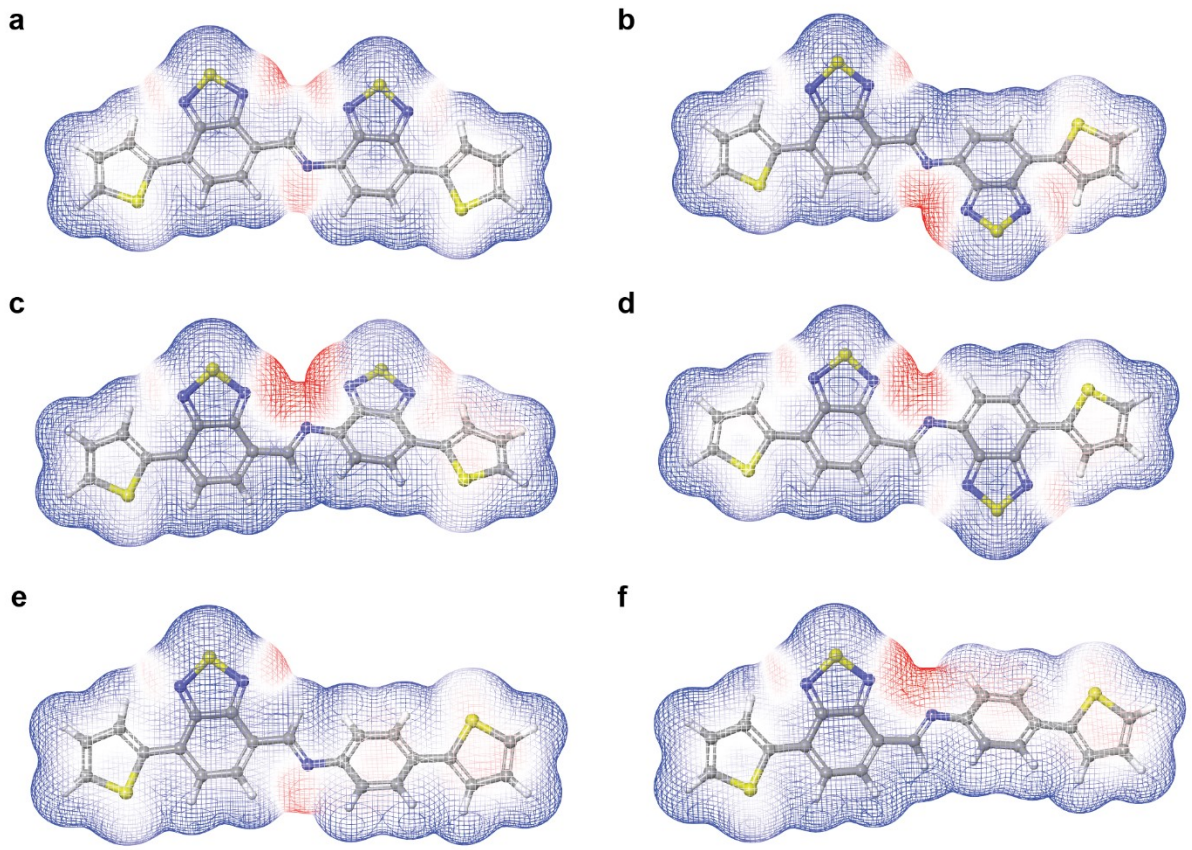

Figure S19. Electrostatic potential surfaces of T-BTiBT-T in the (a) same-anti, (b) opp-anti, (c) same-syn, (d) opp-syn conformations as well as T-BTiPh-T in the (e) anti and (f) syn conformations. Color scale from -30.0 to 10.0 kcal/mol with red indicating electronegative potential and blue indicating electropositive potential. The most favored conformations have electron density that is spread out over the entire molecule.

DFT-Optimized Model for T-BT-T

Total energy: -1842.2390 hartrees
Cartesian coordinates (from left to right: atom, x, y, z in Å):

S1	0.0000000000	3.8021000000	1.9130000000	C15	0.0000000000	-2.9395000000	0.3730000000
C2	0.0000000000	2.9395000000	0.3730000000	S16	0.0000000000	-3.8021000000	1.9130000000
C3	0.0000000000	3.8456000000	-0.6685000000	C17	0.0000000000	-5.3392000000	1.1155000000
C4	0.0000000000	5.2030000000	-0.2453000000	C18	0.0000000000	-5.2030000000	-0.2453000000
C5	0.0000000000	5.3392000000	1.1155000000	C19	0.0000000000	-3.8456000000	-0.6685000000
C6	0.0000000000	1.4815000000	0.3351000000	H20	0.0000000000	3.5306000000	-1.7020000000
C7	0.0000000000	0.7057000000	1.4837000000	H21	0.0000000000	6.0445000000	-0.9282000000
C8	0.0000000000	-0.7057000000	1.4837000000	H22	0.0000000000	6.2490000000	1.6999000000
C9	0.0000000000	-1.4815000000	0.3351000000	H23	0.0000000000	1.1949000000	2.4527000000
C10	0.0000000000	-0.7307000000	-0.8957000000	H24	0.0000000000	-1.1949000000	2.4527000000
C11	0.0000000000	0.7307000000	-0.8957000000	H25	0.0000000000	-6.2490000000	1.6999000000
N12	0.0000000000	1.2536000000	-2.1264000000	H26	0.0000000000	-6.0445000000	-0.9282000000
S13	0.0000000000	0.0000000000	-3.1838000000	H27	0.0000000000	-3.5306000000	-1.7020000000
N14	0.0000000000	-1.2536000000	-2.1264000000				

DFT-Optimized Model for T-BTiBT-T (same-anti conformer)

Total energy: -2673.1488 hartrees
Cartesian coordinates (from left to right: atom, x, y, z in Å):

C1	0.6164000000	6.1516000000	-0.0254000000	N23	-2.4286000000	2.3593000000	0.3962000000
C2	0.3672000000	4.7175000000	-0.0120000000	S24	-3.2870000000	3.7499000000	0.5523000000
C3	1.3832000000	3.7829000000	-0.1897000000	N25	-2.0805000000	4.8491000000	0.3774000000
C4	1.1804000000	2.3872000000	-0.1781000000	C26	-0.9495000000	4.1603000000	0.1879000000
C5	-0.0634000000	1.8089000000	0.0141000000	C27	-0.2698000000	7.1958000000	0.1522000000
C6	-0.2731000000	0.3653000000	0.0375000000	C28	0.3366000000	8.4785000000	0.0781000000
N7	0.7415000000	-0.4258000000	-0.0945000000	C29	1.6834000000	8.4197000000	-0.1559000000
C8	0.6615000000	-1.8074000000	-0.0817000000	S30	2.2417000000	6.7875000000	-0.2925000000
C9	1.8618000000	-2.4946000000	-0.1830000000	H31	2.3985000000	4.1341000000	-0.3449000000
C10	1.9651000000	-3.9019000000	-0.1831000000	H32	2.0264000000	1.7239000000	-0.3219000000
C11	0.8745000000	-4.7539000000	-0.0802000000	H33	-1.2978000000	0.0180000000	0.1733000000
C12	1.0137000000	-6.2054000000	-0.0713000000	H34	2.7628000000	-1.8961000000	-0.2656000000
C13	0.0418000000	-7.1827000000	-0.1552000000	H35	2.9598000000	-4.3267000000	-0.2771000000
C14	0.5594000000	-8.5064000000	-0.1326000000	H36	-1.0090000000	-6.9414000000	-0.2314000000
C15	1.9223000000	-8.5460000000	-0.0259000000				
S16	2.6057000000	-6.9575000000	0.0558000000	H37	-0.0590000000	-9.3943000000	-0.1939000000
C17	-0.4067000000	-4.0958000000	0.0196000000				
N18	-1.5906000000	-4.7070000000	0.1216000000	H38	2.5677000000	-9.4127000000	0.0146000000
S19	-2.7374000000	-3.5372000000	0.2040000000	H39	-1.3224000000	7.0282000000	0.3302000000
N20	-1.7767000000	-2.2053000000	0.1207000000	H40	-0.2083000000	9.4078000000	0.1947000000
C21	-0.5167000000	-2.6388000000	0.0210000000	H41	2.3831000000	9.2379000000	-0.2569000000
C22	-1.1554000000	2.7179000000	0.1987000000				

DFT-Optimized Model for T-BTiPh-T (anti conformer)

Total energy: -2166.6664 hartrees
Cartesian coordinates (from left to right: atom, x, y, z in Å):

H1	-0.0700000000	-1.5395000000	1.1158000000
C2	-0.6680000000	-0.8132000000	0.5758000000
C3	-0.0042000000	0.1801000000	-0.1207000000
C4	1.4508000000	0.2858000000	-0.1568000000
N5	2.1937000000	-0.5539000000	0.4710000000
C6	3.5880000000	-0.4790000000	0.3817000000
C7	4.3303000000	-0.9041000000	1.4971000000
C8	5.7156000000	-0.8552000000	1.4890000000
C9	6.4212000000	-0.4258000000	0.3479000000
C10	7.8862000000	-0.4230000000	0.3482000000
C11	8.7369000000	-1.2267000000	1.0734000000
C12	10.1156000000	-0.9588000000	0.8419000000
C13	10.3158000000	0.0492000000	-0.0603000000
S14	8.8133000000	0.6971000000	-0.6363000000
C15	5.6747000000	-0.0350000000	-0.7779000000
C16	4.2863000000	-0.0542000000	-0.7636000000
C17	-0.8275000000	1.1196000000	-0.8196000000
N18	-0.3750000000	2.1460000000	-1.5488000000
S19	-1.6974000000	2.9142000000	-2.1457000000
N20	-2.8828000000	1.9795000000	-1.5003000000
C21	-2.2798000000	1.0196000000	-0.7893000000
C22	-2.9310000000	-0.0346000000	-0.0485000000
C23	-4.3801000000	-0.1748000000	0.0037000000
C24	-5.3584000000	0.6477000000	-0.5200000000
C25	-6.6810000000	0.1945000000	-0.2676000000
C26	-6.7182000000	-0.9729000000	0.4452000000
S27	-5.1302000000	-1.5461000000	0.8239000000
C28	-2.0754000000	-0.9110000000	0.6108000000
H29	1.8557000000	1.1223000000	-0.7384000000
H30	3.7907000000	-1.2437000000	2.3754000000
H31	6.2651000000	-1.1400000000	2.3806000000
H32	8.3800000000	-2.0108000000	1.7310000000
H33	10.9235000000	-1.5010000000	1.3196000000
H34	11.2528000000	0.4518000000	-0.4190000000
H35	6.1908000000	0.2582000000	-1.6876000000
H36	3.7370000000	0.2192000000	-1.6591000000
H37	-5.1168000000	1.5467000000	-1.0683000000
H38	-7.5690000000	0.7164000000	-0.6041000000
H39	-7.5841000000	-1.5333000000	0.7696000000
H40	-2.5012000000	-1.7225000000	1.1929000000

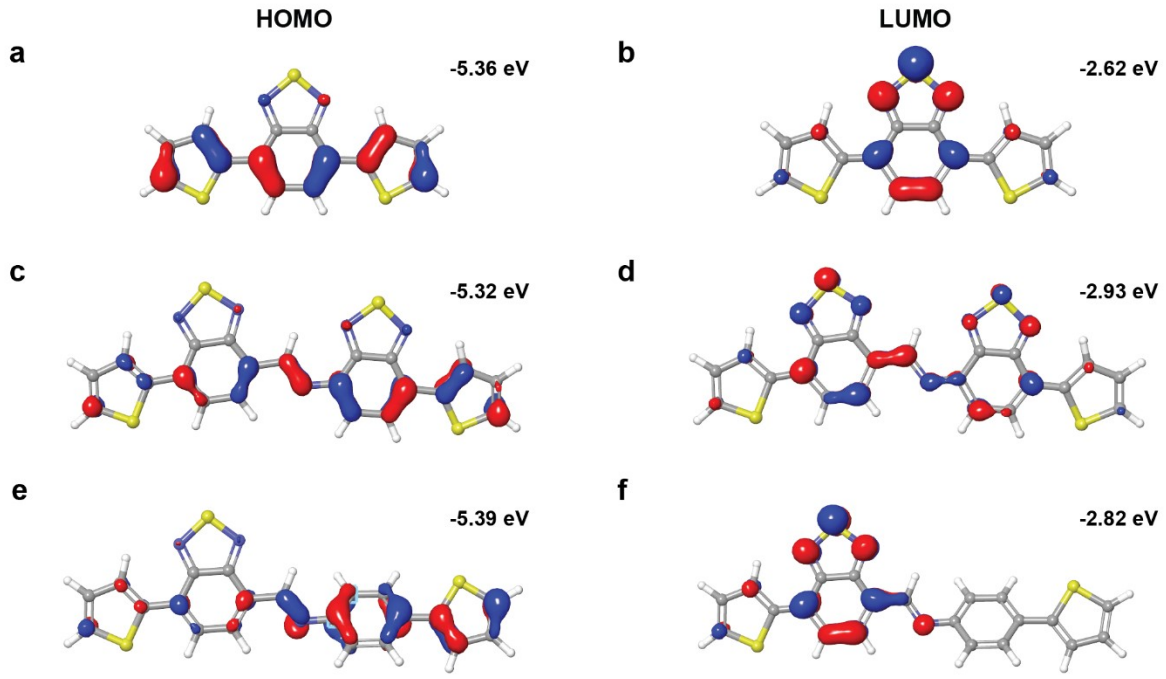

Figure S20. HOMO and LUMO orbitals and their corresponding energies (calculated at the

B3LYP-D3/6-31G** level of theory) of the DFT-optimized models of (a,b) T-BT-T, (c,d) T-BTiBT-T, and (e, f) T-BTiPh-T. Orbital isosurfaces are illustrated at 0.05 electrons Bohr^{-3}.

DFT-Optimized Model for dialdehyde-functionalized BT-IDT-BT

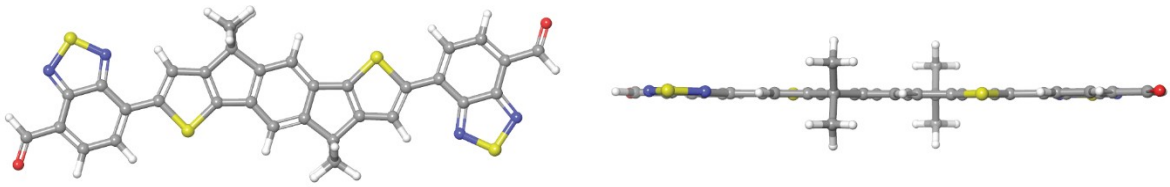

Figure S21. The DFT-optimized (B3LYP-D3/6-31G**) gas-phase model of dialdehyde-functionalized BT-IDT-BT from different views. The alkyl chains on IDT were truncated to methyl groups to simplify the calculations.

Total energy: -3270.7460 hartrees
Cartesian coordinates (from left to right: atom, x, y, z in Å):

O1	-2.7736000000	-4.0247000000	-9.1977000000
C2	-2.0969000000	-3.0765000000	-8.8348000000
C3	-1.8729000000	-2.7325000000	-7.4166000000
C4	-2.4313000000	-3.4848000000	-6.4012000000
C5	-2.2402000000	-3.1872000000	-5.0360000000
C6	-1.4750000000	-2.1141000000	-4.5791000000
C7	-0.8726000000	-1.3003000000	-5.6153000000
N8	-0.1012000000	-0.2245000000	-5.4290000000
S9	0.3216000000	0.3275000000	-6.9161000000
N10	-0.4541000000	-0.7724000000	-7.8563000000
C11	-1.0751000000	-1.6148000000	-7.0226000000
C12	-1.2923000000	-1.8299000000	-3.1697000000
C13	-0.5795000000	-0.7966000000	-2.5735000000
C14	-0.6236000000	-0.8399000000	-1.1691000000
C15	-0.0556000000	-0.0073000000	-0.0338000000
C16	1.4874000000	-0.0059000000	-0.0518000000
C17	-0.5961000000	1.4384000000	-0.0697000000
C18	-1.3641000000	-1.8955000000	-0.6730000000
S19	-2.0332000000	-2.8752000000	-1.9299000000
C20	-1.3728000000	-1.8923000000	0.7734000000
C21	-0.5969000000	-0.7725000000	1.1793000000
C22	-0.4074000000	-0.4921000000	2.5226000000
C23	-1.0036000000	-1.3484000000	3.4595000000
C24	-1.0025000000	-1.3511000000	4.9060000000
S25	-0.3167000000	-0.3811000000	6.1611000000
C26	-1.0374000000	-1.4379000000	7.4034000000
C27	-0.8291000000	-1.1672000000	8.8130000000
C28	-1.4083000000	-1.9939000000	9.8517000000
N29	-2.1821000000	-3.0686000000	9.6687000000
S30	-2.5693000000	-3.6409000000	11.1578000000
N31	-1.7765000000	-2.5501000000	12.0944000000
C32	-1.1755000000	-1.6959000000	11.2581000000
C33	-0.0569000000	-0.0974000000	9.2658000000
C34	0.1632000000	0.1845000000	10.6300000000
C35	-0.3711000000	-0.5812000000	11.6483000000
C36	-0.1156000000	-0.2555000000	13.0653000000
O37	0.5673000000	0.6893000000	13.4254000000
C38	-1.7591000000	-2.4662000000	6.8083000000
C39	-1.7350000000	-2.4117000000	5.4034000000
C40	-2.3120000000	-3.2385000000	4.2677000000
C41	-1.7732000000	-4.6844000000	4.2918000000
C42	-3.8553000000	-3.2392000000	4.2960000000
C43	-1.7796000000	-2.4678000000	3.0540000000
C44	-1.9699000000	-2.7479000000	1.7105000000
H45	-1.6027000000	-2.4068000000	-9.5650000000
H46	-3.0407000000	-4.3374000000	-6.6857000000
H47	-2.7218000000	-3.8368000000	-4.3118000000
H48	-0.0569000000	-0.0574000000	-3.1628000000
H49	1.8813000000	0.5362000000	0.8140000000
H50	1.8802000000	-1.0263000000	-0.0272000000
H51	-0.2332000000	2.0056000000	0.7936000000
H52	-0.2603000000	1.9485000000	-0.9784000000
H53	0.1857000000	0.3596000000	2.8432000000
H54	0.4078000000	0.5614000000	8.5390000000
H55	0.7772000000	1.0349000000	10.9110000000
H56	-0.5918000000	-0.9361000000	13.7974000000
H57	-2.2702000000	-3.2127000000	7.3987000000

H58	-2.1429000000	-5.2463000000	3.4279000000
H59	-0.6800000000	-4.6949000000	4.2673000000
H60	-4.2200000000	-3.7319000000	5.2032000000
H61	-2.5592000000	-3.6024000000	1.3900000000
H62	-1.6894000000	1.4474000000	-0.0531000000
H63	1.8573000000	0.4844000000	-0.9581000000
H64	-2.1034000000	-5.1993000000	5.1997000000
H65	-4.2546000000	-3.7789000000	3.4312000000
H66	-4.2476000000	-2.2186000000	4.2762000000

*Assignment of the electronic transitions (CAM-B3LYP-D3/6-31G++** level of TD-DFT):*
(Number corresponding to the HOMO: 167)

Restricted Singlet Excited State 1:

Excitation energy = 0.0880396665 hartrees 2.39568122 eV 517.53 nm

excitation	X coeff.
166 => 169	-0.36999
167 => 168	-0.90524
167 => 170	-0.12464

Transition dipole moment (debye):
X= 0.7173 Y= 1.0393 Z= 14.1444 Tot= 14.2007

Oscillator strength, f= 1.8321

Restricted Singlet Excited State 2:

Excitation energy = 0.1009308017 hartrees 2.74646685 eV 451.43 nm

excitation	X coeff.
165 => 169	0.10979
166 => 168	-0.47091
166 => 170	0.10031
167 => 169	-0.85768

Transition dipole moment (debye):
X= -0.0808 Y= 0.0413 Z= -0.0100 Tot= 0.0913

Oscillator strength, f= 0.0001

Restricted Singlet Excited State 3:

Excitation energy = 0.1277537889 hartrees 3.47635747 eV 356.65 nm

excitation	X coeff.
161 => 168	0.58919
161 => 169	-0.54913
161 => 171	-0.29736
161 => 172	0.38573
161 => 174	0.24320

Transition dipole moment (debye):
X= -0.0665 Y= 0.0460 Z= 0.0044 Tot= 0.0809

Oscillator strength, f= 0.0001

Restricted Singlet Excited State 4:

Excitation energy = 0.1277823315 hartrees 3.47713416 eV 356.57 nm

excitation	X coeff.
160 => 168	0.58927
160 => 169	0.54883
160 => 171	0.29726
160 => 172	0.38588
160 => 174	-0.24361

Transition dipole moment (debye):
X= -0.0667 Y= 0.0458 Z= 0.0040 Tot= 0.0810

Oscillator strength, f= 0.0001

Restricted Singlet Excited State 5:

Excitation energy = 0.1328173102 hartrees 3.61414290 eV 343.05 nm

excitation	X coeff.
157 => 169	0.10720
164 => 168	-0.10864
165 => 168	0.27924
166 => 169	-0.48492
166 => 171	0.21396
167 => 170	0.75115

Transition dipole moment (debye):
X= 0.3263 Y= 0.4465 Z= -3.7619 Tot= 3.8023

Oscillator strength, f= 0.1981

Restricted Singlet Excited State 6:

Excitation energy = 0.1351632859 hartrees 3.67798014 eV 337.10 nm

excitation	X coeff.
164 => 169	0.15580
165 => 169	-0.30610
166 => 168	0.78095
166 => 170	0.12608
167 => 169	-0.46723

Transition dipole moment (debye):
X= 0.0322 Y= -0.0137 Z= 0.0016 Tot= 0.0350

Oscillator strength, f= 0.0000

Restricted Singlet Excited State 7:

Excitation energy = 0.1462889132 hartrees 3.98072386 eV 311.46 nm

excitation	X coeff.
157 => 169	0.17203
164 => 168	-0.15260
165 => 168	0.38837
166 => 169	-0.55895
166 => 171	-0.13780
166 => 174	-0.10141
167 => 168	0.35112
167 => 170	-0.53671

Transition dipole moment (debye):
X= 0.4333 Y= 0.6060 Z= 3.5184 Tot= 3.5964

Oscillator strength, f= 0.1953

Restricted Singlet Excited State 8:

Excitation energy = 0.1523401618 hartrees 4.14538672 eV 299.09 nm

excitation	X coeff.
157 => 168	-0.12116
162 => 169	0.15007
163 => 168	0.37588
164 => 169	0.26582
165 => 169	-0.15062
165 => 171	0.12006
166 => 170	-0.46688
166 => 172	-0.12983
167 => 171	-0.60908
167 => 174	-0.21105

Transition dipole moment (debye):
X= -0.0297 Y= 0.0184 Z= 0.0022 Tot= 0.0351

Oscillator strength, f= 0.0000

Restricted Singlet Excited State 9:

Excitation energy = 0.1547719300 hartrees 4.21155850 eV 294.39 nm

excitation	X coeff.
157 => 169	0.12873
158 => 168	-0.30813
159 => 169	-0.26970
162 => 168	0.43224
163 => 169	0.50454
163 => 174	0.10775
164 => 168	0.48947
166 => 171	-0.11485
167 => 172	-0.17343

Transition dipole moment (debye):
X= 0.9403 Y= 1.2726 Z= -0.6183 Tot= 1.6989

Oscillator strength, f= 0.0461

Restricted Singlet Excited State 10:

Excitation energy = 0.1558574397 hartrees 4.24109672 eV 292.34 nm

excitation	X coeff.
157 => 168	-0.29749
158 => 169	0.38819
159 => 168	0.31398
159 => 170	-0.10047
162 => 169	-0.34416
163 => 168	-0.50147
164 => 169	-0.21527
165 => 169	-0.16099
166 => 170	-0.23525
166 => 184	0.10121
167 => 171	-0.19688
167 => 174	-0.22503

Transition dipole moment (debye):
X= -0.0344 Y= 0.0053 Z= -0.0029 Tot= 0.0350

Oscillator strength, f= 0.0000

Restricted Singlet Excited State 11:

Excitation energy = 0.1592689537 hartrees 4.33392874 eV 286.08 nm

excitation	X coeff.
158 => 168	0.19686
159 => 169	0.17170
162 => 168	-0.25319
162 => 170	-0.14610
164 => 168	0.35799
164 => 170	0.20748
164 => 176	0.10981
165 => 168	0.31055
165 => 170	0.19647
165 => 172	-0.10777
165 => 176	-0.14263
166 => 169	0.10451
167 => 172	0.12885
167 => 176	-0.61990

Transition dipole moment (debye):
X= -1.0998 Y= -1.5426 Z= -0.3144 Tot= 1.9205

Oscillator strength, f= 0.0606

Restricted Singlet Excited State 12:

Excitation energy = 0.1618692312 hartrees 4.40468589 eV 281.48 nm

excitation	X coeff.
157 => 169	0.21349
158 => 168	-0.53676
159 => 169	-0.43905
162 => 168	-0.33689

```
 162 =>  170   -0.12471
 163 =>  169   -0.27944
 164 =>  168   -0.19152
 166 =>  174    0.12553
 167 =>  176   -0.23216
 167 =>  184   -0.14192

 Transition dipole moment (debye):
   X=    2.3365    Y=    3.2701    Z=    0.2074  Tot=    4.0244

 Oscillator strength, f=    0.2705

 ----------------------------------------------------------------------------
 Restricted Singlet Excited State  13:
 ----------------------------------------

 Excitation energy =  0.1619521765 hartrees       4.40694295 eV
281.34 nm

  excitation     X coeff.
 ------------   ---------
 157 =>  168   -0.14465
 158 =>  168    0.10608
 158 =>  169    0.45003
 159 =>  168    0.48473
 162 =>  169    0.21626
 163 =>  168    0.43657
 164 =>  169    0.23088
 166 =>  172    0.15368
 166 =>  184    0.11533
 167 =>  171    0.27210
 167 =>  188   -0.10283

 Transition dipole moment (debye):
   X=   -0.4585    Y=   -0.6649    Z=   -0.0496  Tot=    0.8092

 Oscillator strength, f=    0.0109

 ----------------------------------------------------------------------------
 Restricted Singlet Excited State  14:
 ----------------------------------------

 Excitation energy =  0.1672733062 hartrees       4.55173825 eV
272.39 nm

  excitation     X coeff.
 ------------   ---------
 156 =>  168   -0.16846
 157 =>  169    0.41906
 159 =>  169    0.20278
 162 =>  168    0.25738
 164 =>  168   -0.24449
 165 =>  168    0.54224
 166 =>  169    0.49814
 167 =>  168   -0.18769
 167 =>  176    0.11634

 Transition dipole moment (debye):
   X=   -0.1471    Y=   -0.2172    Z=    0.2697  Tot=    0.3763

 Oscillator strength, f=    0.0024

 ----------------------------------------------------------------------------
 Restricted Singlet Excited State  15:
 ----------------------------------------

 Excitation energy =  0.1686940041 hartrees       4.59039741 eV
270.09 nm

  excitation     X coeff.
 ------------   ---------
 156 =>  169   -0.21048
 157 =>  168    0.49145
 158 =>  169    0.11698
 159 =>  168    0.32986
 162 =>  169    0.16904
 164 =>  169   -0.21535
 165 =>  169    0.48830
 166 =>  168    0.26306
 166 =>  172   -0.16329
 167 =>  171   -0.37378

 Transition dipole moment (debye):
   X=   -0.0203    Y=    0.0167    Z=    0.0195  Tot=    0.0327

 Oscillator strength, f=    0.0000

 ----------------------------------------------------------------------------
 Restricted Singlet Excited State  16:
 ----------------------------------------

 Excitation energy =  0.1706463724 hartrees       4.64352405 eV
267.00 nm

  excitation     X coeff.
 ------------   ---------
 158 =>  168    0.12095
 159 =>  169    0.10059
 162 =>  168   -0.19781
 163 =>  169   -0.11302
 164 =>  172   -0.10083
 165 =>  168    0.18134
 165 =>  170    0.22971
 166 =>  171   -0.42142
 166 =>  174    0.12683
 167 =>  172   -0.72701
 167 =>  176    0.14453

 Transition dipole moment (debye):
   X=    0.2925    Y=    0.4205    Z=    3.7965  Tot=    3.8309

 Oscillator strength, f=    0.2584

 ----------------------------------------------------------------------------
 Restricted Singlet Excited State  17:
 ----------------------------------------

 Excitation energy =  0.1723892114 hartrees       4.69094912 eV
264.31 nm

  excitation     X coeff.
 ------------   ---------
 154 =>  168    0.34564
 154 =>  169    0.39863
 154 =>  170   -0.17646
 154 =>  171   -0.16162
 155 =>  168    0.48515
 155 =>  169    0.46415
 155 =>  170   -0.24687
 155 =>  171   -0.18798
 160 =>  171   -0.12780
 160 =>  172   -0.10869

 Transition dipole moment (debye):
   X=    0.0104    Y=    0.0158    Z=    0.0029  Tot=    0.0191

 Oscillator strength, f=    0.0000

 ----------------------------------------------------------------------------
 Restricted Singlet Excited State  18:
```

Excitation energy = 0.1724131849 hartrees 4.69160147 eV 264.27 nm

excitation	X coeff.
154 => 168	0.48488
154 => 169	-0.46436
154 => 170	-0.24703
154 => 171	0.18823
155 => 168	-0.34561
155 => 169	0.39858
155 => 170	0.17552
155 => 171	-0.16140
161 => 171	0.12849
161 => 172	-0.10919

Transition dipole moment (debye):
X= 0.0116 Y= 0.0161 Z= -0.0223 Tot= 0.0299

Oscillator strength, f= 0.0000

Restricted Singlet Excited State 19:

Excitation energy = 0.1806447143 hartrees 4.91559278 eV 252.23 nm

excitation	X coeff.
159 => 169	-0.10758
162 => 168	-0.38262
164 => 168	0.44107
165 => 168	0.33394
166 => 171	0.11574
167 => 172	0.22447
167 => 176	0.61842

Transition dipole moment (debye):
X= -0.8664 Y= -1.2474 Z= 0.1122 Tot= 1.5230

Oscillator strength, f= 0.0432

Restricted Singlet Excited State 20:

Excitation energy = 0.1811609193 hartrees 4.92963943 eV 251.51 nm

excitation	X coeff.
157 => 168	-0.20521
157 => 170	0.11921
158 => 169	0.16031
159 => 168	0.12039
165 => 171	0.11064
166 => 168	-0.13987
166 => 170	0.29479
166 => 172	-0.44593
167 => 171	-0.26615
167 => 174	0.64820

Transition dipole moment (debye):
X= -0.0254 Y= 0.0123 Z= -0.0061 Tot= 0.0289

Oscillator strength, f= 0.0000

DFT-Optimized Model for aldehyde-amino-functionalized BT-IDT-BT

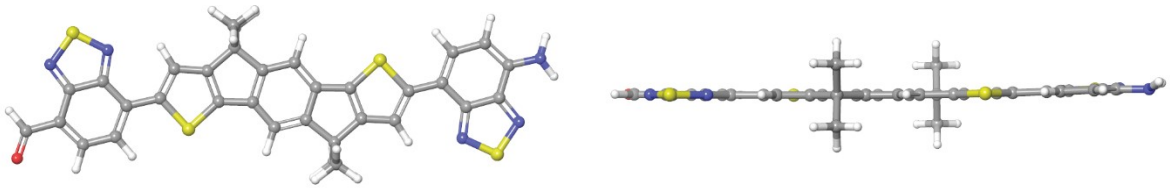

Figure S22. The DFT-optimized (B3LYP-D3/6-31G**) gas-phase model of aldehyde-amino-functionalized BT-IDT-BT from different views. The alkyl chains on IDT were truncated to methyl groups to simplify the calculations.

Total energy: -3212.7759 hartrees
Cartesian coordinates (from left to right: atom, x, y, z in Å):

N1	-2.1625000000	-2.9743000000	8.7510000000	C32	-0.0762000000	-0.0763000000	-9.2809000000
C2	-1.9951000000	-2.7133000000	7.4135000000				
C3	-2.5027000000	-3.4823000000	6.3828000000	C33	0.1047000000	0.2212000000	-10.6461000000
C4	-2.2461000000	-3.1795000000	5.0243000000				
C5	-1.4811000000	-2.1097000000	4.5751000000	C34	-0.4485000000	-0.5390000000	-11.6601000000
C6	-0.9373000000	-1.2806000000	5.6221000000				
N7	-0.1798000000	-0.1865000000	5.4760000000	C35	-0.2359000000	-0.1933000000	-13.0775000000
S8	0.1535000000	0.3856000000	6.9810000000				
N9	-0.6484000000	-0.7306000000	7.8838000000	C36	-1.7152000000	-2.4751000000	-6.8100000000
C10	-1.1982000000	-1.5852000000	7.0192000000				
C11	-1.2539000000	-1.8363000000	3.1634000000	C37	-1.6637000000	-2.4322000000	-5.4076000000
C12	-0.5222000000	-0.8160000000	2.5763000000				
C13	-0.5393000000	-0.8712000000	1.1655000000	C38	-2.2314000000	-3.2599000000	-4.2694000000
C14	0.0498000000	-0.0485000000	0.0322000000				
C15	1.5926000000	-0.0638000000	0.0662000000	C39	-3.7745000000	-3.2540000000	-4.2812000000
C16	-0.4735000000	1.4030000000	0.0581000000				
C17	-1.2753000000	-1.9219000000	0.6641000000	C40	-1.6982000000	-4.7078000000	-4.3038000000
S18	-1.9760000000	-2.8874000000	1.9195000000				
C19	-1.2712000000	-1.9252000000	-0.7802000000	C41	-1.6827000000	-2.4962000000	-3.0597000000
C20	-0.4864000000	-0.8110000000	-1.1865000000	C42	-1.8730000000	-2.7765000000	-1.7162000000
C21	-0.2954000000	-0.5323000000	-2.5290000000	H43	-3.1139000000	-4.3495000000	6.6156000000
				H44	-2.6911000000	-3.8457000000	4.2912000000
C22	-0.9012000000	-1.3827000000	-3.4672000000	H45	-0.0095000000	-0.0726000000	3.1692000000
				H46	2.0020000000	0.4752000000	-0.7946000000
C23	-0.9154000000	-1.3798000000	-4.9131000000	H47	1.9585000000	0.4206000000	0.9775000000
				H48	-0.0945000000	1.9648000000	-0.8020000000
S24	-0.2468000000	-0.4041000000	-6.1730000000	H49	-1.5665000000	1.4242000000	0.0291000000
C25	-0.9999000000	-1.4448000000	-7.4113000000	H50	0.3008000000	0.3175000000	-2.8499000000
				H51	0.3979000000	0.5810000000	-8.5588000000
C26	-0.8258000000	-1.1598000000	-8.8188000000	H52	0.7012000000	1.0817000000	-10.9343000000
C27	-1.4221000000	-1.9825000000	-9.8530000000	O53	0.4262000000	0.7634000000	-13.4473000000
N28	-2.1778000000	-3.0683000000	-9.6620000000	H54	-2.2443000000	-3.2132000000	-7.3957000000
S29	-2.6004000000	-3.6286000000	-11.1465000000	H55	-4.1671000000	-3.7938000000	-3.4133000000
N30	-1.8432000000	-2.5187000000	-12.0917000000	H56	-4.1613000000	-2.2315000000	-4.2542000000
C31	-1.2299000000	-1.6669000000	-11.2619000000	H57	-2.0582000000	-5.2699000000	-3.4359000000

H58	-2.0411000000	-5.2200000000	-5.2088000000
H59	-2.4705000000	-3.6251000000	-1.3952000000
H60	-4.1517000000	-3.7421000000	-5.1859000000
H61	-0.6048000000	-4.7211000000	-4.2930000000
H62	1.9734000000	-1.0887000000	0.0443000000
H63	-0.1429000000	1.9111000000	0.9699000000
H64	-0.7255000000	-0.8706000000	-13.8043000000
H65	-1.9380000000	-2.2217000000	9.3856000000
H66	-2.9339000000	-3.5629000000	9.0248000000

*Assignment of the electronic transitions (CAM-B3LYP-D3/6-31G++** level of TD-DFT):*
(Number corresponding to the HOMO: 164)

Restricted Singlet Excited State 1:

Excitation energy = 0.0863932138 hartrees 2.35087896 eV 527.40 nm

excitation	X coeff.
163 => 165	0.36286
163 => 166	-0.24089
164 => 165	0.77337
164 => 166	0.40566
164 => 167	0.11345

Transition dipole moment (debye):
X= 0.6575 Y= 0.9918 Z= -12.8920 Tot= 12.9468

Oscillator strength, f= 1.4943

Restricted Singlet Excited State 2:

Excitation energy = 0.0952345516 hartrees 2.59146400 eV 478.43 nm

excitation	X coeff.
162 => 166	0.12488
163 => 165	-0.34433
163 => 166	-0.31779
163 => 167	0.10228
164 => 165	-0.32825
164 => 166	0.78681

Transition dipole moment (debye):
X= 0.2656 Y= 0.1963 Z= 0.6185 Tot= 0.7012

Oscillator strength, f= 0.0048

Restricted Singlet Excited State 3:

Excitation energy = 0.1235571245 hartrees 3.36216042 eV 368.76 nm

excitation	X coeff.
162 => 165	0.33449
163 => 165	0.58277
163 => 166	-0.17201
163 => 168	0.13320
164 => 165	-0.27970
164 => 167	-0.57863
164 => 168	-0.17650

Transition dipole moment (debye):
X= 0.2422 Y= 0.4566 Z= 3.8856 Tot= 3.9198

Oscillator strength, f= 0.1959

Restricted Singlet Excited State 4:

Excitation energy = 0.1282932315 hartrees 3.49103645 eV 355.15 nm

excitation	X coeff.
158 => 165	-0.79723
158 => 166	0.10172
158 => 168	0.46457
158 => 170	-0.28024
158 => 188	-0.11217

Transition dipole moment (debye):
X= -0.0671 Y= 0.0474 Z= 0.0064 Tot= 0.0824

Oscillator strength, f= 0.0001

Restricted Singlet Excited State 5:

Excitation energy = 0.1298830932 hartrees 3.53429879 eV 350.80 nm

excitation	X coeff.
162 => 165	-0.15634
162 => 166	0.18617
163 => 165	-0.46730
163 => 166	-0.24398
163 => 167	-0.17195
163 => 170	0.12735
164 => 165	0.40396
164 => 166	-0.23593
164 => 167	-0.56563
164 => 168	-0.19107

Transition dipole moment (debye):
X= -0.0597 Y= -0.0994 Z= 5.0316 Tot= 5.0330

Oscillator strength, f= 0.3395

Restricted Singlet Excited State 6:

Excitation energy = 0.1450437403 hartrees 3.94684099 eV 314.14 nm

excitation	X coeff.
157 => 166	-0.15006
162 => 165	0.21251
162 => 166	0.44209
163 => 166	-0.65199
164 => 165	-0.14006
164 => 166	-0.32976
164 => 167	0.35750

Transition dipole moment (debye):
X= 0.4085 Y= 0.5873 Z= -2.1768 Tot= 2.2913

Oscillator strength, f= 0.0786

Restricted Singlet Excited State 7:

Excitation energy = 0.1480913724 hartrees 4.02977127 eV 307.67 nm

excitation	X coeff.
157 => 165	0.16385
159 => 165	0.20431
162 => 165	0.20036
162 => 166	-0.13216
162 => 167	-0.11795
163 => 165	-0.10601
163 => 167	-0.55517
164 => 167	-0.10065
164 => 168	0.51563
164 => 170	0.39580

Transition dipole moment (debye):
X= -0.0207 Y= -0.1822 Z= -0.0397 Tot= 0.1877

Oscillator strength, f= 0.0005

Restricted Singlet Excited State 8:

Excitation energy = 0.1544974013 hartrees 4.20408819 eV 294.91 nm

excitation	X coeff.
155 => 165	0.43385
157 => 165	0.10287
159 => 165	-0.70756
160 => 165	-0.32523
161 => 165	-0.17643
162 => 165	0.11589
163 => 168	-0.12828
164 => 170	0.14771

Transition dipole moment (debye):
X= 0.5998 Y= 0.8238 Z= 0.3314 Tot= 1.0716

Oscillator strength, f= 0.0183

Restricted Singlet Excited State 9:

Excitation energy = 0.1578393840 hartrees 4.29502817 eV 288.67 nm

excitation	X coeff.
155 => 165	0.15060
157 => 165	-0.11117
159 => 165	-0.21161
160 => 165	0.21080
160 => 167	0.20259
161 => 165	0.25731
161 => 167	0.17149
162 => 165	-0.23591
162 => 174	-0.18501
163 => 165	0.13125
163 => 166	-0.11073
163 => 174	0.15337
164 => 170	0.17480
164 => 174	0.67064

Transition dipole moment (debye):
X= 0.2816 Y= 0.3645 Z= -0.2781 Tot= 0.5381

Oscillator strength, f= 0.0047

Restricted Singlet Excited State 10:

Excitation energy = 0.1595281613 hartrees 4.34098214 eV 285.61 nm

excitation	X coeff.
154 => 165	0.14734
155 => 165	0.28647
156 => 165	0.15888
157 => 165	0.37519
159 => 165	0.22342
160 => 165	0.21743
162 => 165	0.50271
163 => 165	-0.28572
163 => 166	0.16887
163 => 167	0.12728
163 => 168	-0.10013
164 => 165	0.11988
164 => 168	-0.27282
164 => 174	0.25265

Transition dipole moment (debye):
X= 0.7904 Y= 1.1854 Z= -1.1655 Tot= 1.8407

Oscillator strength, f= 0.0558

Restricted Singlet Excited State 11:

Excitation energy = 0.1615385378 hartrees 4.39568726 eV 282.06 nm

excitation	X coeff.
155 => 165	0.65940
156 => 165	-0.19305
157 => 165	-0.29609
159 => 165	0.39173
162 => 165	-0.20182
163 => 165	0.12042

163 => 170 0.12087
164 => 174 -0.22808

Transition dipole moment (debye):
X= 1.6466 Y= 2.3561 Z= 0.1254 Tot= 2.8772

Oscillator strength, f= 0.1380

Restricted Singlet Excited State 12:

Excitation energy = 0.1648020684 hartrees 4.48449245 eV 276.47 nm

excitation	X coeff.
156 => 166	-0.60681
157 => 166	0.24532
160 => 166	0.26155
161 => 165	-0.14272
161 => 166	-0.37597
163 => 181	0.13503
163 => 182	0.10155
163 => 183	0.13647
164 => 169	0.15748
164 => 181	-0.21817
164 => 182	-0.15095
164 => 183	-0.19855

Transition dipole moment (debye):
X= 0.6077 Y= 0.8825 Z= 0.6670 Tot= 1.2621

Oscillator strength, f= 0.0271

Restricted Singlet Excited State 13:

Excitation energy = 0.1681525453 hartrees 4.57566356 eV 270.96 nm

excitation	X coeff.
155 => 165	-0.19462
156 => 166	0.13869
159 => 165	0.11928
160 => 166	0.18845
161 => 165	-0.26032
161 => 166	-0.40804
161 => 167	-0.16517
161 => 168	-0.10083
162 => 166	-0.17722
162 => 167	0.12774
163 => 166	-0.13467
163 => 168	-0.39029
164 => 168	-0.36054
164 => 169	-0.16851
164 => 170	0.28389
164 => 181	0.16676
164 => 188	-0.12086

Transition dipole moment (debye):
X= -0.3899 Y= -0.4931 Z= -1.7532 Tot= 1.8625

Oscillator strength, f= 0.0602

Restricted Singlet Excited State 14:

Excitation energy = 0.1687393323 hartrees 4.59163085 eV 270.02 nm

excitation	X coeff.
156 => 166	-0.12895
162 => 169	-0.19885
163 => 168	0.13274
163 => 169	0.40512
164 => 168	0.11716
164 => 169	-0.77696
164 => 171	0.12473
164 => 173	0.10352

Transition dipole moment (debye):
X= 0.1362 Y= 0.3985 Z= 0.9204 Tot= 1.0122

Oscillator strength, f= 0.0178

Restricted Singlet Excited State 15:

Excitation energy = 0.1723580266 hartrees 4.69010053 eV 264.35 nm

excitation	X coeff.
146 => 165	0.10237
151 => 165	0.83763
151 => 166	-0.14737
151 => 167	-0.33801
151 => 168	0.22093
158 => 165	-0.11906
158 => 167	0.11018
158 => 168	-0.15411

Transition dipole moment (debye):
X= 0.0007 Y= -0.0064 Z= -0.0060 Tot= 0.0088

Oscillator strength, f= 0.0000

Restricted Singlet Excited State 16:

Excitation energy = 0.1727692552 hartrees 4.70129063 eV 263.72 nm

excitation	X coeff.
155 => 165	-0.14768
156 => 166	-0.23315
157 => 165	0.11745
157 => 166	0.29290
160 => 165	-0.17038
160 => 166	-0.31088
161 => 165	0.16867
161 => 166	0.39729
162 => 166	-0.15985
163 => 166	-0.14510
163 => 167	-0.29568
163 => 168	-0.25230
163 => 170	0.12390
163 => 181	0.12454
164 => 167	0.11155
164 => 168	-0.27433
164 => 170	0.11892
164 => 181	-0.12338

164 => 183 -0.13094

Transition dipole moment (debye):
X= 0.6133 Y= 0.8631 Z= -1.3182 Tot= 1.6908

Oscillator strength, f= 0.0510

Restricted Singlet Excited State 17:

Excitation energy = 0.1743053141 hartrees 4.74308892 eV 261.40 nm

excitation	X coeff.
163 => 169	-0.13805
163 => 173	-0.13635
164 => 171	0.81592
164 => 173	0.16440
164 => 176	-0.19137
164 => 184	-0.12847
164 => 186	0.15511
164 => 189	-0.16177

Transition dipole moment (debye):
X= 0.1074 Y= -0.1950 Z= -0.3535 Tot= 0.4178

Oscillator strength, f= 0.0031

Restricted Singlet Excited State 18:

Excitation energy = 0.1750206339 hartrees 4.76255377 eV 260.33 nm

excitation	X coeff.
154 => 165	-0.12653
154 => 166	0.10978
156 => 165	-0.16433
156 => 166	-0.22270
157 => 165	-0.24071
159 => 165	0.10850
160 => 165	-0.24792
161 => 166	0.12744
162 => 165	0.23402
162 => 166	0.40536
162 => 167	0.20475
163 => 166	0.25898
163 => 167	0.18093
164 => 167	-0.11229
164 => 168	0.12358
164 => 170	0.43036
164 => 171	-0.12740
164 => 174	0.17166
164 => 182	-0.10202

Transition dipole moment (debye):
X= 0.4009 Y= 0.6488 Z= -2.0860 Tot= 2.2210

Oscillator strength, f= 0.0891

Restricted Singlet Excited State 19:

Excitation energy = 0.1780368408 hartrees 4.84462893 eV 255.92 nm

excitation	X coeff.
155 => 165	0.10935
157 => 165	-0.14649
159 => 165	0.23053
160 => 165	-0.45989
160 => 167	-0.10607
161 => 165	-0.44859
162 => 166	-0.14194
163 => 168	0.14082
164 => 170	-0.32402
164 => 174	0.44843

Transition dipole moment (debye):
X= -0.8141 Y= -1.1874 Z= 0.1944 Tot= 1.4528

Oscillator strength, f= 0.0388

Restricted Singlet Excited State 20:

Excitation energy = 0.1787007797 hartrees 4.86269563 eV 254.97 nm

excitation	X coeff.
147 => 166	0.16982
150 => 166	0.16268
152 => 165	0.11492
152 => 166	0.87360
152 => 167	-0.22073
152 => 168	-0.13109
152 => 170	-0.11834
153 => 166	0.14388

Transition dipole moment (debye):
X= 0.0756 Y= 0.0681 Z= -0.0842 Tot= 0.1321

Oscillator strength, f= 0.0003

DFT-Optimized Model for diamino-functionalized BT-IDT-BT

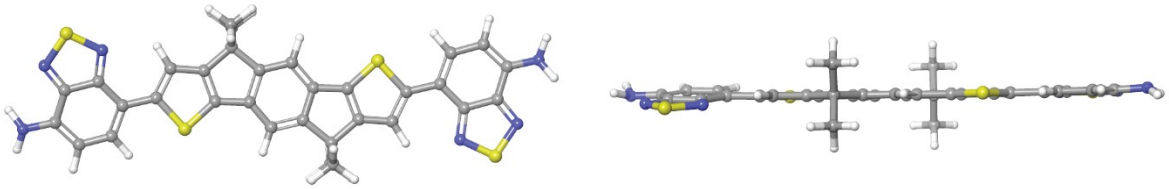

Figure S23. The DFT-optimized (B3LYP-D3/6-31G**) gas-phase model of diamino-functionalized BT-IDT-BT from different views. The alkyl chains on IDT were truncated to methyl groups to simplify the calculations.

Total energy: -3154.8038 hartrees
Cartesian coordinates (from left to right: atom, x, y, z in Å):

N1	-2.2238000000	-2.8712000000	8.7663000000
C2	-1.9853000000	-2.6674000000	7.4255000000
C3	-2.5079000000	-3.4318000000	6.4002000000
C4	-2.2674000000	-3.1287000000	5.0380000000
C5	-1.5012000000	-2.0632000000	4.5812000000
C6	-0.9308000000	-1.2460000000	5.6239000000
N7	-0.1457000000	-0.1726000000	5.4701000000
S8	0.2383000000	0.3747000000	6.9721000000
N9	-0.5762000000	-0.7258000000	7.8835000000
C10	-1.1750000000	-1.5525000000	7.0242000000
C11	-1.2849000000	-1.7916000000	3.1678000000
C12	-0.5438000000	-0.7839000000	2.5718000000
C13	-0.5716000000	-0.8428000000	1.1612000000
C14	0.0266000000	-0.0374000000	0.0203000000
C15	1.5690000000	-0.0764000000	0.0497000000
C16	-0.4731000000	1.4225000000	0.0354000000
C17	-1.3252000000	-1.8842000000	0.6680000000
S18	-2.0311000000	-2.8352000000	1.9310000000
C19	-1.3240000000	-1.8981000000	-0.7779000000
C20	-0.5234000000	-0.8008000000	-1.1913000000
C21	-0.3252000000	-0.5353000000	-2.5369000000
C22	-0.9396000000	-1.3839000000	-3.4684000000
C23	-0.9477000000	-1.3939000000	-4.9151000000
S24	-0.2562000000	-0.4384000000	-6.1834000000
C25	-1.0263000000	-1.4696000000	-7.4149000000
C26	-0.8542000000	-1.1759000000	-8.8300000000
C27	-1.2856000000	-2.0828000000	-9.8649000000
N28	-1.8837000000	-3.2689000000	-9.7002000000
S29	-2.1739000000	-3.8840000000	-11.1968000000
N30	-1.5512000000	-2.6727000000	-12.1199000000
C31	-1.0953000000	-1.7522000000	-11.2679000000
C32	-0.2744000000	-0.0021000000	-9.2946000000
C33	-0.0840000000	0.3236000000	-10.6598000000
C34	-0.4765000000	-0.5234000000	-11.6783000000
C35	-1.7507000000	-2.4866000000	-6.8153000000
C36	-1.7042000000	-2.4351000000	-5.4053000000
C37	-2.2907000000	-3.2463000000	-4.2633000000
C38	-3.8333000000	-3.2191000000	-4.2839000000
C39	-1.7793000000	-4.7021000000	-4.2837000000
C40	-1.7383000000	-2.4824000000	-3.0540000000
C41	-1.9364000000	-2.7481000000	-1.7089000000
H42	-1.5902000000	-2.4051000000	9.4002000000
H43	-2.5065000000	-3.7973000000	9.0494000000
H44	-3.1291000000	-4.2902000000	6.6392000000
H45	-2.7243000000	-3.7915000000	4.3093000000
H46	-0.0139000000	-0.0472000000	3.1583000000
H47	1.9840000000	0.4470000000	-0.8182000000
H48	1.9466000000	0.4107000000	0.9549000000
H49	-0.0885000000	1.9702000000	-0.8314000000
H50	-1.5656000000	1.4601000000	0.0094000000
H51	0.2847000000	0.3026000000	-2.8633000000
H52	0.0543000000	0.7372000000	-8.5703000000
H53	0.3847000000	1.2719000000	-10.9069000000
H54	-2.2837000000	-3.2243000000	-7.3977000000
H55	-4.2395000000	-3.7473000000	-3.4148000000
H56	-4.2049000000	-2.1907000000	-4.2661000000
H57	-2.1538000000	-5.2538000000	-3.4149000000
H58	-2.1224000000	-5.2153000000	-5.1883000000

H59	-2.5466000000	-3.5857000000	-1.3823000000
H60	-4.2123000000	-3.7075000000	-5.1879000000
H61	-0.6863000000	-4.7309000000	-4.2648000000
H62	1.9328000000	-1.1076000000	0.0360000000
H63	-0.1316000000	1.9340000000	0.9415000000
N64	-0.2773000000	-0.2935000000	-13.0212000000
H65	-0.8301000000	-0.8584000000	-13.6504000000
H66	-0.1440000000	0.6635000000	-13.3110000000

*Assignment of the electronic transitions (CAM-B3LYP-D3/6-31G++** level of TD-DFT):*
(Number corresponding to the HOMO: 161)

Restricted Singlet Excited State 1:

Excitation energy = 0.0879376233 hartrees 2.39290448 eV 518.13 nm

excitation	X coeff.
159 => 162	-0.13666
159 => 164	0.10479
160 => 163	0.48731
161 => 162	-0.84464

Transition dipole moment (debye):
X= -0.6908 Y= -0.8970 Z= 10.2656 Tot= 10.3279

Oscillator strength, f= 0.9679

Restricted Singlet Excited State 2:

Excitation energy = 0.0927828607 hartrees 2.52475010 eV 491.08 nm

excitation	X coeff.
159 => 163	0.19518
160 => 162	-0.54333
160 => 164	0.11620
161 => 163	0.79964

Transition dipole moment (debye):
X= -0.0505 Y= 0.0847 Z= -0.5356 Tot= 0.5446

Oscillator strength, f= 0.0028

Restricted Singlet Excited State 3:

Excitation energy = 0.1199371719 hartrees 3.26365650 eV 379.89 nm

excitation	X coeff.
159 => 162	0.25717
160 => 163	-0.35150
160 => 167	-0.24546
161 => 162	-0.14441
161 => 164	-0.83140

Transition dipole moment (debye):
X= 0.2096 Y= 0.3554 Z= 8.3116 Tot= 8.3219

Oscillator strength, f= 0.8571

Restricted Singlet Excited State 4:

Excitation energy = 0.1341198316 hartrees 3.64958631 eV 339.72 nm

excitation	X coeff.
155 => 162	-0.15730
159 => 163	0.42700
160 => 162	-0.66740
160 => 164	-0.10441
161 => 163	-0.55302

Transition dipole moment (debye):
X= -0.0437 Y= 0.0335 Z= -0.0509 Tot= 0.0750

Oscillator strength, f= 0.0001

Restricted Singlet Excited State 5:

Excitation energy = 0.1394829920 hartrees 3.79552533 eV 326.66 nm

excitation	X coeff.
155 => 163	-0.19762
159 => 162	0.45330
160 => 163	-0.55292
160 => 167	0.11826
161 => 162	-0.46264
161 => 164	0.43107

Transition dipole moment (debye):
X= 0.4084 Y= 0.5447 Z= -3.0799 Tot= 3.1542

Oscillator strength, f= 0.1432

Restricted Singlet Excited State 6:

Excitation energy = 0.1452841275 hartrees 3.95338225 eV 313.62 nm

excitation	X coeff.
153 => 162	0.11171
155 => 162	0.13658
157 => 162	0.12564
159 => 163	-0.20913
160 => 162	-0.15485
160 => 164	-0.62640
161 => 167	-0.64339

Transition dipole moment (debye):
X= -0.0210 Y= 0.0096 Z= -0.1110 Tot= 0.1134

Oscillator strength, f= 0.0002

Restricted Singlet Excited State 7:

Excitation energy = 0.1576665453 hartrees 4.29032499 eV 288.99 nm

excitation	X coeff.
156 => 162	0.12797
156 => 164	0.17922
158 => 162	-0.18845
158 => 164	-0.24693
159 => 172	-0.26144
161 => 172	0.83657
161 => 173	0.13646

Transition dipole moment (debye):
X= 0.1659 Y= 0.2426 Z= 0.8922 Tot= 0.9393

Oscillator strength, f= 0.0144

Restricted Singlet Excited State 8:

Excitation energy = 0.1639856633 hartrees 4.46227694 eV 277.85 nm

excitation	X coeff.
153 => 162	0.28491
153 => 163	-0.37843
154 => 162	-0.30686
156 => 162	-0.21767
157 => 162	-0.20639
157 => 163	0.29321
158 => 162	-0.22102
159 => 162	-0.22225
159 => 178	-0.10936
160 => 163	-0.19023
160 => 165	0.13196
160 => 166	-0.13045
160 => 179	-0.21189
161 => 165	0.13800
161 => 166	-0.22731
161 => 178	-0.21388
161 => 179	-0.15167

Transition dipole moment (debye):
X= 0.5237 Y= 0.9425 Z= 0.5429 Tot= 1.2072

Oscillator strength, f= 0.0247

Restricted Singlet Excited State 9:

Excitation energy = 0.1643632826 hartrees 4.47255248 eV 277.21 nm

excitation	X coeff.
153 => 162	0.29885
153 => 163	0.10513
154 => 162	0.26782
154 => 163	0.40433
156 => 162	0.10166
156 => 163	0.19691
157 => 162	-0.33681
157 => 163	-0.16617
158 => 162	0.10616
158 => 163	0.19084
159 => 162	0.13755
159 => 163	0.10301
160 => 163	0.12226
160 => 166	-0.19036
160 => 178	-0.22721
161 => 165	0.29264
161 => 178	0.15444
161 => 179	-0.20671

Transition dipole moment (debye):
X= -0.1105 Y= -0.6100 Z= -0.3137 Tot= 0.6948

Oscillator strength, f= 0.0082

Restricted Singlet Excited State 10:

Excitation energy = 0.1646015199 hartrees 4.47903525 eV 276.81 nm

excitation	X coeff.
152 => 162	0.14981
153 => 163	-0.22077
154 => 162	-0.19915
155 => 163	-0.33781
157 => 163	-0.18167
159 => 162	0.54968
160 => 163	0.46837
160 => 165	0.11723
160 => 167	-0.11811
160 => 179	-0.10813
161 => 162	0.19391
161 => 166	-0.18589
161 => 178	-0.17658

Transition dipole moment (debye):
X= 0.5967 Y= 1.0382 Z= -0.4274 Tot= 1.2714

Oscillator strength, f= 0.0275

Restricted Singlet Excited State 11:

Excitation energy = 0.1655808997 hartrees 4.50568553 eV 275.17 nm

excitation	X coeff.
153 => 162	-0.13680
154 => 163	-0.13119
157 => 162	0.24965
158 => 163	-0.10969
159 => 163	-0.21221
159 => 165	0.17741
160 => 162	-0.14799
160 => 166	-0.38713
161 => 165	0.60385
161 => 167	0.10061

161 => 168 -0.33178
161 => 181 0.10996

Transition dipole moment (debye):
X= -0.1412 Y= -0.1105 Z= -0.0130 Tot= 0.1798

Oscillator strength, f= 0.0006

Restricted Singlet Excited State 12:

Excitation energy = 0.1664462905 hartrees 4.52923401 eV 273.74 nm

excitation X coeff.
---
153 => 163 -0.18369
154 => 162 -0.16885
156 => 162 -0.12386
159 => 166 0.23527
160 => 165 -0.47541
161 => 166 0.66480
161 => 170 -0.11935
161 => 174 -0.10727

Transition dipole moment (debye):
X= 0.5805 Y= 0.6363 Z= 0.4309 Tot= 0.9630

Oscillator strength, f= 0.0159

Restricted Singlet Excited State 13:

Excitation energy = 0.1669482047 hartrees 4.54289179 eV 272.92 nm

excitation X coeff.
---
152 => 163 0.17246
153 => 162 -0.14236
155 => 162 -0.44314
156 => 163 -0.15356
159 => 163 0.52103
160 => 162 0.35109
161 => 163 0.10231
161 => 165 0.13329
161 => 167 -0.39908
161 => 168 -0.18811

Transition dipole moment (debye):
X= -0.0766 Y= 0.0315 Z= 0.1036 Tot= 0.1327

Oscillator strength, f= 0.0003

Restricted Singlet Excited State 14:

Excitation energy = 0.1690131162 hartrees 4.59908089 eV 269.58 nm

excitation X coeff.
---
153 => 163 0.15508
154 => 162 0.16933
155 => 163 -0.25091
156 => 162 -0.38255
157 => 163 0.37511
157 => 167 -0.12806
158 => 162 -0.42834
158 => 164 -0.15301
159 => 162 0.19710
159 => 164 0.19201
160 => 163 0.11319
160 => 167 0.22711
161 => 168 0.15572
161 => 178 0.19273
161 => 182 -0.13636
161 => 184 -0.11309

Transition dipole moment (debye):
X= -0.6226 Y= -0.8703 Z= -0.5265 Tot= 1.1926

Oscillator strength, f= 0.0248

Restricted Singlet Excited State 15:

Excitation energy = 0.1696694397 hartrees 4.61694036 eV 268.54 nm

excitation X coeff.
---
155 => 162 0.11105
156 => 163 0.12618
157 => 162 -0.19465
158 => 162 -0.10293
158 => 163 0.11972
159 => 165 -0.15052
160 => 166 0.23169
160 => 170 0.11904
160 => 174 0.10711
161 => 165 -0.20442
161 => 168 -0.73143
161 => 171 -0.11123
161 => 181 0.12764
161 => 186 0.14097

Transition dipole moment (debye):
X= -0.2821 Y= -0.4773 Z= -0.2175 Tot= 0.5956

Oscillator strength, f= 0.0062

Restricted Singlet Excited State 16:

Excitation energy = 0.1715312425 hartrees 4.66760259 eV 265.63 nm

excitation X coeff.
---
153 => 162 -0.31870
154 => 163 -0.31316
155 => 162 0.23493
155 => 164 0.10665
156 => 163 0.29073
156 => 167 -0.10684
157 => 162 -0.47455
157 => 164 -0.11624
158 => 163 0.29635
159 => 179 0.11019
160 => 164 -0.17918
160 => 166 -0.10310
160 => 178 0.22324
161 => 165 0.10932
161 => 168 0.21492

161 => 177 0.11796
161 => 179 0.18958

Transition dipole moment (debye):
X= -0.1002 Y= 0.0907 Z= 0.0050 Tot= 0.1352

Oscillator strength, f= 0.0003

Restricted Singlet Excited State 17:

Excitation energy = 0.1761840478 hartrees 4.79421187 eV 258.61 nm

excitation	X coeff.
155 => 162	0.14065
159 => 163	-0.17367
159 => 167	0.23023
160 => 162	-0.17276
160 => 164	0.66141
161 => 163	-0.18841
161 => 167	-0.54107
161 => 185	-0.11706
161 => 194	-0.10324
161 => 195	0.22873

Transition dipole moment (debye):
X= -0.7018 Y= -0.5200 Z= -0.4317 Tot= 0.9743

Oscillator strength, f= 0.0174

Restricted Singlet Excited State 19:

Excitation energy = 0.1787346915 hartrees 4.86361841 eV 254.92 nm

excitation	X coeff.
144 => 163	0.10621
147 => 162	-0.22819
147 => 163	0.16309
149 => 162	-0.58960
149 => 163	0.58797
149 => 164	0.21096
149 => 167	0.12738
150 => 162	0.10384

Transition dipole moment (debye):
X= -0.0302 Y= -0.0913 Z= 0.3139 Tot= 0.3283

Oscillator strength, f= 0.0020

Restricted Singlet Excited State 20:

Excitation energy = 0.1789567473 hartrees 4.86966086 eV 254.61 nm

excitation	X coeff.
147 => 162	-0.16778
147 => 163	-0.25243
148 => 162	0.51802
148 => 163	0.57664
148 => 164	-0.19732
148 => 167	0.11601

Transition dipole moment (debye):
X= 0.1032 Y= 0.0792 Z= 0.0702 Tot= 0.1478

Oscillator strength, f= 0.0004

Restricted Singlet Excited State 18:

Excitation energy = 0.1777519796 hartrees 4.83687746 eV 256.33 nm

excitation	X coeff.
160 => 164	0.11105
160 => 168	0.25858
160 => 183	-0.12602
160 => 188	-0.13159
161 => 169	-0.32135
161 => 170	-0.43776
161 => 174	-0.41391
161 => 175	0.32359
161 => 182	0.19650
161 => 184	-0.19945

149 => 162 0.14885
159 => 164 -0.13147
160 => 167 -0.11751

Transition dipole moment (debye):
X= -0.1242 Y= -0.2367 Z= 0.8025 Tot= 0.8458

Oscillator strength, f= 0.0132

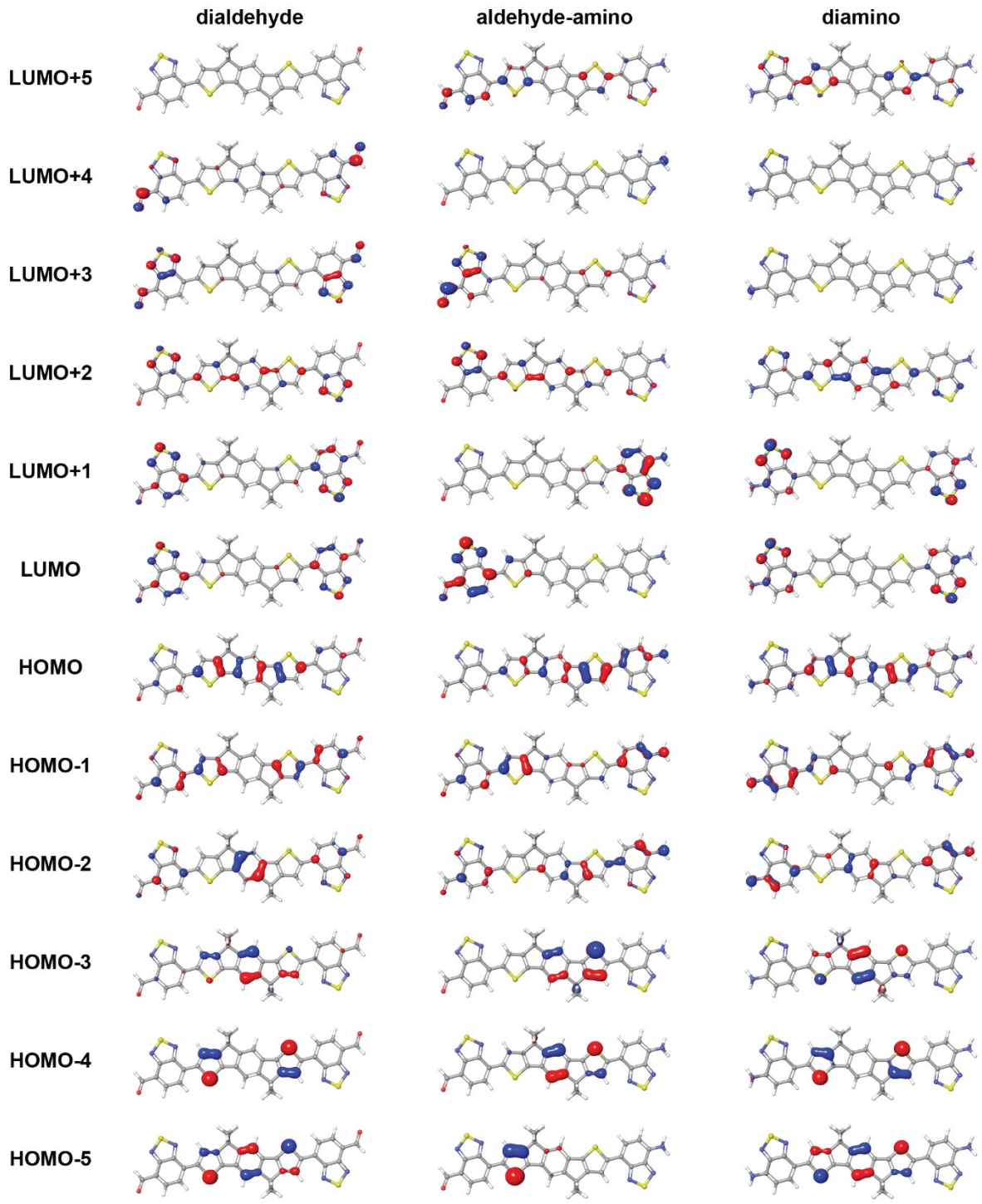

Figure S24. Frontier molecular orbitals levels (calculated at the CAM-B3LYP-D3/6-31G++** level of theory) of the DFT-optimized models of dialdehyde-, aldehyde-amino-, and diamino-functionalized BT-IDT-BT degradation products. Orbital isosurfaces are illustrated at 0.05 electrons $Bohr^{-3}$.

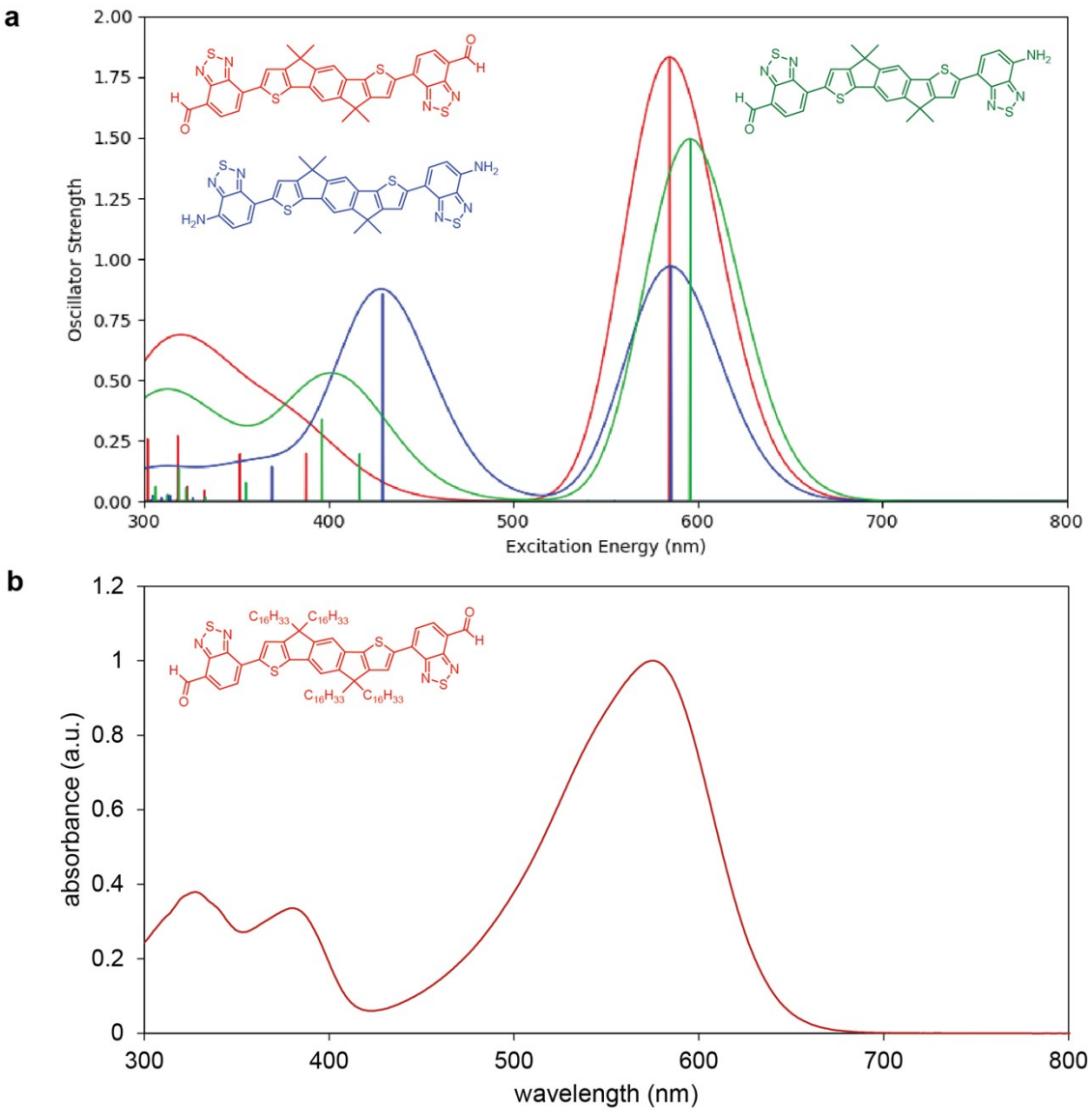

Figure S25. (a) Simulated UV-vis absorbance spectra of the models of BT-IDT-BT degradation products from TD-DFT (calculated at the CAM-B3LYP-D3/6-31G++** level of theory). The alkyl chains on IDT were truncated to methyl groups to simplify the calculations. The spectra were rendered, without vibronic character, using Gaussian band-shapes (fwhm of 0 and 40 nm). The energies of the transitions were scaled by a factor of 1.13 relative to their assignments above (pages S22-36). (b) Experimental UV-vis absorbance spectrum of dialdehyde-functionalized BT-IDT-BT in THF (~0.01 mg/mL) used as reference for scaling.

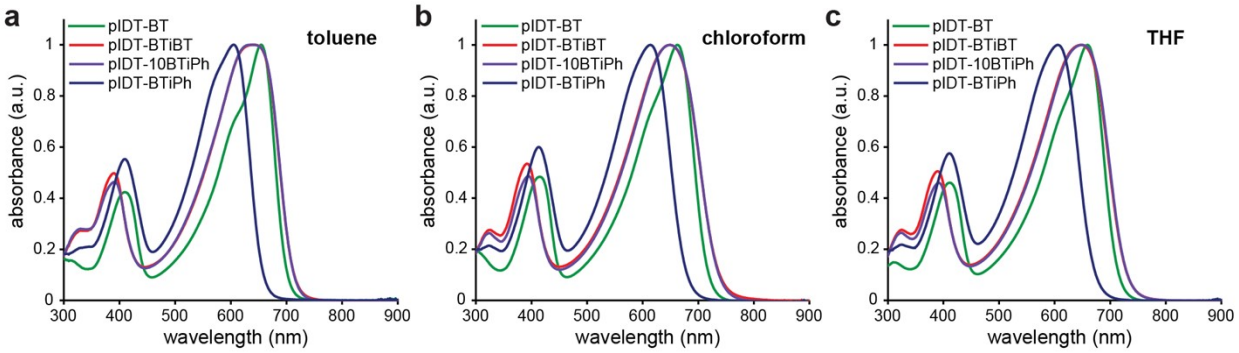

Figure S26. Normalized UV-vis absorption spectra for pIDT-BT, pIDT-BTiBT, pIDT-10BTiPh, and pIDT-BTiBT in (a) toluene, (b) chloroform, and (c) THF solutions (0.01 mg/mL).

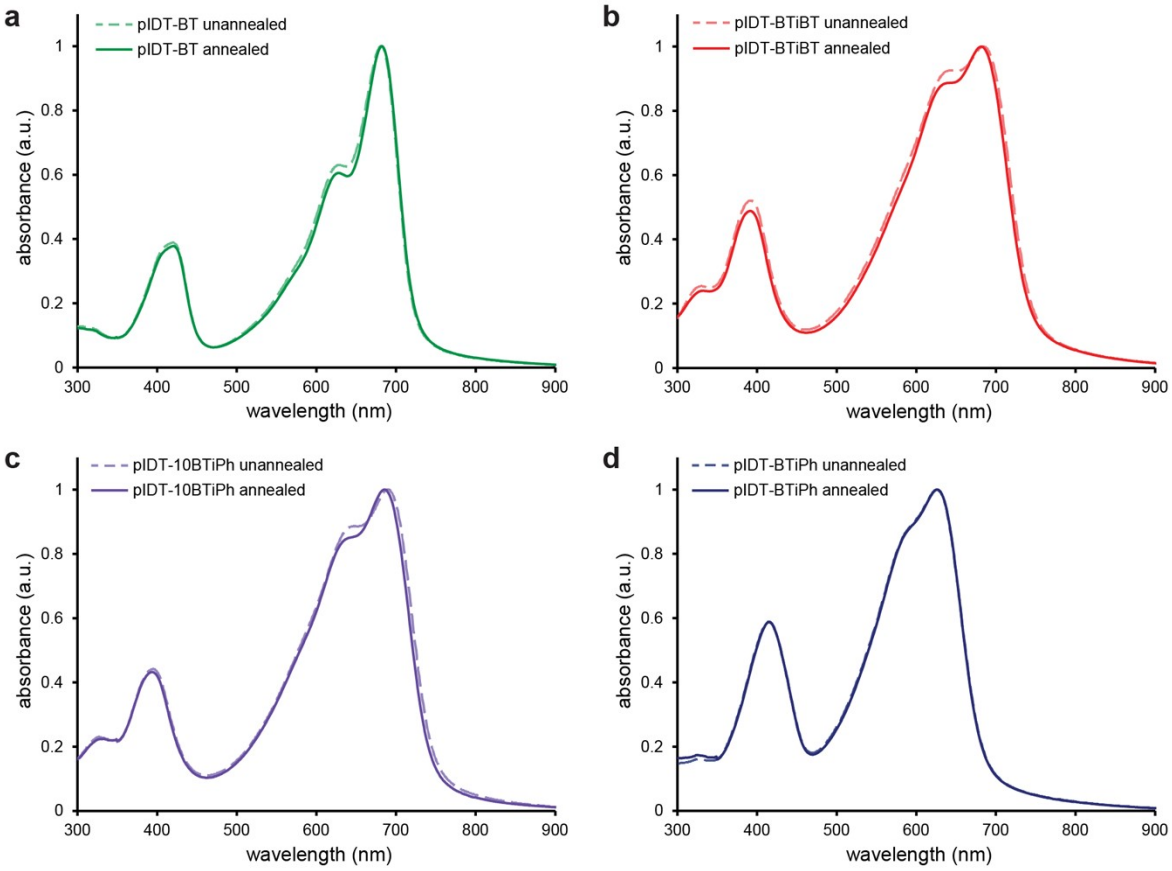

Figure S27. Normalized UV-vis absorption spectra of unannealed and annealed thin films for (a) pIDT-BT, (b) pIDT-BTiBT, (c) pIDT-10BTiPh, and (d) pIDT-BTiPh spincoated from chlorobenzene solution (10 mg/mL).

Table S2. Measured HOMO Energies by PESA and Calculated LUMO Energies

polymer	HOMO[a] (eV)	absorption onset[b] (nm)	optical band gap[c] (eV)	calculated LUMO[d] (eV)
pIDT-BT	-5.40	729	1.70	-3.70
pIDT-BTiBT	-5.60	745	1.66	-3.66
pIDT-10BTiPh	-5.60	748	1.66	-3.66
pIDT-BTiPh	-5.55	688	1.80	-3.75

[a]Ionization potentials determined from the onset of photoemission in PESA. [b]Onset of absorption was taken from UV-vis spectra of polymer thin films spincoated onto glass substrates and annealed at 80 or 150 °C for 30 min. [c]Optical band gaps were calculated using the Tauc relation. [d]LUMO energies were estimated by subtracting optical band gap values from the corresponding HOMO energies.

Table S3. Relevant Crystallographic Parameters from GIXD

polymer	lamellar fwhm (Å^{-1})[a]	lamellar CCL (Å)[b]	$\pi-\pi$ fwhm (Å^{-1})[c]	$\pi-\pi$ CCL (Å)[b,d]	backbone fwhm (Å^{-1})[e]	backbone CCL (Å)[b]
pIDT-BTiBT	0.04	168.7	0.17	37.7	0.02	308.3
pIDT-10BTiPh	0.04	156.0	0.17	38.1	0.03	228.7
pIDT-BTiPh	-	-	0.18	34.7	-	-
pIDT-BT	0.03	187.4	0.21	29.8	0.02	327.9

[a]Extracted from fitting the (100) diffraction peak. [b]Calculated based on the peak fwhm using the Scherrer equation $CCL = \frac{2\pi K}{fwhm}$, where CCL = crystallite coherence length and K = shape factor = 1.0.[5,6] [c]Extracted from fitting the (010) diffraction peak. [d]Due to the overlapping scattering from the OTS surface modification as well as amorphous alkyl chains, the (010) peak was not deconvoluted. Therefore, we do not believe the $\pi-\pi$ fwhm and CCL values reported are accurate. [e]Extracted from fitting the (002) diffraction peak.

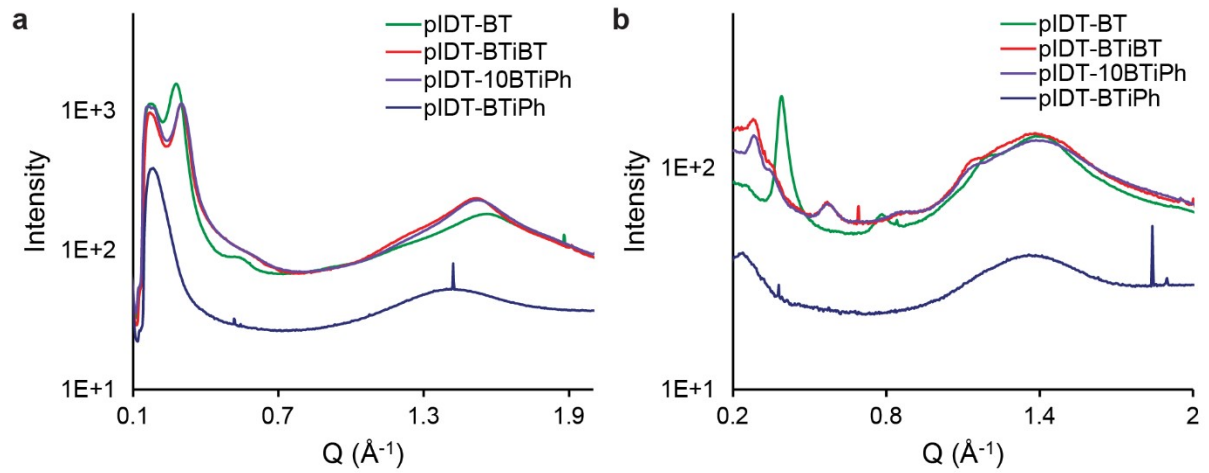

Figure S28. Integrated GIXD line profiles taken from cake segments drawn (a) out-of-plane (azimuthal angle, $\chi = 0 \pm 30°$) and (b) in-plane ($\chi = 75 \pm 15°$) for IDT-based polymers.

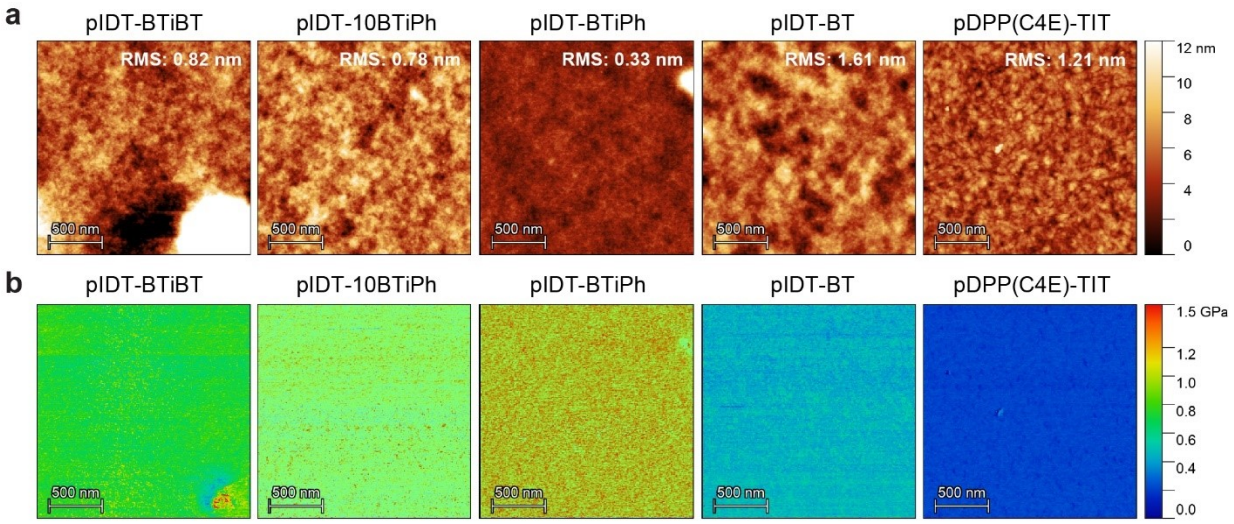

Figure S29. AFM (a) height and (b) DMT modulus images of degradable IDT and reference polymers spincoated from chlorobenzene solutions onto OTS-SiO_2 substrates after annealing for 30 min under nitrogen. For height images, root mean square (RMS) surface roughness values are shown. Large (> 500 nm) aggregates were omitted from calculated RMS roughness values.

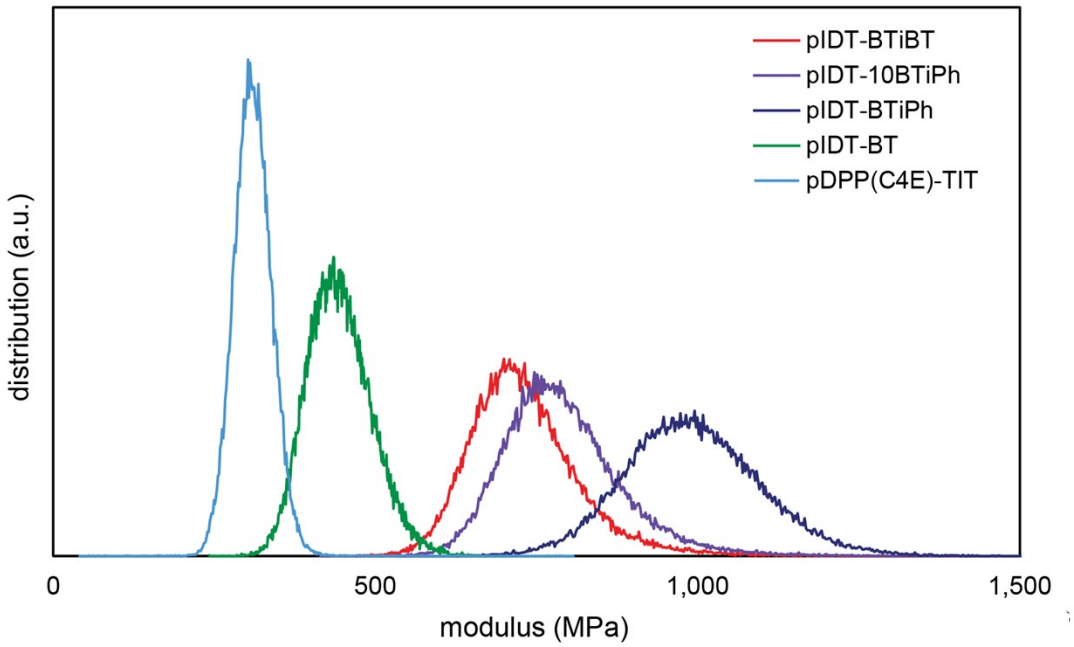

Figure S30. AFM-based DMT modulus distribution of degradable IDT and reference polymers.

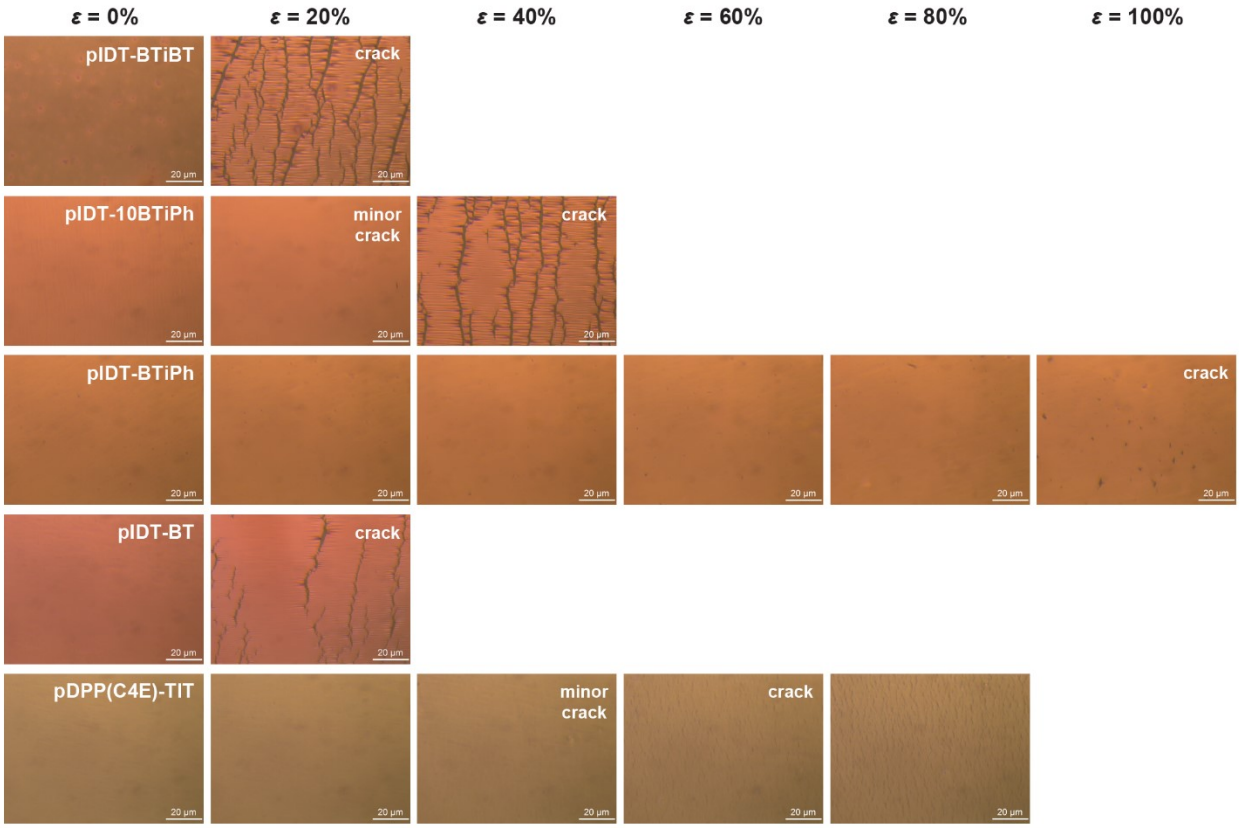

Figure S31. Optical microscope images of polymer films on PDMS elastomer at different strain (ε) values. Crack onset strain marked by "crack."

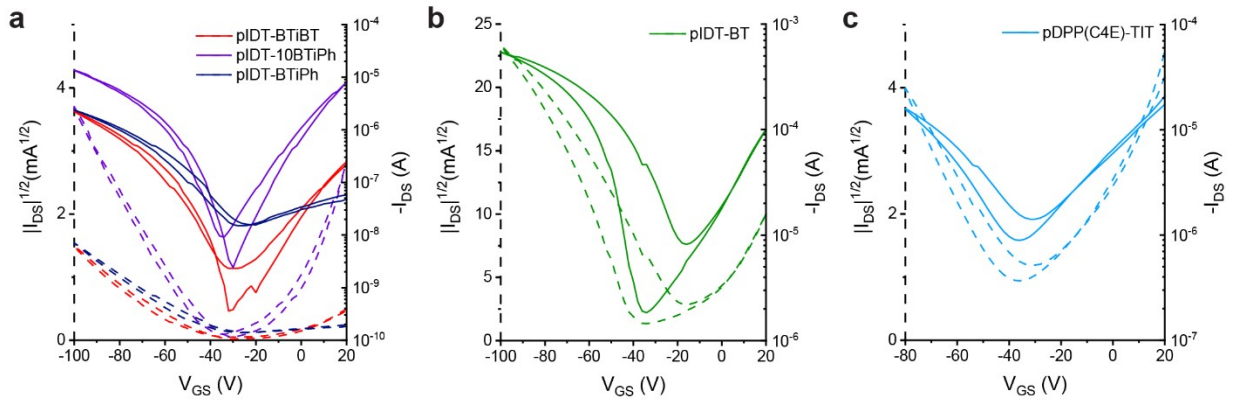

Figure S32. Representative TGBC transfer curves with dual sweep of V_{GS} for (a) degradable IDT-based polymers (V_{DS} = −100 V), (b) pIDT-BT (V_{DS} = −100 V), and (c) pDPP(C4E)-TIT (V_{DS} = −80 V).

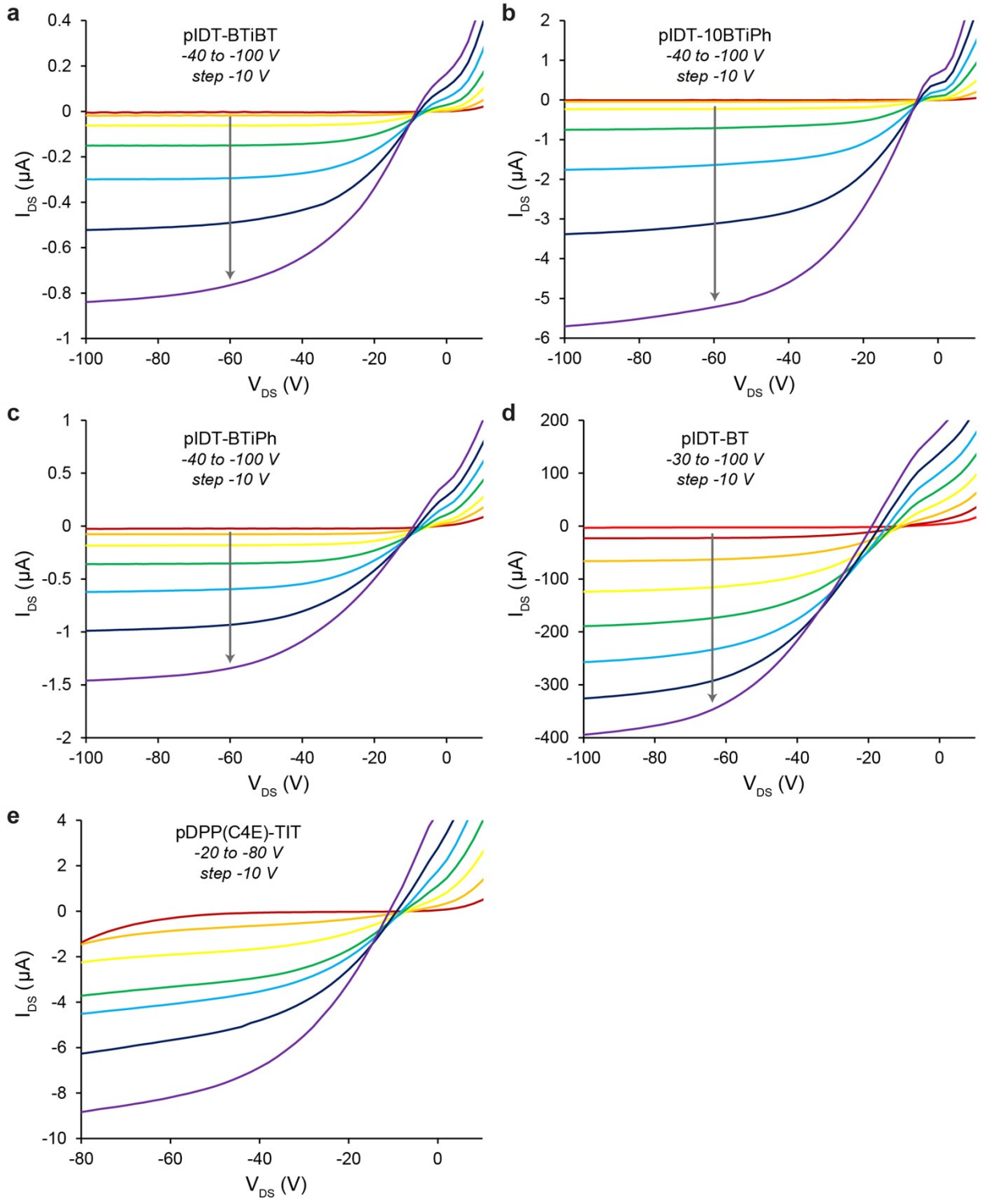

Figure S33. TGBC output curves for (a) pIDT-BTiBT, (b) pIDT-10BTiPh, (c) pIDT-BTiPh, (d) pIDT-BT, (e) pDPP(C4E)-TIT TGBC FETs.

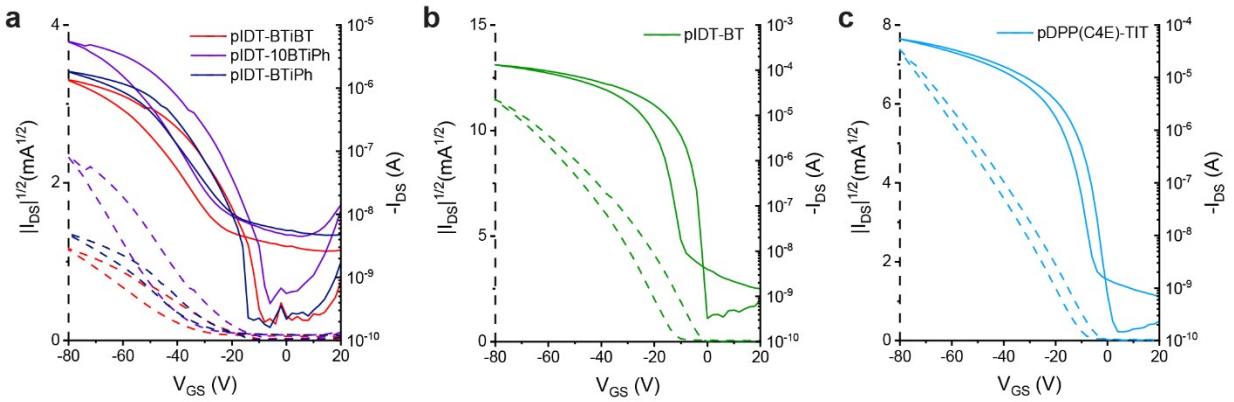

Figure S34. Representative BGTC transfer curves with dual sweep of V_{GS} for (a) degradable IDT-based polymers (V_{DS} = −80 V), (b) pIDT-BT (V_{DS} = −80 V), and (c) pDPP(C4E)-TIT (V_{DS} = −80 V).

Table S4. CYTOP Dielectric Thicknesses

batch	thickness (nm)[a]
1	710 ± 10
2	710 ± 30
3	647 ± 7

[a]Averaged from five different points on CYTOP dielectric.

Table S5. Extracted Parameters for FETs

polymer	BGTC configuration[a]			TGBC configuration[b]		
	μ_{sat} ($cm^2/V{\cdot}s$)	I_{on}/I_{off}	V_t (V)	μ_{sat} ($cm^2/V{\cdot}s$)	I_{on}/I_{off}	V_t (V)
pIDT-BTiBT	3.2 ± 0.7 E-3	10^4	−16.2	0.016 ± 0.002	10^4	−45.8
pIDT-10BTiPh	0.019 ± 0.002	10^4	−19.7	0.08 ± 0.01	10^4	−41.8
pIDT-BTiPh	0.008 ± 0.002	10^4	−19.9	0.010 ± 0.002	10^2	−35.3
pIDT-BT	0.52 ± 0.02	10^5	−0.3	1.4 ± 0.1	10^2	−12.3
pDPP(C4E)-TIT	0.13 ± 0.01	10^5	−0.2	0.04 ± 0.03	10^1	−7.9

[a]11.5 nF/cm^2 was used as the capacitance for 300 nm SiO_2. [b]Capacitance for CYTOP dielectric was calculated each batch from CYTOP thickness measurements. 2.6-2.9 nF/cm^2 was used as the capacitance using $C = \varepsilon_0 \frac{A}{d}$.

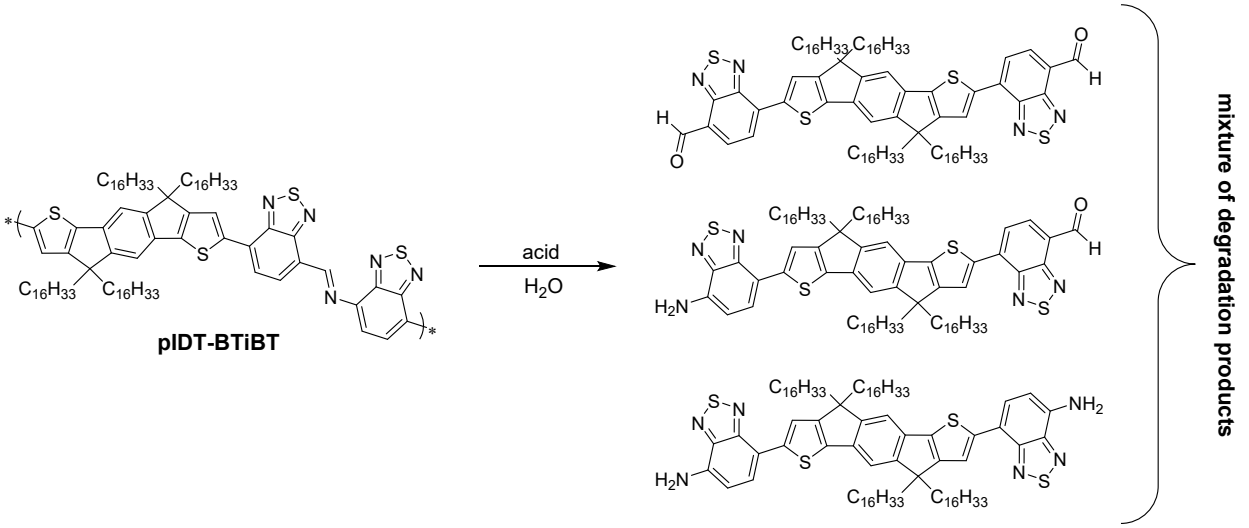

Figure S35. Scheme for degradation of pIDT-BTiBT which produces a mixture of degradation products upon reaction with acid and water.

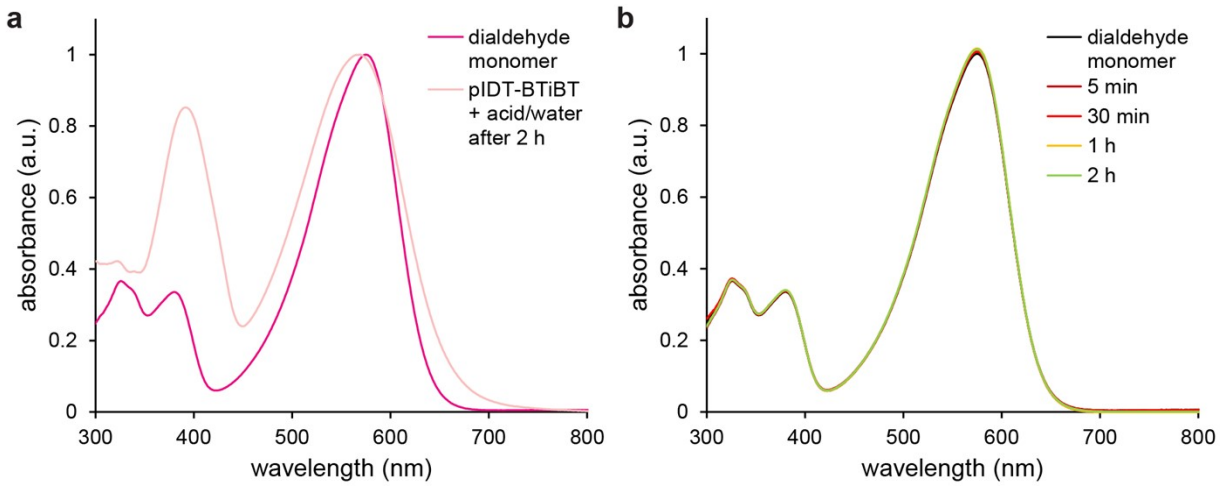

Figure S36. Experimental UV-vis spectra for (a) dialdehyde-functionalized BT-IDT-BT degradation product compared with pIDT-BTiBT after completely degraded in THF and (b) dialdehyde-functionalized BT-IDT-BT in THF solution with 150x molar excess of TFA and water.

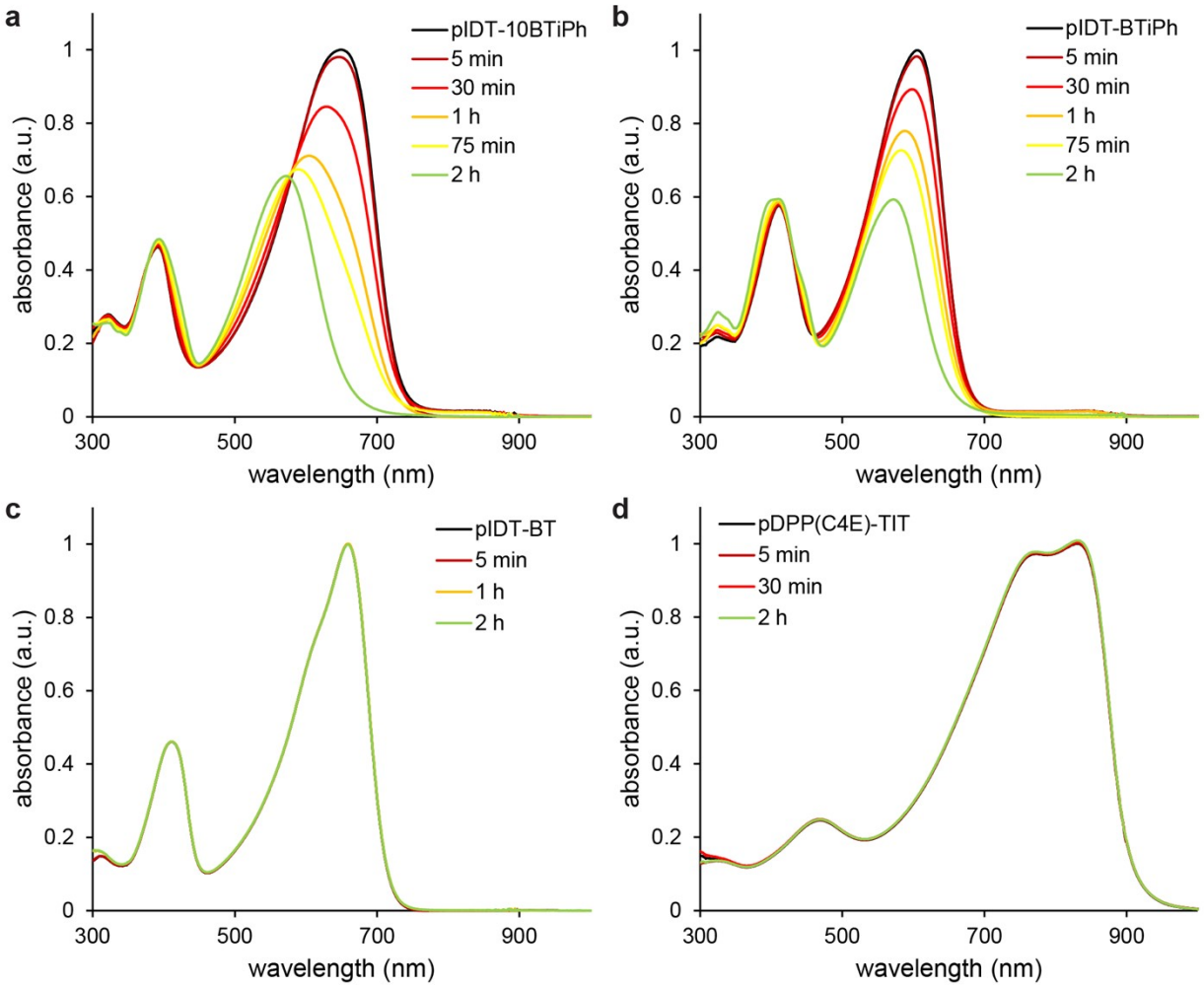

Figure S37. UV-vis spectra for (a) pIDT-10BTiPh, (b) pIDT-BTiPh, (c) pIDT-BT, and (d) pDPP(C4E)-TIT in THF solution with 150x molar excess of TFA and water.

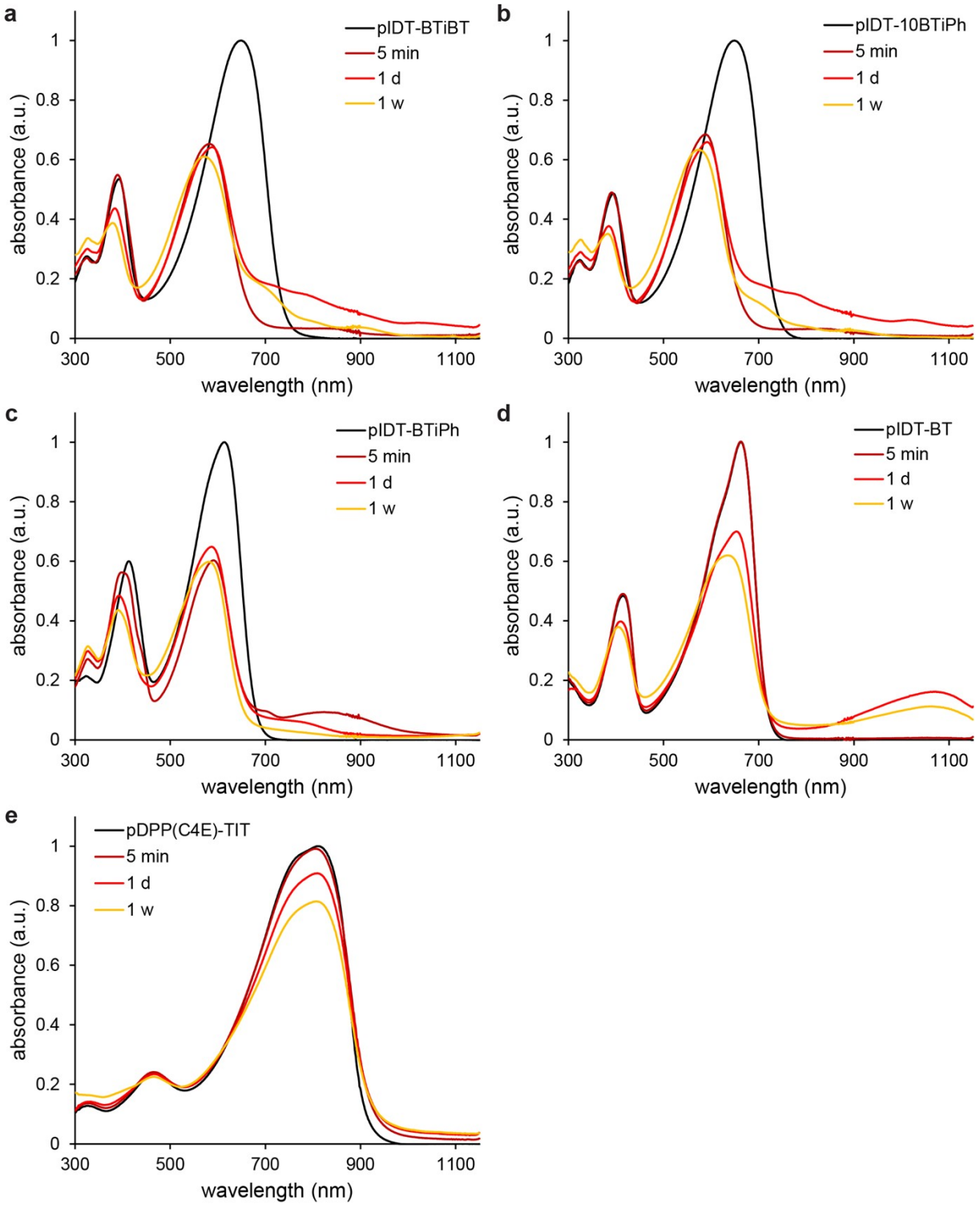

Figure S38. UV-vis spectra for (a) pIDT-BTiBT, (b) pIDT-10BTiPh, (c) pIDT-BTiPh, (d) pIDT-BT, and (e) pDPP(C4E)-TIT in chloroform solution with 150x molar excess of TFA and water.

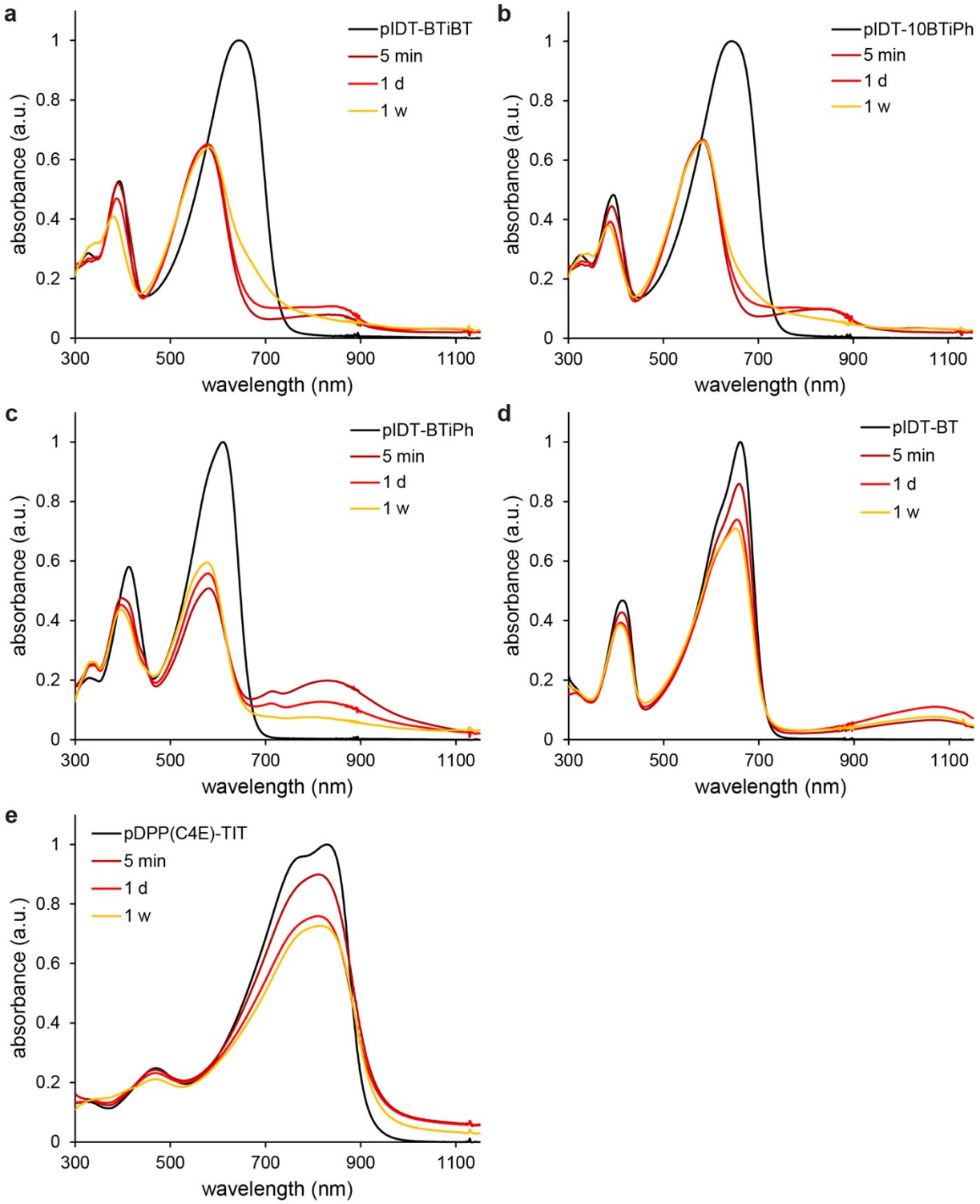

Figure S39. UV-vis spectra for (a) pIDT-BTiBT, (b) pIDT-10BTiPh, (c) pIDT-BTiPh, (d) pIDT-BT, and (e) pDPP(C4E)-TIT in chlorobenzene solution with 150x molar excess of TFA and water.

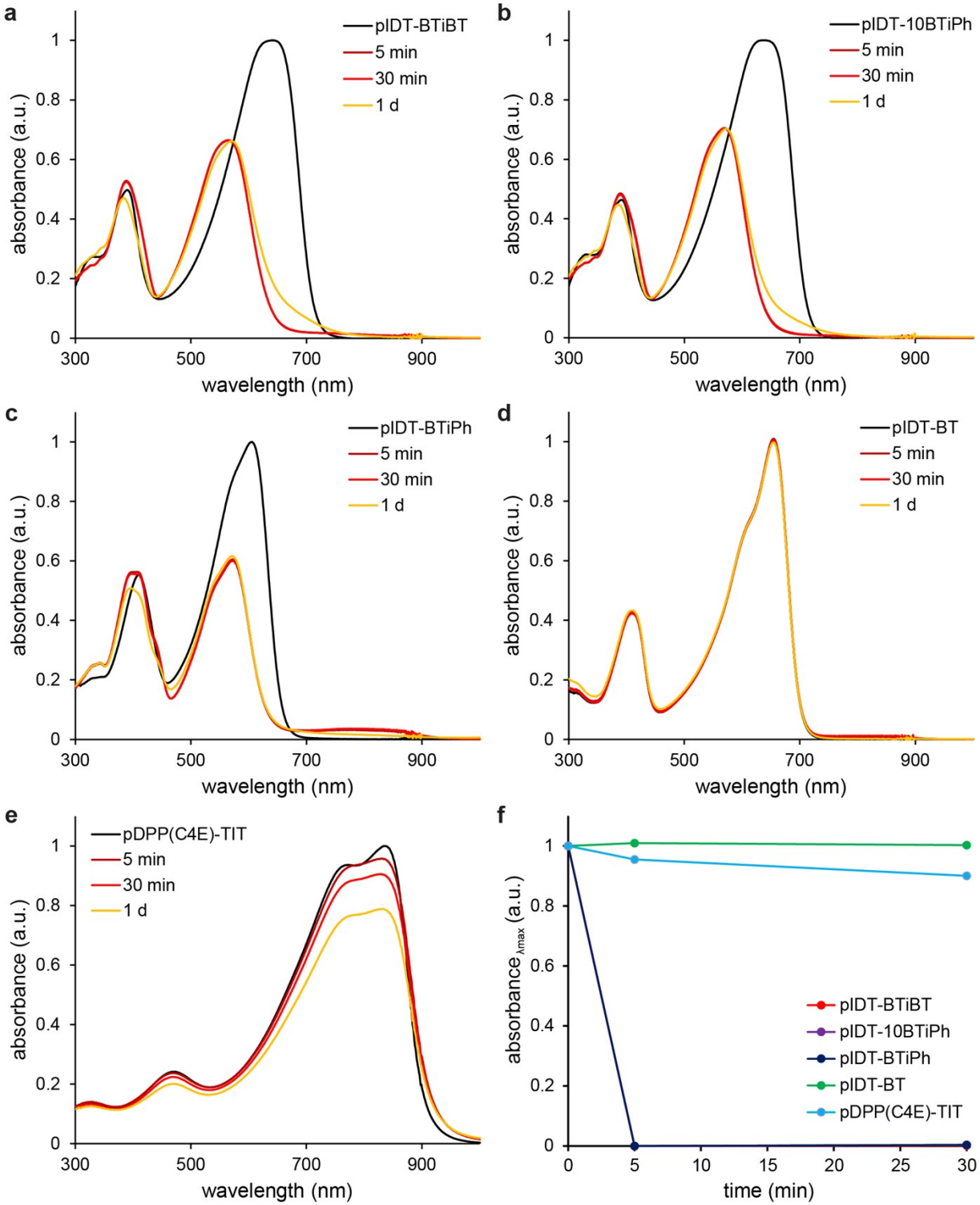

Figure S40. UV-vis spectra for (a) pIDT-BTiBT, (b) pIDT-10BTiPh, (c) pIDT-BTiPh, (d) pIDT-BT, and (e) pDPP(C4E)-TIT in toluene solution with 150x molar excess of TFA and water. (f) UV-vis absorption intensities at λ_{max} are plotted over time for degradation of all polymers in toluene solution.

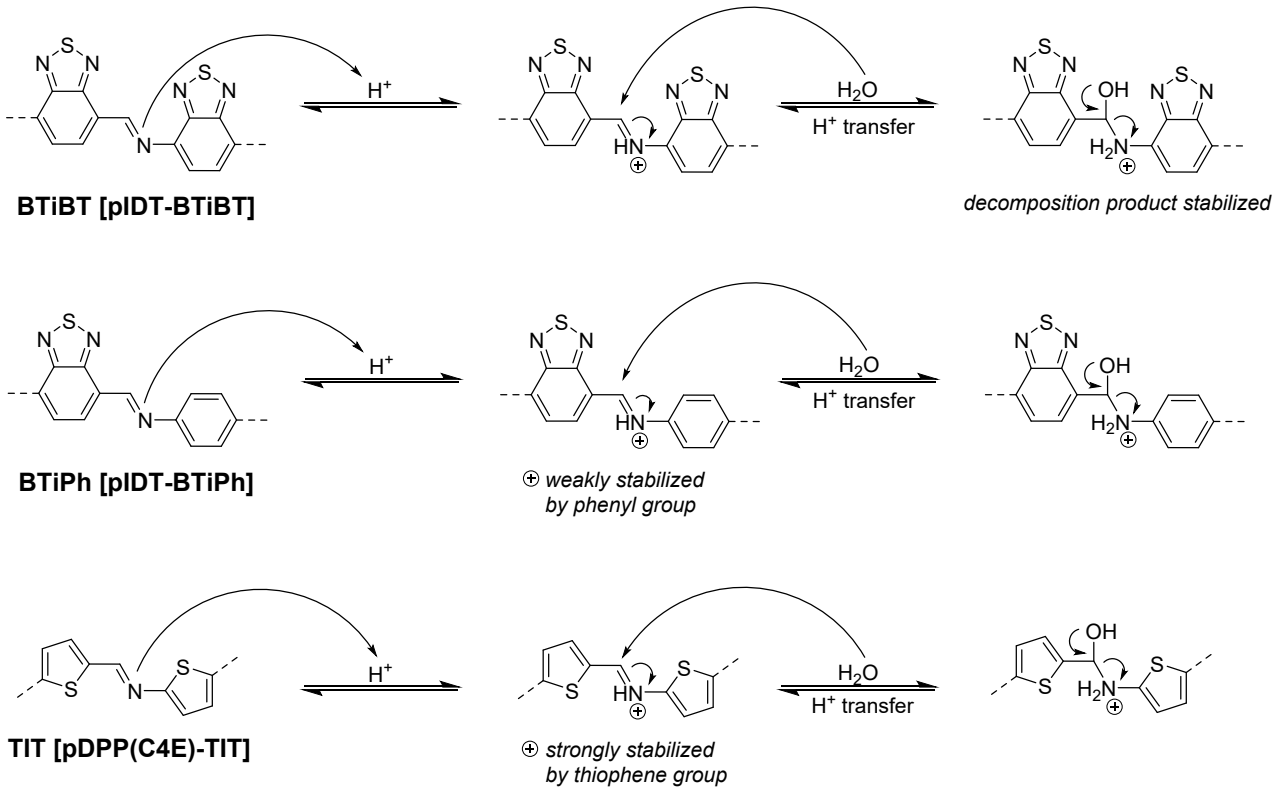

Figure S41. Proposed mechanisms for the imine hydrolysis of pIDT-BTiBT, pIDT-BTiPh, and pDPP(C4E)-TIT. The electronic effects of the hydrolytic attack and decomposition of the tetrahedral intermediate steps are noted.

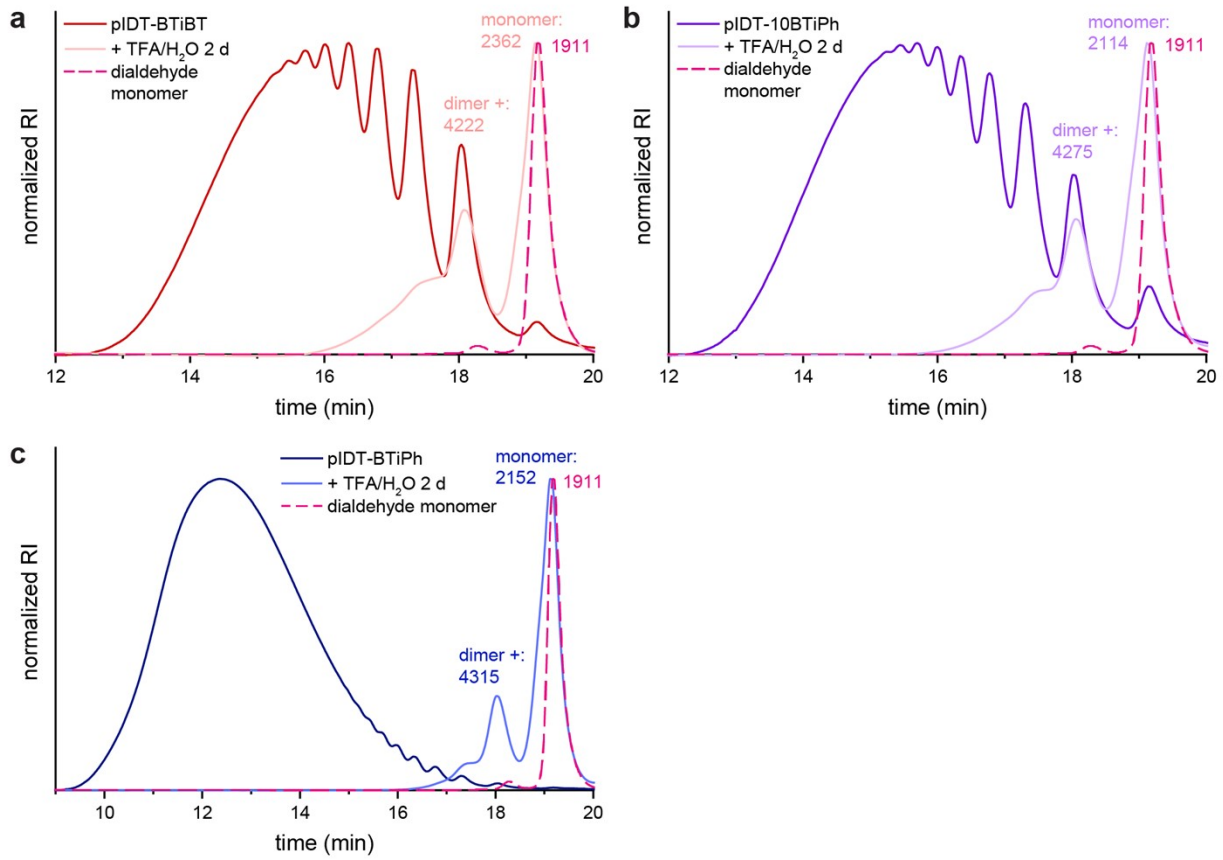

Figure S42. GPC chromatograms taken in THF at 40 °C for (a) pIDT-BTiBT, (b) pIDT-10BTiPh, and (c) pIDT-BTiPh before and after degradation in THF solution with 150x molar excess of TFA and water compared with that of synthesized dialdehyde-functionalized BT-IDT-BT. Calculated M_n values (kg/mol) are shown.

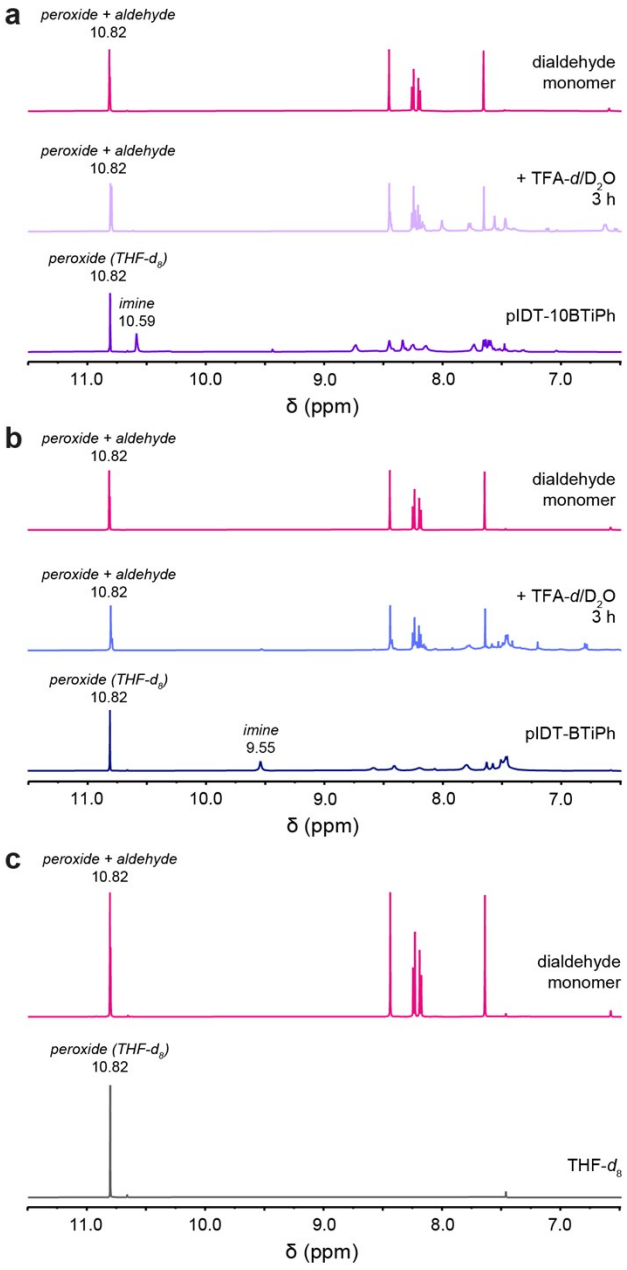

Figure S43. NMR degradation experiments of (a) pIDT-10BTiPh and (b) pIDT-BTiPh before and after degradation in THF-d_8 solution (~5 mg/mL) with 150x molar excess of TFA-*d* and D_2O compared with that of synthesized dialdehyde-functionalized BT-IDT-BT. (c) NMR of the solvent THF-d_8 was taken to demonstrate the existence of the peroxide impurity that overlapped with the aldehyde peak of the degradation products.

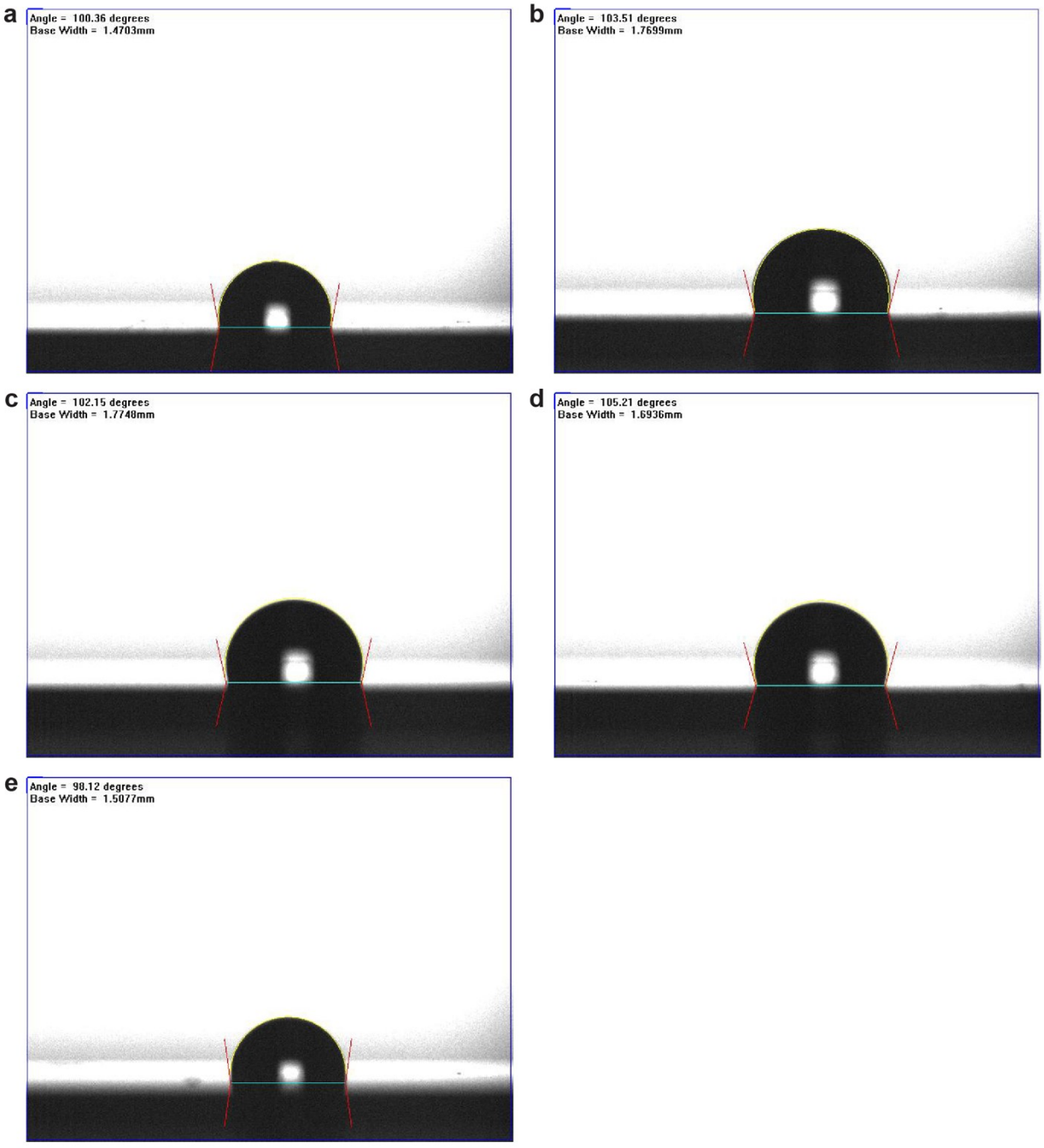

Figure S43. Contact angle measurements of (a) pIDT-BTiBT, (b) pIDT-10BTiPh (c) pIDT-BTiPh, (d) pIDT-BT, and (e) pDPP(C4E)-TIT thin films.

Table S6. Thicknesses of the Polymer Thin Films

polymer	trial 1 (nm)	trial 2 (nm)	trial 3 (nm)	average thickness (nm)[a]
pIDT-BTiBT	68.0	72.0	66.0	69 ± 3
pIDT-10BTiPh	74.5	67.5	69.9	71 ± 4
pIDT-BTiPh	67.1	66.0	67.1	66.7 ± 0.6
pIDT-BT	74.7	71.9	60.9	69 ± 7
pDPP(C4E)-TIT	66.8	67.9	76.9	71 ± 6

[a]Averaged from three different points on the polymer film.

Table S7. Average Contact Angle Measurements for Polymer Thin Films[a]

polymer	trial 1 (°)	trial 2 (°)	trial 3 (°)	average (°)
pIDT-BTiBT	102.89	100.36	100.11	101 ± 1
pIDT-10BTiPh	103.66	103.51	103.46	103.5 ± 0.1
pIDT-BTiPh	102.15	101.18	102.72	102.0 ± 0.6
pIDT-BT	105.21	105.23	105.16	105.20 ± 0.03
pDPP(C4E)-TIT	99.49	95.86	98.12	98 ± 2

[a]Distilled water was used for contact angle measurements.

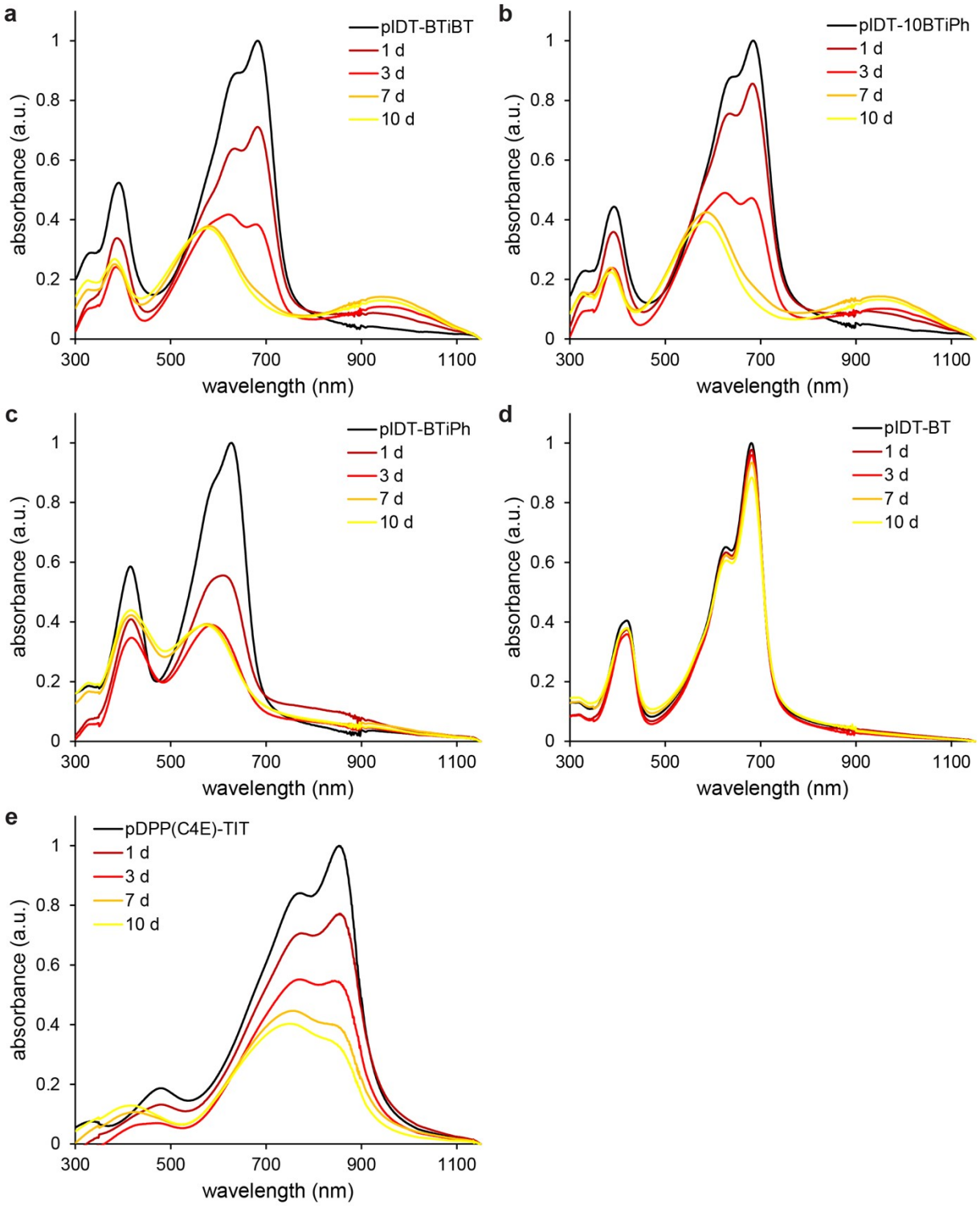

Figure S45. UV-vis spectra for (a) pIDT-BTiBT, (b) pIDT-10BTiPh (c) pIDT-BTiPh, (d) pIDT-BT, and (e) pDPP(C4E)-TIT as annealed thin films on PDMS degraded over time by submerging in 0.5 M TFA aqueous solution at 70 °C.

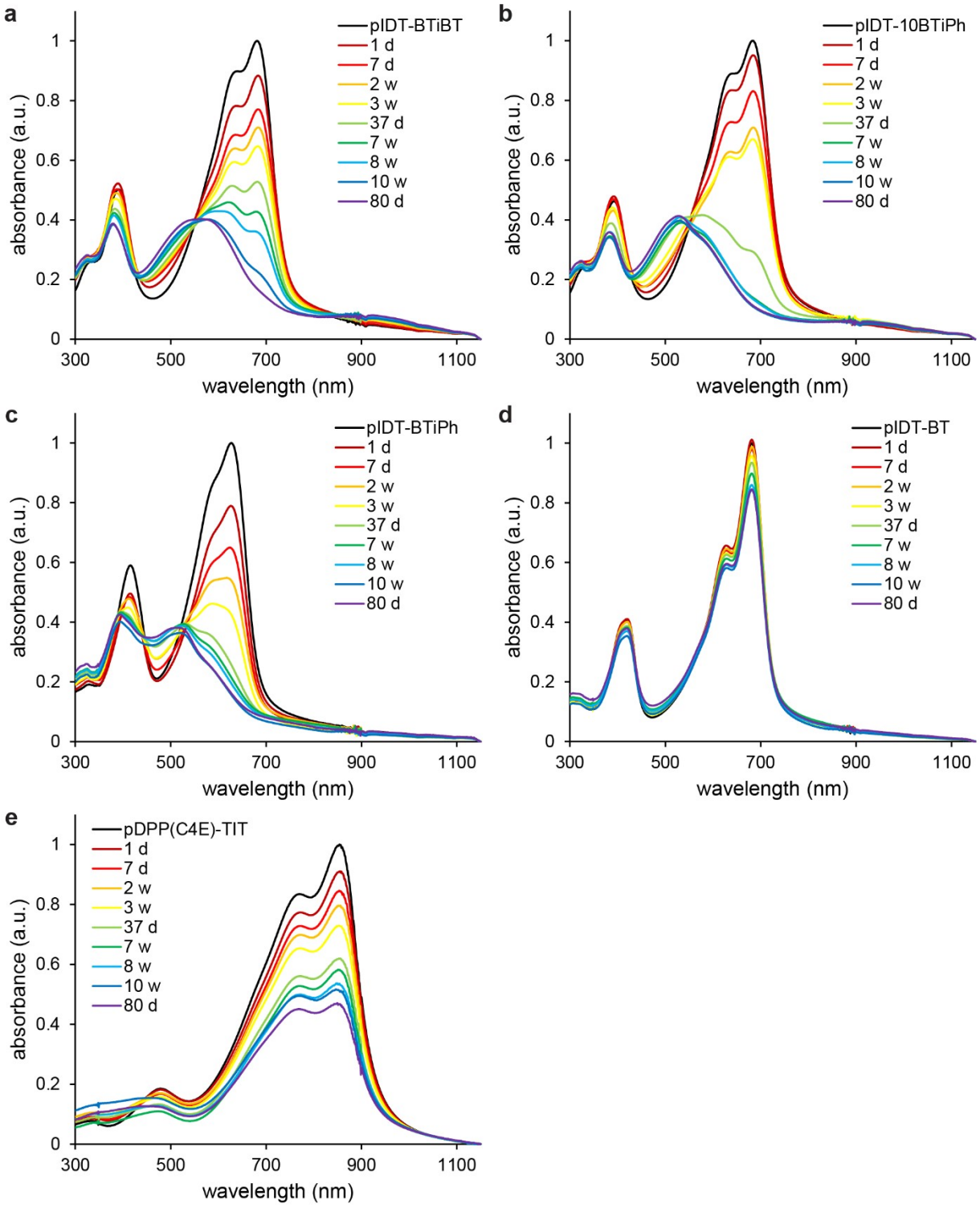

Figure S46. UV-vis spectra for (a) pIDT-BTiBT, (b) pIDT-10BTiPh (c) pIDT-BTiPh, (d) pIDT-BT, and (e) pDPP(C4E)-TIT as annealed thin films on PDMS degraded over time by submerging in 0.1 M HCl aqueous solution at 70 °C.

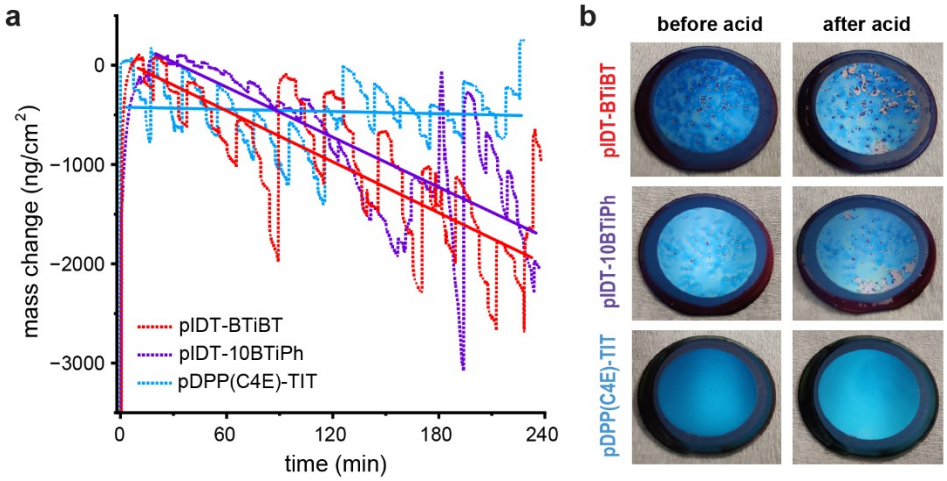

Figure S47. (a) Mass changes of thin films monitored by quartz crystal microbalance (QCM) for 0.1 M HCl at 65 °C. The solid lines display the linear fit. (b) Images of the measured polymers before and after flow of 0.1 M HCl at 65 °C.

References

(1) Jaguar: A high-performance quantum chemistry software program with strengths in life and materials sciences - Bochevarov - 2013 - International Journal of Quantum Chemistry - Wiley Online Library. https://onlinelibrary.wiley.com/doi/10.1002/qua.24481 (accessed 2023-04-21).

(2) Wadsworth, A.; Chen, H.; Thorley, K. J.; Cendra, C.; Nikolka, M.; Bristow, H.; Moser, M.; Salleo, A.; Anthopoulos, T. D.; Sirringhaus, H.; McCulloch, I. Modification of Indacenodithiophene-Based Polymers and Its Impact on Charge Carrier Mobility in Organic Thin-Film Transistors. J. Am. Chem. Soc. **2020**, 142 (2), 652–664. https://doi.org/10.1021/jacs.9b09374.

(3) Chen, H.; Wadsworth, A.; Ma, C.; Nanni, A.; Zhang, W.; Nikolka, M.; Luci, A. M. T.; Perdigão, L. M. A.; Thorley, K. J.; Cendra, C.; Larson, B.; Rumbles, G.; Anthopoulos, T. D.; Salleo, A.; Costantini, G.; Sirringhaus, H.; McCulloch, I. The Effect of Ring Expansion in Thienobenzo[b]Indacenodithiophene Polymers for Organic Field-Effect Transistors. J. Am. Chem. Soc. **2019**, 141 (47), 18806–18813. https://doi.org/10.1021/jacs.9b09367.

(4) Zhao, B.; Pei, D.; Jiang, Y.; Wang, Z.; An, C.; Deng, Y.; Ma, Z.; Han, Y.; Geng, Y. Simultaneous Enhancement of Stretchability, Strength, and Mobility in Ultrahigh-Molecular-Weight Poly(Indacenodithiophene- Co -Benzothiadiazole). Macromolecules **2021**, 54 (21), 9896–9905. https://doi.org/10.1021/acs.macromol.1c01513.

(5) Smilgies, D.-M. Scherrer Grain-Size Analysis Adapted to Grazing-Incidence Scattering with Area Detectors. J Appl Cryst **2009**, 42 (6), 1030–1034. https://doi.org/10.1107/S0021889809040126.

(6) Rivnay, J.; Mannsfeld, S. C. B.; Miller, C. E.; Salleo, A.; Toney, M. F. Quantitative Determination of Organic Semiconductor Microstructure from the Molecular to Device Scale. Chem. Rev. **2012**, 112 (10), 5488–5519. https://doi.org/10.1021/cr3001109.